NAVAL POSTGRADUATE SCHOOL

MONTEREY, CALIFORNIA

THESIS

SIMULATED E-BOMB EFFECTS ON ELECTRONICALLY EQUIPPED TARGETS

by

Enes Yurtoğlu

September 2009

Thesis Advisor:	Terry Smith
Second Reader:	Dan Boger

Approved for public release; distribution is unlimited

REPORT DOCUMENTATION PAGE		Form Approved OMB No. 0704-0188

1. AGENCY USE ONLY *(Leave blank)*	2. REPORT DATE	3. REPORT TYPE AND DATES COVERED
	September 2009	Master's Thesis

4. TITLE AND SUBTITLE Simulated E-Bomb Effects on Electronically Equipped Targets	5. FUNDING NUMBERS
6. AUTHOR(S) Enes Yurtoğlu	
7. PERFORMING ORGANIZATION NAME(S) AND ADDRESS(ES) Naval Postgraduate School Monterey, CA 93943-5000	8. PERFORMING ORGANIZATION REPORT NUMBER
9. SPONSORING /MONITORING AGENCY NAME(S) AND ADDRESS(ES) N/A	10. SPONSORING/MONITORING AGENCY REPORT NUMBER

11. SUPPLEMENTARY NOTES The views expressed in this thesis are those of the author and do not reflect the official policy or position of the Department of Defense or the U.S. Government.

12a. DISTRIBUTION / AVAILABILITY STATEMENT	12b. DISTRIBUTION CODE
Approved for public release; distribution is unlimited	

13. ABSTRACT

Like High Altitude Electromagnetic Pulse (HEMP), high power microwaves (HPM) produce intense energies, which may overload or damage various electrical system components such as microcircuits. This thesis investigates possible effects of a hypothetically designed HEMP-like weapon, an "e-bomb," on electronically equipped target systems.

The procedure to determine these possible effects is to estimate the electromagnetic coupling from first principles and simulations using a coupling model program (CEMPAT), pursuing a feasible geometry of attack, practical antennas, best coupling approximations of ground conductivity and permittivity, a reasonable system of interest representation from specifications, threat waveshape and operating frequency. The analysis procedure investigates roles of these factors contributes to the e-bomb coupling scenario.

Those possible e-bomb effect results are then compared to a published and experimentally created threshold level table to determine whether any upset or damage is formed on the target system. Based on this comparison, the results are evaluated with respect to the factors that caused them to exceed, or not exceed, the threshold levels. Additionally, a conventional weapon attack scenario for the same target system is created. Its results are compared to the e-bomb attack. Finally, operational recommendations are given along with advantages and disadvantages for each type of attack.

14. SUBJECT TERMS High Altitude Electromagnetic Pulses, High power microwaves, electromagnetic coupling, e-bomb, electronically equipped targets, threshold level, upset, damage, burnout, conventional weapon, attack scenario, directed energy, threat environment, damage assessment, E-Field, cable shielding.	15. NUMBER OF PAGES 127
	16. PRICE CODE

17. SECURITY CLASSIFICATION OF REPORT	18. SECURITY CLASSIFICATION OF THIS PAGE	19. SECURITY CLASSIFICATION OF ABSTRACT	20. LIMITATION OF ABSTRACT
Unclassified	Unclassified	Unclassified	UU

NSN 7540-01-280-5500 Standard Form 298 (Rev. 8-98)
Prescribed by ANSI Std. Z39.18

THIS PAGE INTENTIONALLY LEFT BLANK

Approved for public release; distribution is unlimited

SIMULATED E-BOMB EFFECTS ON ELECTRONICALLY EQUIPPED TARGETS

Enes Yurtoğlu
1st Lieutenant, Turkish Air Force
B.S., Turkish Air Force Academy, 2002

Submitted in partial fulfillment of the
requirements for the degree of

MASTER OF SCIENCE IN ELECTRONIC WARFARE SYSTEMS ENGINEERING

from the

NAVAL POSTGRADUATE SCHOOL
September 2009

Author: Enes Yurtoğlu

Approved by: Lt. Col. Terry Smith
Thesis Advisor

Dr. Dan Boger
Second Reader

Dr. Dan Boger
Chairman, Department of Information Science

THIS PAGE INTENTIONALLY LEFT BLANK

ABSTRACT

Like High Altitude Electromagnetic Pulse (HEMP), high power microwaves (HPM) produce intense energies, which may overload or damage various electrical system components such as microcircuits. This thesis investigates possible effects of a hypothetically designed HEMP-like weapon, an “e-bomb,” on electronically equipped target systems.

The procedure to determine these possible effects is to estimate the electromagnetic coupling from first principles and simulations using a coupling model program (CEMPAT), pursuing a feasible geometry of attack, practical antennas, best coupling approximations of ground conductivity and permittivity, a reasonable system of interest representation from specifications, threat waveshape and operating frequency. The analysis procedure investigates roles of these factors contributes to the e-bomb coupling scenario.

Those possible e-bomb effect results are then compared to a published and experimentally created threshold level table to determine whether any upset or damage is formed on the target system. Based on this comparison, the results are evaluated with respect to the factors that caused them to exceed, or not exceed, the threshold levels. Additionally, a conventional weapon attack scenario for the same target system is created. Its results are compared to the e-bomb attack. Finally, operational recommendations are given along with advantages and disadvantages for each type of attack.

THIS PAGE INTENTIONALLY LEFT BLANK

Disclaimer

The views expressed in this thesis are those of the author and do not reflect the official policy or position of the Turkish Republic, the Turkish Armed Forces, the Turkish Land Forces, the Turkish Naval Forces, the Turkish Air Force, the U.S. Navy or the Naval Postgraduate School.

THIS PAGE INTENTIONALLY LEFT BLANK

TABLE OF CONTENTS

LIST OF FIGURES

THIS PAGE INTENTIONALLY LEFT BLANK

LIST OF TABLES

THIS PAGE INTENTIONALLY LEFT BLANK

ACKNOWLEDGMENTS

I would like to express my gratitude to the great Turkish Nation, to the Turkish Armed Forces, born from the heart of the great nation, and my sponsor, the Turkish Air Force, for providing me this opportunity to obtain my Master of Science degree in the United States at the Naval Postgraduate School.

I am heartily thankful to my advisor, Lt. Col. Terry Smith, USAF, whose encouragement, guidance and support from the initial to the final level enabled me to develop an understanding of this thesis subject.

I offer my regards and blessings to my parents, Münevver Yurtoğlu and Cemali Yurtoğlu, who have always been there for me and supported me throughout all my life. Everything they have done for me is invaluable.

Mostly, I would like to thank my beautiful wife, Deniz, for her great support and love that she gave to me while I struggled through the completion of my master's degree at the Naval Postgraduate School, as well as her devotion throughout all of my professional endeavors leading to this degree. Moreover, I would like to thank to her for being a very good mother to my little son, Semih, and being a good wife to me. Thank God you are in my life.

THIS PAGE INTENTIONALLY LEFT BLANK

EXECUTIVE SUMMARY

Nuclear weapons detonated at very high altitudes create High Altitude Electromagnetic Pulse (HEMP). At specific ranges, this pulse can overload or damage various electrical system components, such as microcircuits. High power microwaves (HPM) can also produce intense energy effects, similar to HEMP. An equivalency to the HPM instantaneous pulses can be created by special equipment that transforms the desired energy, using high frequency generators and stored battery power, into intense radiated microwaves. It can also be possible to create the same effect on the electronic devices by aiming a powerful electromagnetic transient, formed by a shaped antenna, against those same electronic system devices.

This issue forms the very core objective of this thesis work. The study investigates possible effects of a hypothetically designed HEMP-like weapon, herein called an “e-bomb,” on electronically equipped target systems such as Integrated Air Defense Systems, Command Control Communications Computers and Intelligence (C^4I) systems.

The procedure followed in this study to determine these possible e-bomb effects is to estimate the electromagnetic coupling from first principles and simulations using appropriate coupling model programs. For example, the research pursues a feasible geometry of attack, practical antennas, best coupling approximations for true fields including the impacts of ground conductivity and permittivity near the deployed target, a reasonable system of interest representation from specifications, and consideration for the threat waveshape and operating frequency. The analysis procedure investigates the role each of these factors contributes to the e-bomb coupling scenario and the end-to-end process is described as follows:

A simple topographical system of interest transmission-line coupling model is created as a target that consists of some mission-essential distributed

equipment nodes, which include electronic device components. This model resembles a mobile, deployed, Integrated Air Defense System (IADS).

Configuration detail of the model is created for each node of the target model, including node functions, specifications, distances to neighboring nodes, and the connection cable types.

Appropriate environmental details of the electromagnetic coupling model like conductivity (σ), permittivity (ε), which are dependent on establishment field, polarization, and load configurations, are estimated in order to better represent true-fielded systems.

A range, which turns out to be the detonation altitude over the target, is selected based on the desired frequency span, antenna diameter, and the geometry for the deployment platform source. This altitude, in-turn, is used to establish the intensity level for illumination of the topographical model, while also considering the corresponding weapons beam width and it's spectral capabilities that might be possible with reasonable delivery systems. A basic approach is employed to define the geometry and to calculate the detonation altitude to ensure the radius of the whole target system area (including all cable lengths) is e-bomb illuminated.

The hypothetical e-bomb created transient pulse used to interact with the modeled IADS system is defined from first principles. The pulse is developed and formatted as the expected amplitude, waveshape and frequency content of an e-bomb as a function of 'range.' The device waveshape is largely unknown for a hypothetical weapon; therefore, the e-bomb pulse is defined based on reasonable approximations of existing and published "open literature" electromagnetic threats that are scaled to the maximum amplitude value that would be associated with the calculated detonation height and the geometry of the assumed target system. A MATLAB program, developed under a previous effort, is used in this part of the development to define the e-bomb weapon E-field intensity as a function of range.

After defining the threat field expected from an e-bomb, as described above, an electromagnetic coupling and interaction program using the threat waveshape and models of the target system was employed to analyze terminal currents throughout the model. These system currents were then converted to their node voltage, delivered power, or energy, at the various representative distributed system nodes (i.e., power, communication, network) throughout the model. In other words, the voltage, power, and energy formed on the electrical device components were calculated using terminal currents as expected to be induced on the cables exposed to radiated outputs from an e-bomb.

A published, experimentally created, threshold level table appropriate for the node electronic components (transistors, diodes, etc.) was then used as the basis for evaluating the potential for upset and damage based on the analyzed voltage, power, and energy results obtained by the interacting model.

All the described results are analyzed individually and collectively. The controlling elements such as source size, environment, and system configuration are inherent to the described analysis. In addition, the effects of shielding methods, where appropriate, are explained and folded into the results.

Operational analysis is conducted to determine which of the controlling elements are the most important to ensure sustained operations of the IADS. A conventional weapon scenario is created for the same target system and probability of damage values are obtained for each system node separately. Similar analysis accomplished by considering conventional weapons and common or differential trends are identified and compared to the e-bomb model findings.

Finally, operational recommendations are given to readers regarding the results and comparisons achieved from this study. In addition, advantages and disadvantages of both e-bomb and conventional attacks are provided based on the obtained results.

As a result, this study claims that with all the principles, theories, and procedures applied to obtain every result, it can be possible to damage or at least upset various types of electrical devices components in an IADS with a hypothetical e-bomb weapon. With respect to the e-bomb attack results, it is determined that the best defense is in the shielding against electromagnetic interference. Shielded cables in the system were significantly less affected than unshielded cables.

Overall, those results and comparisons provide an idea of how to best use such a weapon against electronically equipped targets, along with comparing and contrasting e-bomb effectiveness against conventional munitions effects on the same target system.

I. INTRODUCTION

A. SCOPE OF THE THESIS

This thesis research seeks to characterize possible effects—upset, damage, burnout—of a hypothetical electromagnetic weapon (identified as *e-bomb* for the remainder of this thesis) on distributed targets composed of electronic components. In addition, this research investigates possible effects of the conventional weapons on the same distributed targets to compare to the hypothetical e-bomb effect results. Throughout, this effort searches and analyzes those potential effects from the view of a military operation's perspective.

The conventional weapon evaluations will include systems such as conventional bombs (i.e., Mark (MK) series weapons) while considering deployment methods, effects, and results on a target. Moreover, Desired Mean Point of Impact (DMPI) considerations will be studied. After analysis of these devices and comparing all of their advantages and disadvantages, some operational recommendations will be given. This operationally based analysis will bring out a comparison picture and let the reader view the potential utility of an electromagnetic weapon.

B. MOTIVATION (WHY DIRECTED ENERGY?)

Open source material available on the Internet reveals that some scientists have already theoretically conceived the basic framework for an electromagnetic weapon. For example, Carlo Kopp, a prominent Australian freelance defense analyst and academic, indicates that because of fundamental dependency upon the modern semiconductor devices, they are globally vulnerable to the attacks from some specifically designed weapons that can damage or destroy those semiconductor components. Prominently, those kinds of weapons are technically feasible and economical to build in comparison to

established weapons of mass destruction. Such weapons can employ a wide range of existing targeting and delivery techniques. These devices are electromagnetic weapons and the most dominant one of this weapon type is the electromagnetic bomb (e-bomb) (Kopp, 1996).

Another scientist, Edl Schamiloglu, who is a professor of electrical and computer engineering at the University of New Mexico in Albuquerque and one of the leading researchers in this field, says “High Power Microwave (HPM) sources are maturing, and one day, in the very near future, they will help revolutionize how U.S. soldiers fight wars” (Abrams, 2003). Lt. Col. Terry Smith, lecturer and Electronic Warfare (EW) Program Officer at Naval Postgraduate School (NPS), implies that because of the potential advantages that these electromagnetic devices might offer, militaries all around the world have shown interest in this emerging technology. A general thought in the global military community is this: The wars of the future will be based on technological power. Electromagnetic weaponry is one of the technologies that potentially offer many tactical and strategic advantages, not the least of which would be their deterrent role preventing foreign aggression with reasonable resource expenditure (Smith, 2009).

Those deliberations and progresses around the world leads this study to search how effective an e-bomb can be against a specific group of targets from the view of military operations. The research will try to simulate an e-bomb attack against a target system including multiple, electronically equipped, DMPIs. In this simulation, the geometry of the attack, deployment methods and a selected platform will be evaluated and demonstrated. Appropriate scenarios and tactics will be included as well. The study will discuss whether an e-bomb can be more practical than conventional weaponry. It will conclude with an analysis of the advantages and disadvantages of DE weapons compared to conventional munitions. In addition, this study will analyze the use of e-bomb against multiple DMPIs simultaneously from the operational perspective of causing no collateral damage.

It is obvious that Directed Energy Weapons (DEW) are at least potentially going to play important roles in future warfare. The use of DEW will lead warfare considerations into a new dimension, and it will cause all the current strategies and tactics to be rearranged.

C. WHAT IS AN E-BOMB?

In order to be able to understand what an e-bomb is, it is needed to begin with an understanding of what Electromagnetic Pulse (EMP) is—an extremely concentrated instantaneous energy field that can disrupt or overload various electrical systems and microcircuits sensitive to power surges (Wilson, 2006). EMP is typically related to one of the weapons' effects from a nuclear burst, but it can be used to describe any very intense, very rapid, burst of energy propagated radially from an emitter.

An e-bomb is a kind of weapon that uses the electromagnetic spectrum, emitting short, but very high power, microwave burst pulses that spikes into the gigawatts power range lasting for only microseconds causing some specific levels of damage by emitting enough energy to overwhelm electronic devices and their components (Pace, 2007). From this definition, an e-bomb can be viewed as a kind of EMP weapon.

It is important for the reader to understand that there is no officially reported example of an e-bomb in the world, nor is it possible to identify any officially recognized operational testing of an e-bomb. Because this information is unavailable in any open-literature environment, the e-bomb for discussion in this thesis is a "hypothetical e-bomb."

There are various kinds of military targets which an e-bomb can potentially be used against. Some important examples of these can include military functions related to telecommunications systems, manufacturing systems, computers used in data processing systems, displays, equipment that is embedded in the military such as signal processors, electronic flight controls,

digital engine control systems and industrial control applications, including road and rail signaling (Kopp, 1996). These examples are in Figure 1.

Considering the typically deployed configuration of these potential targets, they are usually gathered in a specific area of operational functions, so an e-bomb can be used against and can affect all of them with just one pulse at a time.

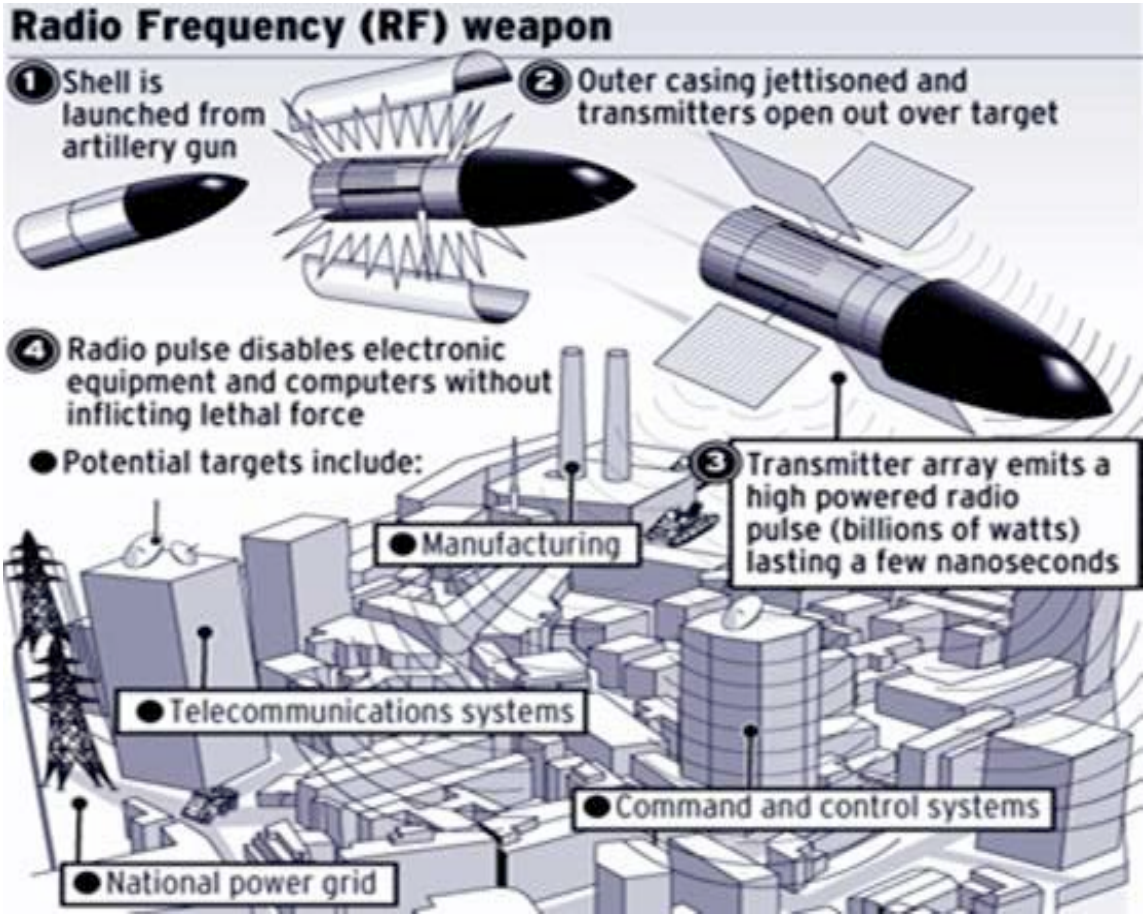

Figure 1. Feasible E-bomb Targets (From: Pace, 2007)

Normally, an e-bomb does cause harm or injury against any human or any lives since its pulse duration is very short. In other words, it is non-lethal and a threat only to operating electronic systems. This provides the opportunity to attack targets against which conventional weapons do very poorly such as, targeting an enemy among civilian neighborhoods using human shields

(Pace, 2007). Therefore, there is the potential advantage of no collateral damage unless the e-bomb affects a facility such as a hospital or any other equipment, related to human life.

On the other hand, there are some other important things to consider when using an e-bomb against those potential targets, from the aspect of an objective to inflict damage. These non-ideal considerations include factors such as triggering undesirable environmental conditions (rain and thick clouds), which can affect the propagation of the electromagnetic wave (and reduce its amplitude), shielded components of the target system, which provides an inherent protection layer against electromagnetic pulse

Chapter II provides further information about an e-bomb including its delivery system, possible effects on targets, coupling methods, and shielding associated with an e-bomb.

D. THE BENEFIT OF THE RESEARCH

This study will help to understand the use of an electromagnetic weapon and its effect on representative targets. In addition, it will provide an opportunity to see the difference between using an electromagnetic weapon and using conventional weapons against a specific target from an operational view.

The research will provide a concept of an electromagnetic weapon. It will focus on a hypothetical e-bomb as a type of electromagnetic pulse weapon. A theoretical application and engagement scenario, supported by two computer programs, is employed to measure the hypothetical e-bomb effects on a target, i.e., Integrated Air Defense System (IADS) for realistic results.

In order to best match a real-world operating scenario, this study incorporates the features and effects of real field components and environmental considerations as a result of coupling efficiency on the DMPIs of the target system. Those real-world coupling factors include soil conductivity, permittivity,

cable length and thickness, and cable height above ground. Moreover, hypothetical e-bomb parameters, i.e., incident angle, frequency, amplitude, and coupling efficiency must also be applied.

The described engagement scenario will be used to show how those sensitive electronic components and the cables connecting each nodes of IADS can be exposed to the effects of the hypothetical e-bomb. Moreover, the results support evaluation of which parameters or conditions have a positive impact and which have a negative impact on the results.

All of these results provide an opportunity to understand how an e-bomb can be used operationally in a battlefield, and how it can be compared to the conventional munitions with respect to their advantages, disadvantages, and effects on electronically equipped targets. The comparison of those effects, advantages and disadvantages, will provide an opportunity to make a decision on method should be used in military operations against indicated targets.

E. RESEARCH ROADMAP

The research roadmap description of this study is comprehensively explained step by step below and those steps can also be viewed in Figure 2 following the steps. The Figure and explanations provide a quick understanding of the whole process of the study.

Step 1. A simple topographical system of interest transmission-line coupling model will be created as a target that consists of some mission-essential distributed equipment nodes. This model will be developed to resemble a mobile, deployed, IADS or Command Control Communications Computers and Intelligence (C^4I) system.

Step 2. A configuration of the model will be outlined and each node of the target model will be defined, including functions and specifications of each node Distances between each other will be indicated. Specifications and configurations of each cable connecting each node will be included.

Step 3. Appropriate environmental details of the model: conductivity (σ), permittivity (ε), polarization, load configurations etc. will be researched in order to better describe true-fielded systems.

Step 4. A range (altitude over the target) of interest will be decided based on the desired frequency range, antenna diameter, and the geometry for the deployment platform source. This altitude, in-turn, will be used to establish the intensity level for illumination of the topographical model while considering the corresponding weapons beam width and it's spectral capabilities.

Step 5. The hypothetical e-bomb created pulse, that is used to interact with the modeled system, will be defined from first principles. The pulse will be developed and formatted as the expected amplitude, waveshape and frequency content of an e-bomb as a function of 'range'. The device waveshape is unknown for a hypothetical weapon; therefore, it will be defined based on reasonable approximations of existing electromagnetic threats that are scaled to the maximum value amplitude of the hypothetical e-bomb 'Field Strength'. A MATLAB program will be used in this part of the method to define the weapon E-field intensity as a function of range.

Step 6. Defining the threat field expected from an e-bomb, as described previously, an electromagnetic coupling and interaction program using the target field strength (E), and models of the target system will be employed to analyze terminal current values throughout the model.

Step 7. These system currents will be converted to the delivered power, or energy, at representative distributed system nodes (power, communication, network, etc.).

Step 8. The threshold values of the voltage, power, and energy formed on the electronic components (transistors, diodes, etc.) at each node, within their modeled environments, will be searched and identified, for upset or burnout threshold level purposes.

Step 9. Those induced powers from the interacting model will be compared to those power threshold levels to determine their potential for either upset or burnout.

Step 10. All the results will be analyzed. The controlling elements like source size, environment, and system configuration will be identified.

Step 11. Operational analysis will be conducted to determine which of the controlling elements are the most important to ensured operations of the IADS.

Step 12. Similar analysis will be accomplished by considering conventional weapons and common or differential trends will be identified.

Step 13. Finally, operational recommendations will be given to readers regarding to the results and comparisons achieved from the study.

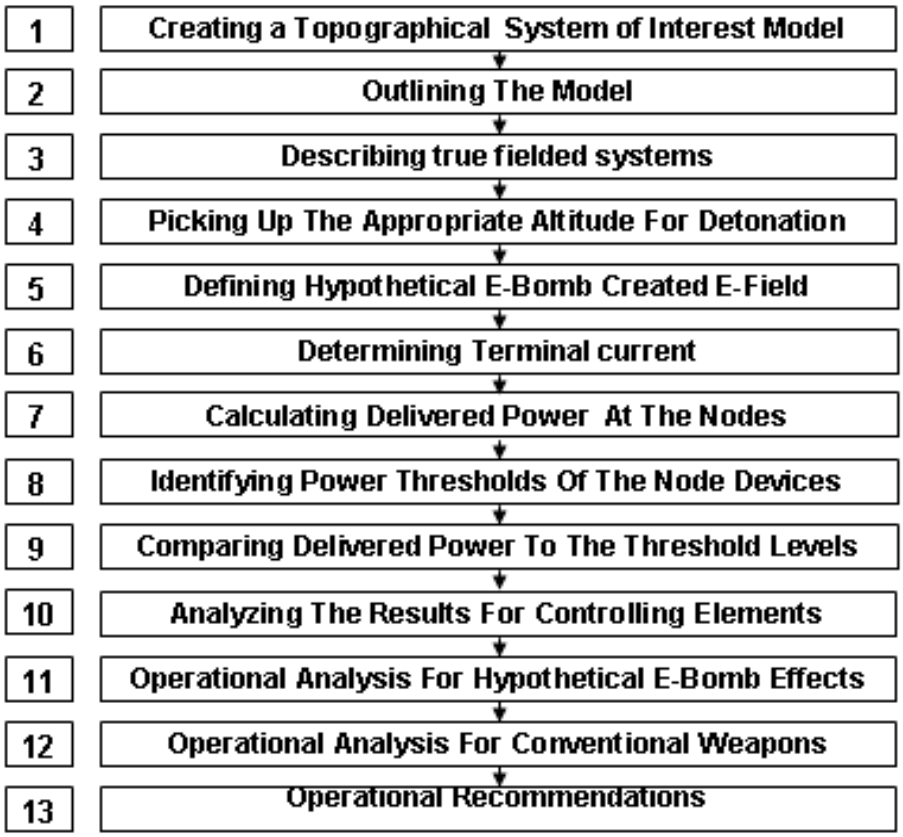

Figure 2. Research Roadmap

II. ASSESSMENT SCENARIO OVERVIEW

This chapter begins with an introduction and examination of terms and definitions involved in this study. Following that, possible systems of interest as targets, various threat models, the attack geometry, modeling, and electromagnetic coupling methods at the very core of this study are covered broadly. Included are some outputs out of the study demonstrating range between the best and worse cases. Selected target system and the threat model are explained specifically.

A. RESEARCH PRINCIPLES

Provided in this section, basic definitions related to the study. The section covers basic concepts and some explanations about Directed Energy (DE), High Power Microwave (HPM) and HPM Weapons. In addition, some DE use examples available in open literature are provided in this section.

1. Basic Definitions

a. Directed Energy

> An umbrella term covering technologies that relate to the production of a beam of concentrated electromagnetic energy or atomic or subatomic particles. (JP1-02 DoD Dictionary of Military and Associated terms)

Some known directed energy types are counted as; High-Energy Lasers (HEL), Charged Particle Beams (CPB), Neutral Particle Beams (NPB), and High Power Microwave (HPM) (Schleher, 1999). Among those energy sources, only HPM were investigated in this study. Using those energy sources, some special weapons can be produced, as it will be covered later in this section.

b. Directed-Energy Weapon (DEW)

> A system using directed energy primarily as a direct means to damage or destroy enemy equipment, facilities, and personnel. (JP1-02 DoD Dictionary of Military and Associated terms)

Since the only interest of this study will be HPM weapons, the possible effects of a hypothetical e-bomb on electronically equipped targets was examined using HPM principles.

c. Directed-Energy Warfare

> Military action involving the use of directed-energy weapons, devices, and countermeasures to either cause direct damage or destruction of enemy equipment, facilities, and personnel, or to determine, exploit, reduce, or prevent hostile use of the electromagnetic spectrum through damage, destruction, and disruption. It also includes actions taken to protect friendly equipment, facilities, and personnel, as well as retain friendly use of the electromagnetic spectrum. (JP1-02 DoD Dictionary of Miltary and Associated terms)

This study provides a good Directed-Energy Warfare scenario while searching the possible effects of an e-bomb on an electronically equipped target. In addition, the e-bomb outputs were compared to a conventional attack scenario against the same target. Both of the attack's results were compared to each other at the end.

d. High Power Microwave

Microwaves can be used at moderate power levels for communications or for radar and are composed of very small wavelengths of centimeters or millimeters. When a powerful chemical detonation is transformed through a special coil device, i.e., a flux compression generator, into a much stronger electromagnetic field, or when combining reactive chemicals or powerful batteries and capacitors are used, it produces High Power Microwave weapons (Wilson, 2006).

Also, HPM generates an intense shock of electromagnetic waves in the microwave range of frequency, which can overload electrical circuitry. The components of this electrical circuitry, such as metal-oxide semiconductors (MOS), metal semiconductor, and bipolar devices, can absorb them resulting in over-heated or melted devices (Abrams, 2003).

Therefore, an HPM weapon should be the best DE weapon among others to give some specific damage levels to an electronically equipped target systems, consisting of multiple DMPIs such as IADS, which are deployed on a feasible territory.

2. Directed Energy and High Power Microwave Weapons (HPMW)

It is possible to create some specially designed weapons out of DE types, such as HEL, CPB, NPB, and HPM, previously mentioned. The most important feature of these weapons is that they attack at the speed of light, which helps defeating theater and ballistic missiles (Schleher, 1999).

At the very basic level, the common concept of DEW is delivering a very large amount of stored energy, which potentially creates structural and incendiary damage effects on desired targets. Nevertheless, two basic problems with DEWs are “getting the projectile to successfully travel a useful distance to hit the target” and “producing useful damage effects.” HPM and HEL weapons are the most damaging DEW sources (Kopp, 2006).

The use and purpose of these described electromagnetic weapons may vary. For example, HEL weapons should probably be used against specifically targeted systems, like UAVs, since they use a very narrow laser beam. HPM weapons should be used against distributed DMPI system nodes, as in IADS, which is included in this thesis.

The interest is not only focused on single pieces of these more complicated systems (radar set, launch station, and transmitter terminal), but also on the complete end-to-end system including peripheral sensors and

support equipment needed to control the combat functions. The below advantages were identified in open-literature sources that identify possible effects that can be achieved from a HPM weapon (Valouch, 2003):

- Very fast effect on the target
- Irrespective weather conditions
- Covering various targets with minimum information about their characteristics.
- Operational attack, which causes denial of activities, neutralization, etc., against electronic assets.
- Minimum collateral damage against sensitive environment either vital or political and means of their reuse after attack.

Taking the use of HPM against multiple DMPIs into consideration, a modeling and analysis simulation effort can effectively lead investigations into the research that helps define what kind of affects can be attributed to those DMPIs. This described simulation was used to uncover some possible beneficial uses for these technologies. Representing a hypothetical e-bomb environment in such a simulation, it appeared that two methods would be the most likely candidates to pursue possible effects on a target like an IADS system: High-Altitude Electromagnetic Pulse (HEMP) and High Power Microwave (HPM).

A high altitude nuclear detonation can cause an EMP, an instantaneous, intense energy field, produced in the atmosphere that is subsequently radiated to operating target systems. At specific ranges, this pulse can overload or damage various electrical systems and microcircuits, which might be especially sensitive to power surges. HEMP is the name for the nuclear burst well above the earth's surface.

The physics basis as to why a high nuclear detonation causes an electromagnetic pulse is that the weapon burst creates gamma radiation that

causes an interaction with air molecules. This process is the ‘Compton Effect.’ Scattered electrons at high energies ionize the atmosphere, which generates a powerful electric field.

As might be expected, the generation of this electric field is highly dependent on the earth’s magnetic field, which varies significantly from position to position. Therefore, the description of the HEMP field depends not only on height above the plane of the earth, as shown in Figure 3, but also on the environment where the burst occurs. This described HEMP signal has a duration from its peak intensity to insignificant levels that is too short to harm (by Joulean heating) the human body. Nevertheless, the HEMP threat signal is a pervasive and potentially divesting transient that is much more effective than a lightning strike and can cause significant damage on operating electronic circuitry (Wilson, 2006).

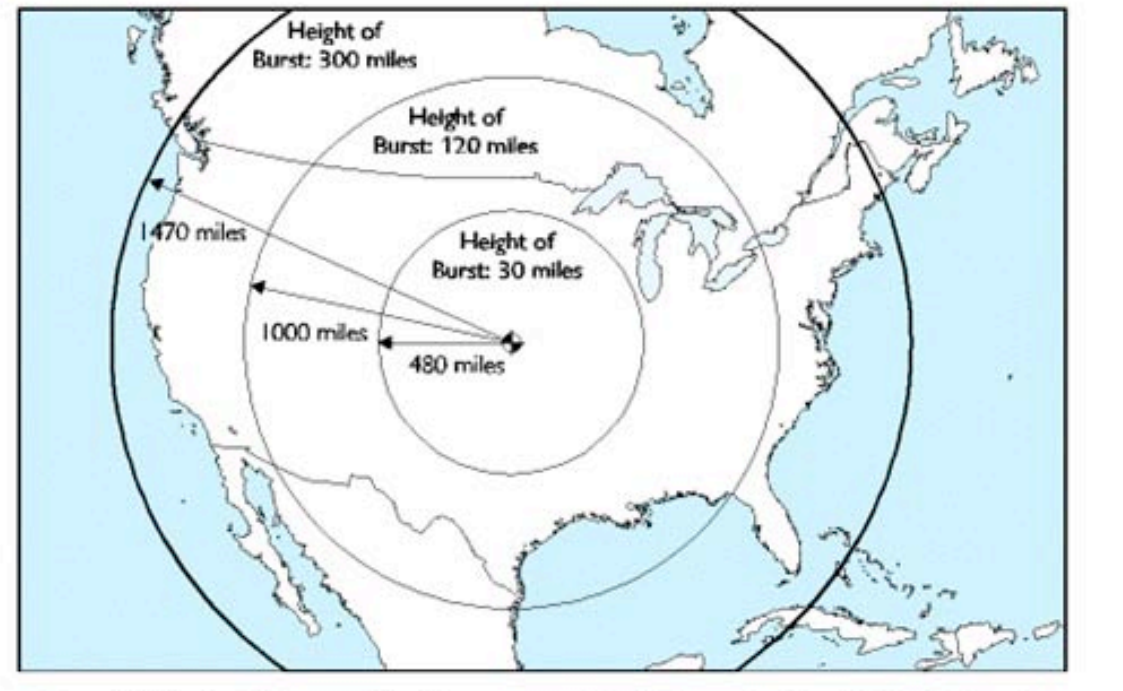

Figure 3. HEMP Affecting Area by Height of Burst (From: Wilson, 2006)

Intense energy effects, including instantaneous electromagnetic pulses, similar to those described for HEMP, are also produced by High power

microwaves. The high-power microwave instantaneous pulses can be created through using special equipments that transform powerful chemicals (by reaction or explosion) or perhaps stored battery power into intense microwaves that can cause very serious damages on electronics within a much smaller footprint than is typically described as the effective range of HEMP (see Figure 3).

HPM energy, however, has an advantage in that it can be focused using a shaped antenna, to produce intense effects within a chosen small area, in a limited distance. Higher-frequency waveforms are possible with HPM radiation, which might make it highly effective against electronic equipment, and perhaps more difficult to defend against. Additionally, HPM weapons are smaller in scale than HEMP weapons and do not require a nuclear capability (Wilson, 2006).

It is very difficult to consider a HEMP methodology, as a weapon. HEMP is too complicated to produce, requires high technology resources and expertise, involves significant effort to employ, and it is expensive to use. Therefore, researchers can instead focus on weaponeering HPM, since it is easier to produce, not as complicated, does not require extensive technology resources, and is cheaper to employ with respect to HEMP, since it can be produced using very basic electronic and physical components.

Nevertheless, there are still other things to consider on how an HPM weapon can be applied on a candidate target as an effective threat, such as the hypothetical e-bomb that is the subject of this thesis. The issues to consider for making a hypothetical e-bomb include design of the hypothetical e-bomb, its deployment methods, its power source, frequency generator, antenna design and shape.

Taking all of these into account, one must evaluate the effects of and decide on various performance parameters such as frequency selection, incident angle, created far field amplitude value and target specifications, i.e., cable diameters, ground conductivity, dielectric constant value, cable length, and cable

height above ground for best coupling purposes. All of those parameters will take the weapon research to some complicated tradeoff situations.

Using a computer program modeling and analysis designed to calculate the relevant values, both physical and performance, for the weapon can provide some major assistance in deciding how best to choose between these tradeoff options. Additionally, using a model approach, the ‘worse case’ parameter values can be identified and used as possible conditions for situations where they might apply. Significant judgment is involved in using models as described. A “worst case” modeling approach that produces orders of magnitude effects above any a reasonably expected weapon might be able to produce is of little utility. However, a “reasonable worst case” approach, such as is used in this study, can be used to address the problem above, but at the same time produce a useful and meaningful result.

After deciding on those “reasonable worst case” values, one must analyze the achieved power level results and match them with the power threshold levels of the sensitive electronic components i.e., transistors, diodes etc. in each node of the target system to determine the impact of the hypothetical high-power microwave source.

Overall, those results and comparisons can provide an idea for how best to use such a weapon against electronically equipped targets. Moreover, using such a weapon provides an opportunity for causing no blast effects and, in the focused mode provided an aimed output directed at the indicated target system, not harming humans. That means no collateral damage worries unless there is, again, an electronically equipped facility nearby with electronic systems that serve to support human critical life functions.

3. Some Directed Energy Applications

There are some examples of DEWs that are laser based and electromagnetic based. Some of these are reported, some presented, and some are theoretical.

One example is from CBS News, reported on March 25, 2003, that the U.S. Air Force hit an Iraqi satellite TV station with a kind of electromagnetic pulse device, and it caused that TV channel be out of order. By this, the US military achieved shutting down a propaganda source (CBS News, 2003).

Another example is a laser weapon. Boeing recently demonstrated its laser gun mounted on an Avenger Combat Vehicle. That gun can shoot down a small Unmanned Air Vehicle (UAV) with its laser beam (Albuquerque, 2009).

Using a focused electromagnetic beam can be a crowd control system. An example of that weapon is the 'Precision Pain,' The Humvee-mounted Active Denial System (ADS), which can strike from at least one-third of a mile away. This weapon causes a short burst of pain lasting a second or two (Shoot to Not Kill, 2003).

B. SYSTEM OF INTEREST MODEL AS A TARGET

A "system of interest" model as a potential target for an e-bomb should be an electronically equipped and distributed system, which may include nodes such as command and control systems composed of computers, electronic control systems, power generators, and cables connecting these nodes to each other.

A selected system of interest model, which will represent a reasonable IADS, is explained in this section including its nodes, features, parameters, protection features against EMP, cables and cable specifications.

1. Shielding Methods, as a Defense against HPM Weapons

As a defense or countermeasure method against electromagnetic interference, therefore, against high power microwave weapons, critical systems

typically use some form of shielding. Those shielding methods when employed as a topological shield for the system are expressed in dB values. For example, a 30 dB shielding provides 1000 times reduction on the effect of the field levels associated with electromagnetic interference.

The most reliable and robust method for a high power microwave protection can be to completely enclose all the sensitive electronic equipments wholly with an electrically conductive metal enclosure (topological shield). This enclosing metal barrier, called Faraday Cage, prevents the effect of electromagnetic field interference to the sensitive equipment (Deveci, 2007). Shielding can be expensive though, and the expense may not be based solely on the dollar costs involved. In an aircraft, for example, the addition of electromagnetic protection shields may add excessive weight to the aircraft design.

There are other effective protection techniques against high power microwave weapons that can be used. Surge protective devices, which limit (by clamping) surge voltages to safe levels work well. The utilization of fiber optic cables, which contain no conductive metal, can also reduce the effect of high power microwave weapon. High power microwave energy couples to metallic objects, and the associated energy is distributed in a system through conductive paths, so fiber optics technology basically removes the coupling method from consideration. Tactical protection methods (as simple as avoidance) can be considered as well. Some more protective techniques, whether, technical or tactical, are (Deveci, 2007):

- Shielding and filtering
- Extreme care in eliminating very small openings
- Gasketing
- Flexible metal jackets on cables
- Multi-layer shielding

- Welded structures
- Non-metallic cables (fiber optics)
- Minimization of metal fixtures and fastenings in non-metallic structures
- Narrow beam antennas with minimum side lobes
- Laser communications
- Internal optical communications
- Conductive foil over joints
- Interval system usage.

In this study, some cables in the system of interest configuration are assumed to have shielding while other cables are assumed to not have any protection against electromagnetic interference. Shielding methods of the target system will not be specified. Only the shielding value will be given in dB value.

Nevertheless, it is difficult for a system to provide 100% shielding against high power microwave weapons because cable connections between the systems nodes are always present in large numbers and these conductive paths can expose the system to electromagnetic interference. Another difficulty associated with complete topological shields is that the cables need to be connected to each other at some distances or they need to be connected to the nodes. In those connection points, possible cracks, connection failures, and worn out materials occur, which expose the cables to electromagnetic interference and penetrating the shielding. Each of these penetrations produces a potential risk to the integrity of the overall topological shield barrier.

2. Possible Target Models and Selected Model for this Study

As mentioned before, a viable target for an e-bomb could be any electronically equipped system of interest providing an important function or

operation. For example, the target system can be an IADS, a radar system, a ship or any kind of C4I system. This study will examine a representative IADS as its system of interest model.

Deciding on the design of the system of interest model as an IADS, a Patriot Missile system is taken as a reference from open sources. The selected system node types and number of the nodes are created with respect to that Patriot missile system. The patriot system node types can be seen in Figure 4. Some nodes in the system of interest model are omitted, and it is assumed that relevant nodes take on omitted node's missions. For example, only one launch station is included in the created model, although there may be more than one, as the Patriot missile system can use up to sixteen launch systems. In addition, a satellite communication system that provides the required communication between the IADS and other friendly systems, in this scenario, is included in the selected model.

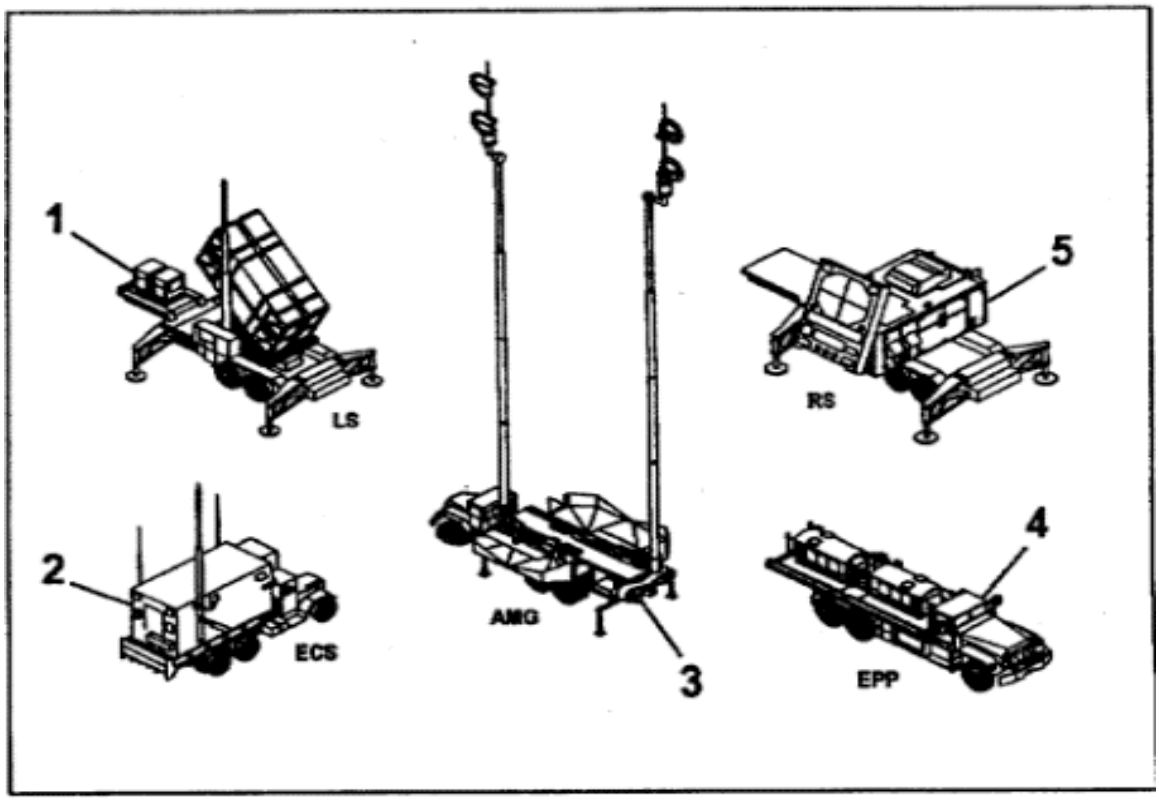

Figure 4. Patriot Missile System Configuration (Introduction to the Patriot)

> “Patriot-unique equipment at the Headquarters and Headquarters Battery (HHB) includes the information and coordination central (ICC), communications relay groups (CRGs), antenna mast groups (AMGs), trailer mounted electric power units (EPUs), and guided missile transporters (GMT). The Patriot firing battery equipment includes the AMG, radar set (RS), engagement control station (ECS), truck mounted electric power plant (EPP), and up to sixteen launching stations (LSs). Both the battalion and firing batteries are equipped with a semitrailer maintenance center.” (Patriot TMD)

Therefore, the target system for this study is a simulated realistic IADS configuration composed of six different, separated nodes. These nodes include an Engagement Command Station (ECS), Launch Station (LS), Antenna Mast Group (AMG), Satellite Communication (SAT COM), Radar Set (RS), and Electric Power Plant (EPP).

Six was an optimum number of nodes for the subject system model Including more than six nodes in the system would be more complicated and cause the study to be hard to analyze the effects of the e-bomb on each node and the cables, which make the connection between them. On the other hand, less than six nodes in the system would not be a realistic and representative model, since in this case it would not provide the required elements of an IADS. As a result, the model configuration is evaluated as a reasonably representative IADS by including six operative nodes.

The straight line sketch provided in Figure 5 shows the system nodes. It simulates each node type and shows distances between each node along with cable types and their specifications. Review of the available literature describing the typical deployed configuration of systems of this type determined the configuration for the illustrated IADS .

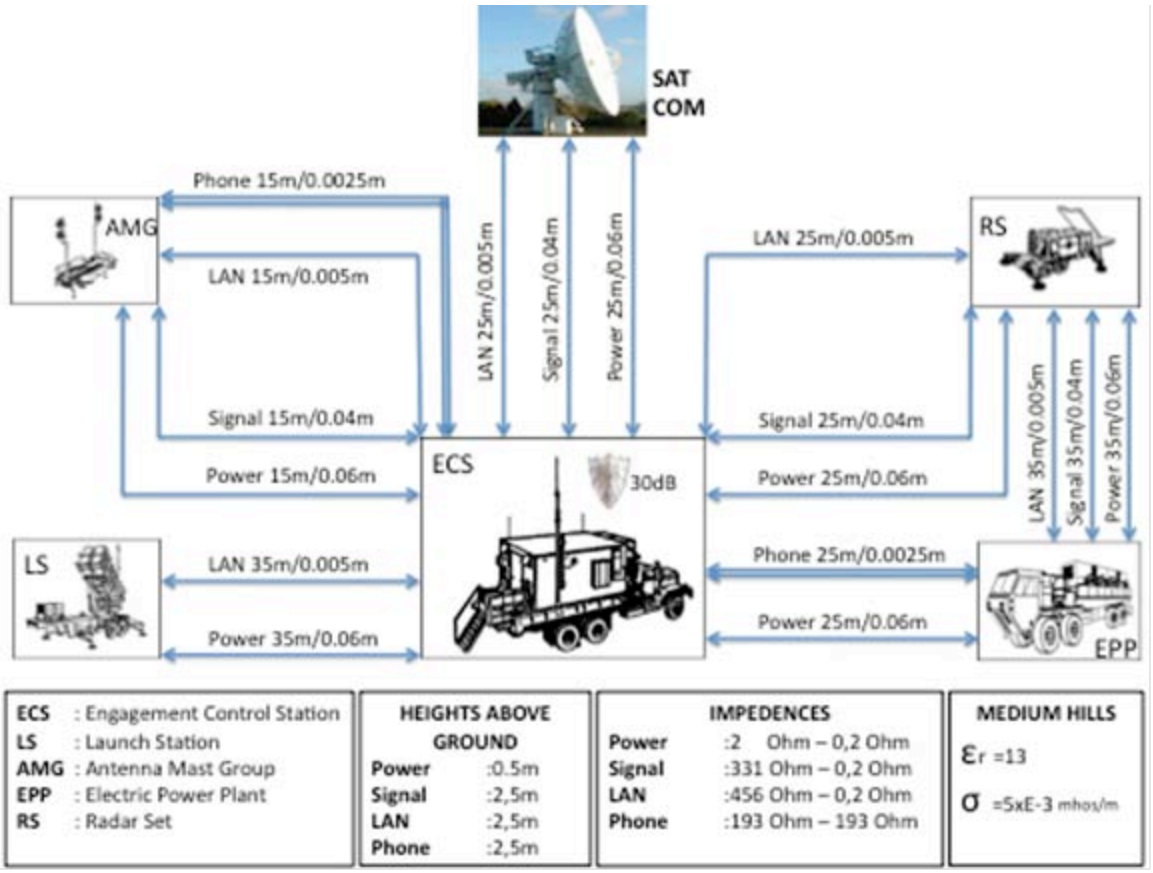

Figure 5. System of Interest Model

For instance, one of the criteria of the Patriot missile system for determining the ground/site reconnaissance or establishment for the fire control system provided by Patriot Battalion and Battery Operations manual (Headquarters Department of Army, 2002) is, “Is the fire control area 30 meters by 35 meters and less then a 10-degree slope?” Therefore, the maximum distance between elements should be 35 meters for the fire control system. Some other distances between other nodes could be less than 35 meters. Figure 6 illustrates the possible establishment configuration of the nodes and distances between them. Since the fire control system takes the major part of the IADS configuration, the same requirement criteria was deployed to the other parts of the selected system of interest model. Consequently, a representative system can be established on a 35-meter radius territory, with an engagement control system (ECS) in the center.

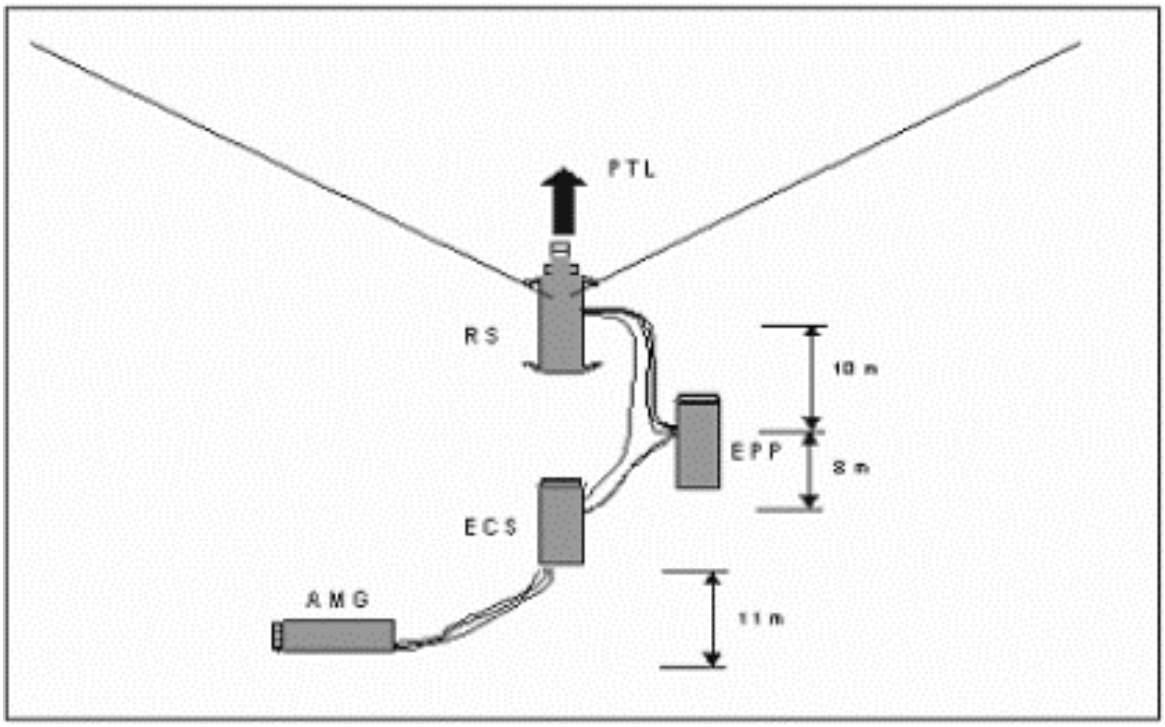

Figure 6. Configuration of the Patriot Missile Fire Control System (From: Headquarters Department of Army, 2002)

Based on this review of the literature, three reasonable distances were established between each node to cover the range of possible deployment configurations. These distances are 35 meters, 25 meters, and 15 meters. Taking possible curvatures on the longer cables into account and to be conservative, cable lengths used in the assessment model were 40 meters, 30 meters, and 15 meters. Their lengths can expected to be different depending on the establishment geometry, i.e., distances between each other, and for the overall configuration of the deployed IADS as well.

The most probable terrain for a system that uses radar should be an unobstructed field in order to provide the best antenna view. Because of that, the system of interest model should be deployed on a medium hill, and the environmental values that will establish electromagnetic coupling (i.e., dielectric constant, ε_r and the conductivity, σ) are shown in Table 1.

Terrain	Dielectric Constant, Ɛr	Conductivity, σ (mhos/m)
Pastoral Land, Medium Hills	13	5XE-5

Table 1. Dielectric Constant and Conductivity Values for IADS Target (From: Vance, 1987)

In the Patriot missile system configuration uses various cable types such as interconnection points of terminal boxes are linked to Electrical Power Plant with power cables and control cables. They are connected to the Radar system with data cable. The interfacing data link to the ECS is connected via shielded cable to protect against Electromagnetic Interference (EMI) and EMP (Patriot Battalion equipment and Organization). Collocated shelter connecting cables include RF cables, control cables, and a prime power cable. Fiber-optic cables link the ECS to the local launching stations (Headquarters Department of Army, 2002).

Based on this Patriot missile system, the system of interest model components are connected to each other with representative, appropriate types of intra-site cabling with respect to their functional purposes. Those connection types and cables are signal transmission, telephone connection, power transmission, and network connection. This study assumed that the signal and network connection cables had 30 dB shielding. The power cable was a five-wired three-phase cable that is a widely used power cable for power feed purposes. The telephone line was composed of two-wire parallel cable type in the system of interest model because of the assumption that some communications between the nodes were via a telephone network. The telephone lines in the model were a ‘two-wire parallel cable’ because they are broadly used in the industry for telephone networks. Other cable types used single pair cabling (see Figure 5).

All of those four cable types were installed to meet the mission requirements of the IADS. For example, since all included transmission and communication lines are required, each type of the cables are laid down between

ECS and AMG, while only power and phone lines are laid down between ECS and EPP, since there is no need for signal and network communications between these nodes.

The features and specifications of the target system cables vary with respect to their functional purpose. Therefore, their thicknesses and material composition differ from each other. There are various types of cable specifications depending on their purpose and their specifications. Research at the industrial product websites determined the nominal outer diameters of the cables used in the system of interest model. Relevant and average cable specifications were selected that can lead the connections, nodes, and the whole IADS to operate effectively. For example, based on that research, industrial companies provide some cable types that have a nominal outer diameter range of 0.26 inches to 0.47 inches. A basic telephone cable at home measures an outer diameter around 2.5 mm.

In addition to their extent, the height of cables above the earth's surface are established from positions reasonably close to the ground where the connections to the equipment nodes of the system are expected. The most effective coupling is most likely at these nodes. (Detailed information about this is in the 'MODELING & EM COUPLING' chapter.)

The Patriot missile system elements are composed of trucks, trailers, launchers, and tractors. Their heights from the ground to their tops range from 2 meters to 4 meters (Headquarters Department of Army, 2002). Since the cable connections to each element are expected to be at the bottom of their body and above their wheels, an average representative height is 2.5 meters except for the power cable that is 0.5 meters. It is more suitable for a power line to be at or near ground level.

Simulated system node type characteristics, i.e., trunk height above ground, launcher specifications, all played an important role in determining those specific heights. Overall, the mentioned values were discretionally based upon

the system design, geometry, and physical specification requirements. Those values determined very close to their realistic values.

Another consideration evaluating the cable selection is their impedance values. Electromagnetic energy couples to intra-site cabling and transfers energy to the equipment node configurations and locations at the left and right ends of the cable. Left and right hand impedance values are decided based upon acquiring the best coupling effect values, and again, as dependent as can be based on their realistic values as determined by a review of the literature. Summarized values of the cables associated with the cable runs shown earlier in Figure 5 can be examined in Table 2.

	LENGTH	HEIGHT	DIAMETER	ZL	ZR
POWER CABLE	40 m	0.5 m	0.06 m	2 ohms	0.2 ohms
	30 m				
	15 m				
SIGNAL CABLE	40 m	2.5 m	0.04 m	331 ohms	0.2 ohms
	30 m				
	15 m				
LAN CABLE	40 m	2.5 m	0.005 m	456 ohms	0.2 ohms
	30 m				
	15 m				
TWO PAIRS PHONE CABLE	40 m	2.5 m	0.0025 m	193 ohms	193 ohms
	30 m				
	15 m				

Table 2. Cable Values of the System of Interest Model

C. THREAT

The previously mentioned four DEW types, indicated in open literature, can each be considered as a viable threat against their relevant targets. In this study, however, which involves an e-bomb, the threat discussions will be limited to an HPM weapon. This thesis does not address the remaining threats.

1. Possible Effects on Targets

Our greatest understanding of system element susceptibilities to hostile electromagnetic threats comes from EMP work. Most electronic equipments are vulnerable to EMP effects in well-understood ways. As an example, almost all of the target equipment items include metal-oxide semiconductor (MOS) devices, which are very sensitive to exposure to high voltage transients. MOS devices can sustain permanent damage with very little coupled energy. A typical voltage in excess of tens of volts can produce a gate breakdown effect, which effectively destroys the device (Kopp, 1993).

Classifying potential e-bomb effects on targets will require a brief introduction to possible effects on electronic equipment. The following discussion introduces the possible effects, with respect to the lethality levels, which require increasing coupled power for the presentation order that follows.

a. Soft Kill

Soft kill is a temporarily disruption in the operation of the target equipment or system, caused by the weapon effect. An example is any computer system caused to reset or transition into an unrecoverable or hung state. The result is a temporary loss of operation, which can seriously compromise the operation of any critically dependent computer system (Kopp, 1996).

In this kill level, it is possible to regain the operational functions of the system by fixing it. Nevertheless, the adversary can gain important time needed to accomplish missions during this time. For example, the adversary can create a corridor for its allies if the soft killed equipment is a radar platform.

b. Hard Kill

Hard kill is a permanent electrical damage, to the target equipment or system, caused by the effect of the weapon. Hard kill necessitates either the repair, or the replacement, of the equipment or system. An example is a

computer system that has experienced damage to its power supply, peripheral interfaces and memory. These effects involve significant deterioration of operational capability and in some cases, based on severity, can render the equipment dependent upon this computer system inoperable for extended periods (Kopp, 1996).

Unlike soft kill, a hard kill level can be applied to the systems, which are the desired main point of impact, and need to be destroyed operationally. This kill level can be applied, especially, in situations where an electronically equipped target has to be hit and collateral damage avoidances are primary for the mission.

2. Delivery Systems and Deployment Methods

E-bombs can be delivered to targets in several ways by using any kind of aircraft and UAV as a platform, which are eligible for carrying desired munitions, aerial bombs such as general-purpose munitions or cruise missile. This study used a general-purpose bomb, BLU-82, in order to meet the desired requirements for coupling purposes and to select a realistic deployment configuration.

An e-bomb consists of both a microwave source and a power source. The microwave source depends on an extremely fast switching device. This could be a virtual cathode oscillator (vircator) tube. In addition, feeding the e-bomb's microwave source requires enormous power (gigawatts).In order to achieve that high power, a Flux Compression Generator (FCG) would be a good choice (Abrams, 2003).

a. The Dish Antenna

Both microwave sources and power source devices can maximize the delivered energy of the e-bomb assuming they are focused and that they can be accommodated in the packaging volume available. Another important

component to consider for the design and shape of the e-bomb is its antenna, which improves the power transfer from the microwave source out of the weapon and into air (Kopp, 1996).

Among all of the described e-bomb components, the most important part affecting the shape and size of the hypothetical e-bomb platform was the antenna. Since most conventional munitions are candidate deployment packages, and are cylindrical shaped, a dish antenna was picked for the best high-gain radiation of the e-bomb output. The diameter of the dish antenna for this study was dependent on the tradeoff issues of acquiring the best coupling purposes of the weapon along with the planned attack geometry, which will be discussed later. Desired coupling could be achieved and delivery systems are available with a cylindrical diameter of 1-meter antenna. In order to fit a 1-meter diameter antenna to a general-purpose bomb, as a platform for an e-bomb, that bomb must be slightly larger than 1 meter in diameter.

A BLU-82 bomb, which will be analyzed later, can meet this requirement since it is wide enough to accommodate a 1-meter diameter dish antenna. The antenna can be mounted at the back 1/3 section of the bomb's dome.

The focal length of the dish antenna will need to be determined for radiated output calculations, as well as other important parameters associated with the operation of a dish antenna. In order to be able to calculate the focal length of a dish antenna, one needs diameter and depth values (Determining The Focal Length of a Parabolic Dish):

$$F = \frac{D^2}{16 \times c} \tag{1}$$

where

D : Diameter of the dish antenna (m)

c : Depth of the dish antenna (m)

The depth of the dish antenna for this study was 0.25 meters, in order to meet the range of performance values commonly expected of dish antenna designs. In this case, the focal length of the dish antenna was 0.25 meters.

b. The Waveguide

A Transverse Electric, TE_{10} mode, waveguide is assumed to feed this antenna. An example of the shape of a waveguide can be seen in Figure 7. The waveguide aperture physical dimensions are (a x b), and the length 'a' of the TE_{10} waveguide, determines the cut-off frequency value, which is an important performance characteristic for deciding the best far field value. The formula used to calculate the cut-off frequency is:

$$f_c = \frac{c}{2 \times a} \tag{2}$$

where

c : speed of light (m/s)

a : waveguide Length (m)

There is only one variable included in the above formula, and it is the length, 'a,' of the waveguide. The cut-off frequency is inversely proportional to the length of the waveguide.

Frequency content below the cutoff limit controlled by the length 'a' are not supported by the feed and will not be propagated. Possible waveguides that can be used for the specified dish antenna are provided in Table 3 with their associated physical dimensions. More information about the waveguide is provided in proper places in the following sections.

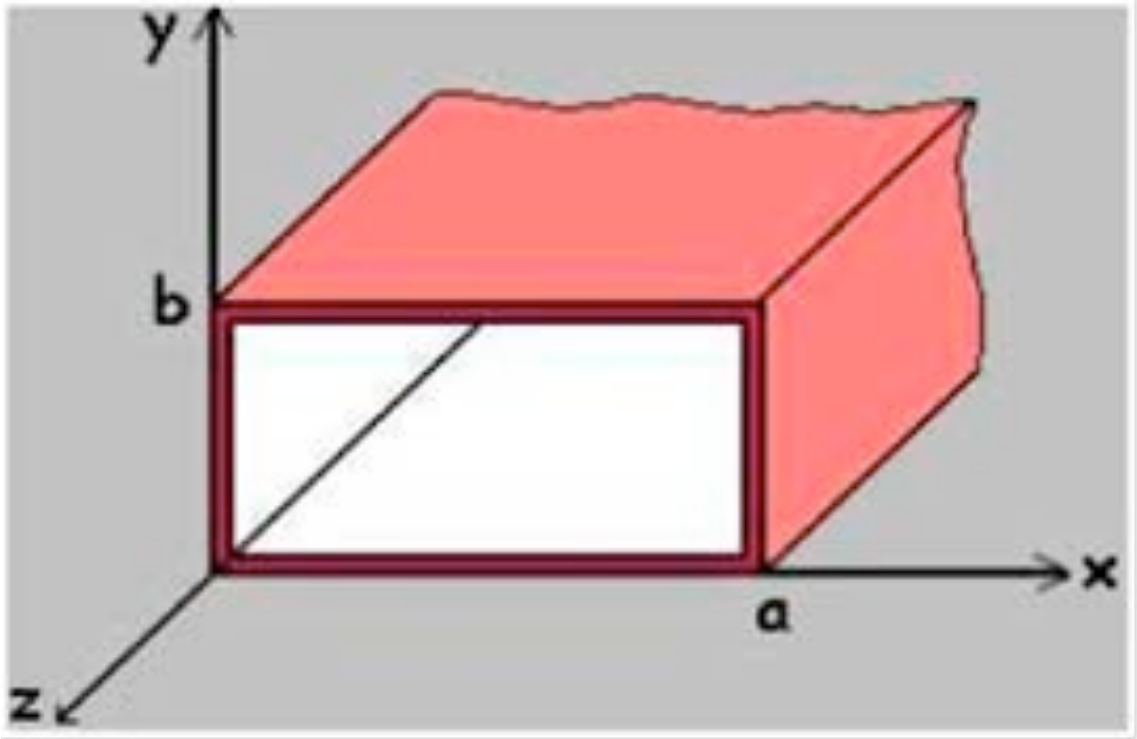

Figure 7. Waveguide Dimension (axb) (From: Ertekin, 2008).

Range	Internal	Internal	Official Designations	
GHz	(inches)	(mm. approx)	U.K. (RCSC)	U.S. (EIA)
0.41 - 0.625	18.0 x 9.0	457.0 x 229 0	WG1	WR1800
0.49 - 0 75	15.0 x 7.5	381.0 x 191.0	WG2	WR1500
0.64 - 0.96	11.5 x 5.75	292.0 x 146 0	WG3	WR1150
0.75 - 1.12	9.75 x 4.875	248.0 x 124.0	WG4	WR975
0.96 - 1.45	7.7 x 3.85	196.0 x 98.0	WG5	WR770

Table 3. Rectangular Waveguide Specifications (From: Microwave Encyclopedia, 2009)

c. The Threat

A theoretical design of an e-bomb is in Figure 8 along with identification of the principal components involved in the design and deployment platform.

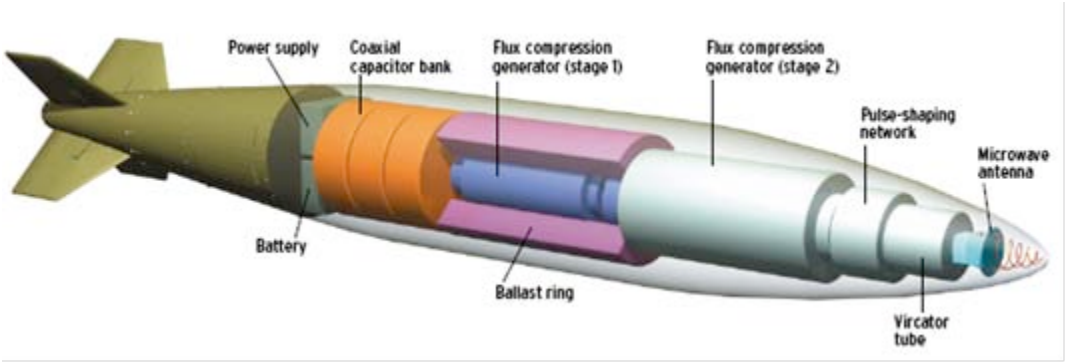

Figure 8. A Theoretical Design for an E-bomb (From: Abrams, 2003)

Since both the power generator and a desired antenna large enough for the desired effect can be very bulky, integrating them to a delivery platform can be a difficult challenge. Figure 8 depicts a commonly accepted delivery platform, i.e., general-purpose bombs, which are carried by most regular aircraft under their fuselage or wings. Some weapons' designs may require large platforms that can accommodate the e-bomb components, which would restrict the delivery system to specific aircraft. Since, the diameter of the dish antenna was decided as 1 meter, based on desired performance, therefore, the width of the bomb must be larger than 1 meter. Because of those requirements, the e-bomb is assumed to be integrated in BLU-82 bomb since that bomb's width is larger than 1 meter and its specifications are suitable for carrying such an e-bomb. The specifications of the BLU-82 Bomb can be seen in Table 4, and a picture of the system is provided in Figure 9.

NAME	DIAMETER	LENGTH	CARRIER
BLU-82	54"/1.37 m	141"/3.58 m	C-130

Table 4. BLU-82 Bomb Specifications (From: BLU-82 Commando Vault, 2009)

Normally, a BLU-82 bomb is an unguided system, and it uses a parachute, which provides a slow glide, facing the dome of the bomb towards the ground, and its parachute is opened after the bomb is dropped off the host aircraft.

Figure 9. BLU-82 Bomb (Defencetalk)

Even though BLU-82 is an unguided system, in this study, it is assumed that an appropriate kit is attached to BLU-82. This makes it a Precision Guided Munition (PGM) that replaces the parachute equipment. The weapon is dropped at a feasible altitude, high enough for the dome of the bomb to turn and face towards the ground, which leads to a 90 degree attack angle postulated for this delivery scenario. With this ability, the bomb will be able to detonate using a fuse at a desired altitude right above the target and at a height selected to ensure full coverage for the entire distributed target at levels that are within 3 dB of the

peak output of the device. A basic geometry is in Figure 10 and the ground footprint is conceptually within the 3 dB beamwidth of the dish antenna.

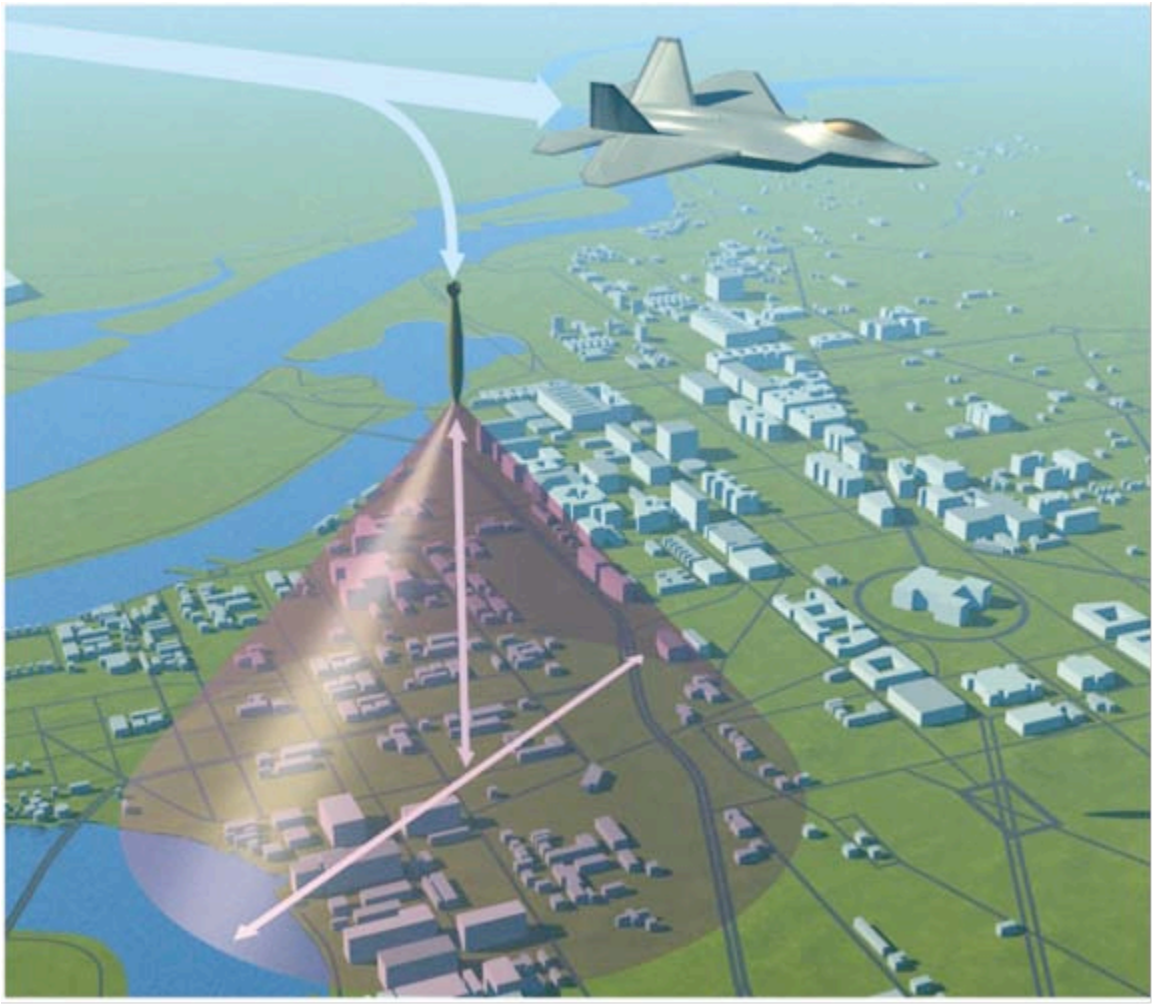

Figure 10. Detonation Altitude and Coverage Area (From: Abrams, 2003)

D. GEOMETRY OF THE ATTACK

In order to establish the attack geometry for the model of the IADS target and the engagement scenario, some parameter values such as frequency selection, and therefore wavelength, antenna diameter, beamwidth angle, had to be calculated based on an assumed target field extent. All of those parameter

values led to tradeoffs in the coupling model. For each competing parameter, the best and the most realistic attack geometry was chosen to meet desired coupling effects.

Among the desired input parameters, only the target field radius of 35 meters is certain because it best represents the maximum extent for a deployed IADS model. All other parameters had to be calculated with appropriate formulas provided in the material that follows. Figure 11 provides the attack geometry view of the e-bomb in this study.

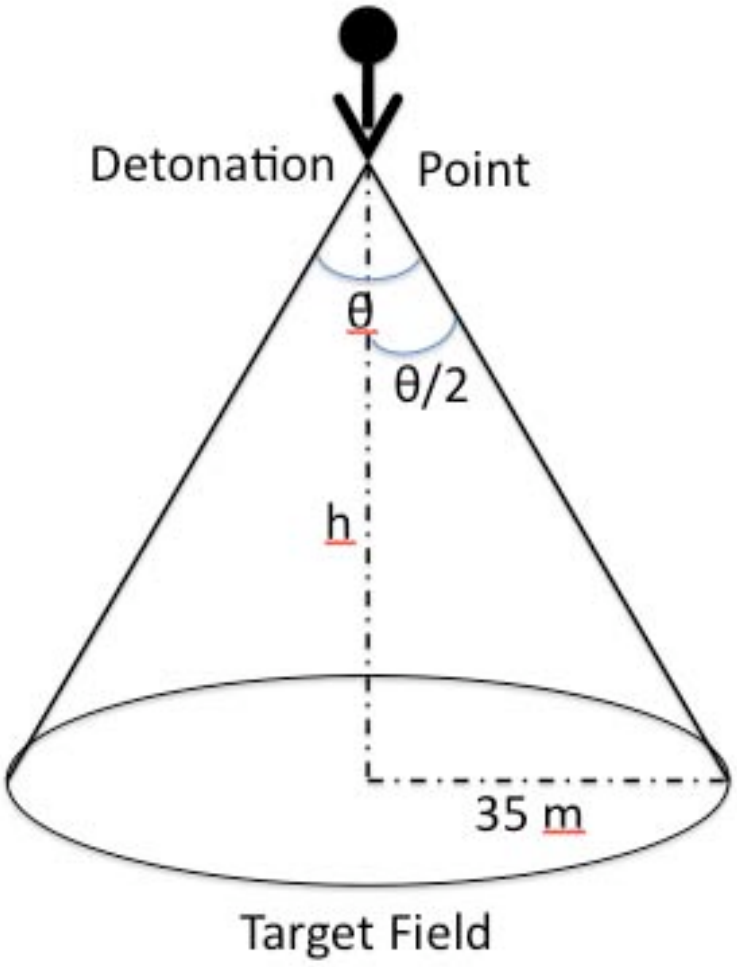

Figure 11. The Attack Geometry

In order to select the performance spectrum of the e-bomb, required resolution of the fundamental dilemma that an e-bomb does not exist, so its spectral content is unknowable. The frequency band for the hypothetical e-bomb in this study adopts a 'Double Exponential E-Field Spectrum,' associated with an unclassified representation of HEMP. This selection is a low-risk approach that relies on a known and modeled hostile electromagnetic waveshape. Detailed information about the unclassified HEMP threat waveshape that has been used can be found in Appendix.

The EMP threat described has significant content at low frequencies (1 to 100 MHz) and does not decay to insignificant levels until well above 1 GHz. At the low end, the e-bomb frequency band was established by the maximum extent of the delivery system and was determined by calculating the cutoff frequency for the feed waveguide. At wavelengths longer than the feed waveguide (i.e., lower in frequency), there will be no propagated field in the guide. The cutoff frequency value is inversely proportional to the length of the selected waveguide length, (a), and it can be calculated by equation 2

In fact, since the frequency band adopts a 'Double Exponential E-Field Spectrum' in this study, the lower frequencies are useful for the e-bomb effect on the target, and it is desired for the best coupling purposes for such an e-bomb design. In the double exponential E-Field spectrum, as shown in Figure 12, lower frequencies correspond to higher E-Field values, which provides more coupling effects on the target field.

Nevertheless, the specifications of the e-bomb are limited to feed longer lengths of the waveguide. This limitation withholds the use of major part of the E-Field amplitude. Therefore, a reasonable waveguide, which provides the less cut-off frequency, was chosen as feasible for the specifications of the e-bomb to feed this waveguide. Because of that, WR1150 type is the best-fit design waveguide for the e-bomb. The specifications of WR1150 waveguide are shown in Table 3.

With respect to the length of WR1150 waveguide, the cut-off frequency of the e-bomb is calculated as 510MHz, and this is used in the other calculations of the study.

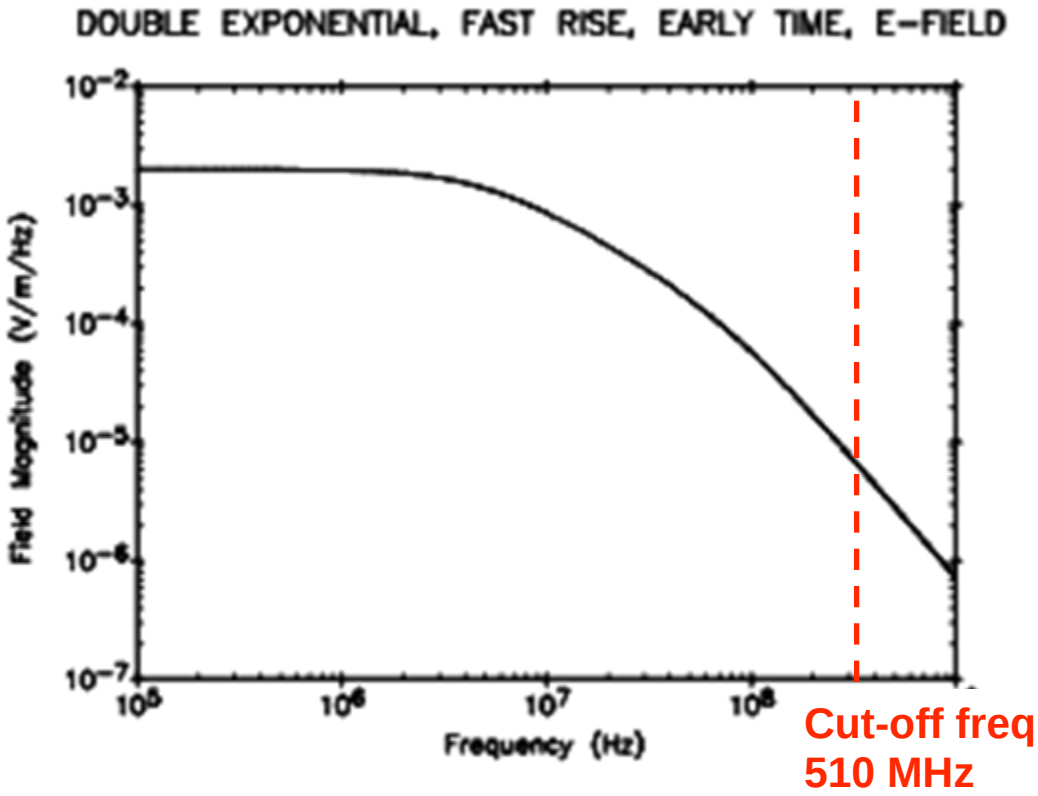

Figure 12. Double Exponential Pulse Spectrum

The main objective of the attack geometry shown in Figure 11 is to calculate the detonation altitude (h). Since the target extent radius is known (35 meters), the 3 dB beamwidth (θ) angle associated with the dish antenna has to be known in order to be able to calculate the detonation altitude.

A rule of thumb formula to calculate a dish antenna 3dB beamwidth angle is shown in equation 3:

$$\theta = 70 \times \frac{\lambda}{D} \tag{3}$$

where

θ : 3dB Beamwidth Angle (degrees)

λ : Wavelength (m)

D : Dish Antenna Diameter (m)

For such a situation, that angle is expected to be very small for a dish antenna. Dividing (θ) by two so that the geometry of the attack scenario can be determined, does not make a big difference for computing the tangent value of (θ). For this particular case, in order to be more precise in values, equation 3 can be written with respect to (θ) angle, as:

$$\frac{\theta}{2} = 35 \times \frac{\lambda}{D} \tag{4}$$

Since,

$$c = 3 \times 10^8 \tag{5}$$

and

$$\lambda = \frac{c}{f} \tag{6}$$

Equation 3 can be modified as:

$$\frac{\theta}{2} = \frac{105 \times 10^8}{f \times D} \tag{7}$$

After calculating that angle, the detonation altitude can be calculated by using the tangent rule. Here, in this formula, the diameter of the dish antenna (D) is known. It is 1 meter. However, the frequency (f) can be any value among the

frequency bandwidth that the radiated system supports. Therefore, the selected frequencies have the main effect on the 3dB beamwidth angle and consequently on the detonation altitude. The tangent formula to calculate the detonation altitude for this particular case is:

$$h = \frac{35}{Tan\left[\frac{\theta}{2}\right]} \tag{8}$$

Out of all those formulas, it can easily be understood that the higher the frequency, the higher the detonation altitude is needed. However, a high altitude is not desired the far E-Field amplitude on the target. The far E-Field amplitude is inversely proportional to the distance (altitude in this case). Therefore, from an attack engagement, the minimum height possible to illuminate the entire target object is needed. And again, the lowest altitude is limited by the cut-off frequency. Figure 13 outlines the altitude and frequency relations used in this study.

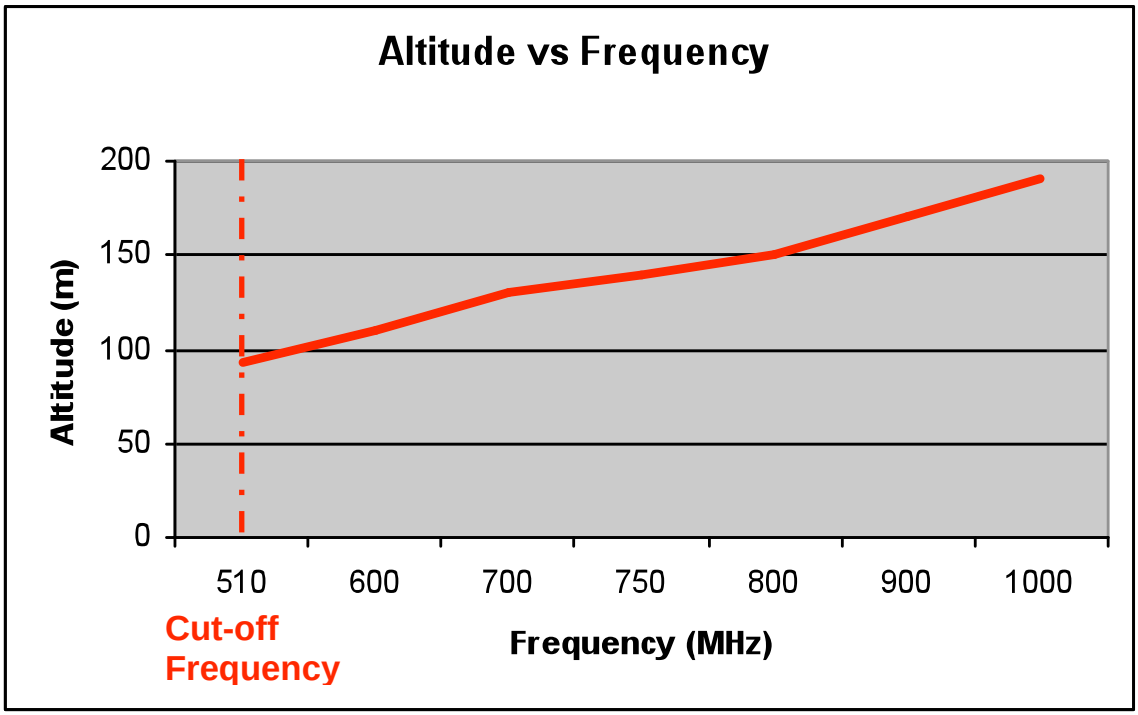

Figure 13. Altitude vs. Frequency Outline

THIS PAGE INTENTIONALLY LEFT BLANK

III. MODELING & ELECTROMAGNETIC COUPLING

A. COUPLING METHODS

The main effect of the electromagnetic field produced by an e-bomb is coupling with interconnecting lines and cables that integrate all the nodes into a system. The model that represents an IADS stimulates voltages and currents created by the electromagnetic field environment. There are many studies that attempt to find computing methods for describing these voltages and currents. The goal of those studies is either to analyze system susceptibility thresholds or to find the most robust method for reducing effects of the coupled electromagnetic field (Ianoz, 2008).

The effect of an incident electromagnetic field on an electronically equipped device within the target may be defined in terms of the coupling to that device and its microwave threshold of disturbance (e.g., stimulus that causes a change of state). For any kind of EMP or e-bomb weapon, the microwave power or stress applied to the device can be calculated by means of the coupling through a reasonable representation of system topology. The disturbance threshold of the device provides an indication of the strength of the device against the microwaves without changing state. After measuring coupling and disturbance thresholds, one can better calculate the threshold of disturbance for the device for system exposure to the weapon. The system susceptibility and the probability of effect, such as upset or damage, can be estimated with probabilistic models for stress (the level of coupled field) and strength (the effect that field causes) (Zacharias, 1992).

The Defense Nuclear Agency (DNA) has previously published a useful threshold level chart, shown in Figure 14, for various kinds of electronic components. The bars on this figure represent the possible damage occurrences on the device when exposed to corresponding power levels. This chart was created from experimental results of damage occurrences from injection testing

(numerous trials) with standard waveforms. As depicted in the chart, power levels corresponding to the bars for each device can lead that device to serious damage results. In this particular case, the goal of an EMP weapon or e-bomb should be achieving those threshold levels as possible as it can. More information about this issue can be found in Chapter V, Damage Assessment.

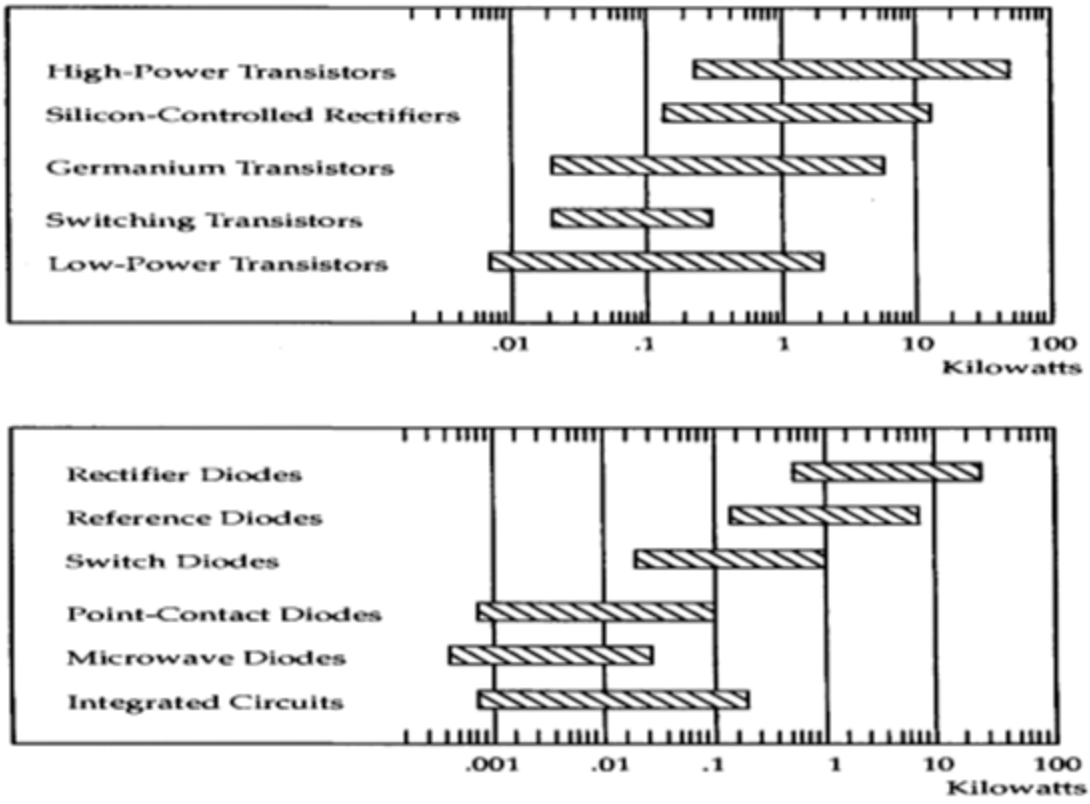

Figure 14. Damage Threshold Power Range of Representative Electronic Components (From: DNA, 1986)

When an illuminating electromagnetic field induces current and voltages in the operating system electronic circuits at levels that are comparable to the normal operating signals, a temporary malfunction can possibly occur and when these induced stresses are at higher levels, those stresses can possibly produce joulian heating to the extent that permanent damage can occur (Ertekin, 2008).

It is known, and has been demonstrated, through many system-level tests that an EMP explosion will result a high voltage electrical spike propagating

along the exposed conductive cables. If the high voltage is sufficiently intense, it can produce breakdown effects on semiconductors. Moreover, if its intensity is high enough, then it can produce thermal damage effects on conductive materials. The proportion of the delivered power, which is coupled to target, can measure the coupling efficiency. This proportion may be expected to vary significantly due to difference in wiring geometry and shielding performance (Kopp, 1996).

Two fundamental coupling methods found in open literature are:

- Front Door Coupling
- Back Door Coupling

Only the Back Door Coupling will be covered in this study since it has some types of cables that are connecting the nodes to each other. Back door coupling is generally an unexpected disturbance while front door coupling (such as the in-band reception on an HF receiver) generally has amplitude and content that are within the system design parameters.

1. Front Door Coupling

> Front door denotes coupling through intentional receptors for electromagnetic energy such as antennas and sensors; power flows through transmission lines designed for that purpose and terminates in a detector or receiver. (Benford, Swegle and Schamiloglu, 2007)

This method does not apply to this study since the e-bomb created E-Field is not aimed at any antennas or sensors on the target system (See Figure 15). Therefore, the coupling method in this study cannot be associated with front door coupling method. In addition, other technical considerations might be needed in order to couple an EMP to an antenna or sensor.

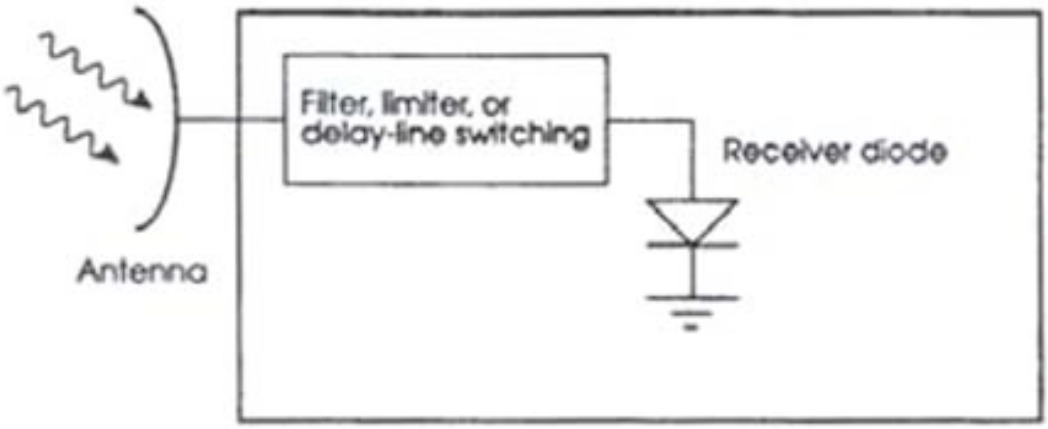

Figure 15. Front Door Coupling (From: Pace, 2007)

2. Back Door Coupling

Backdoor denotes coupling through apertures intended for other purposes or incidental to the construction of the target system. Backdoor coupling paths include seams, cracks, hatches, access panels, windows, doors, and unshielded or improperly shielded wires. (Benford, Swegle and Schamiloglu, 2007)

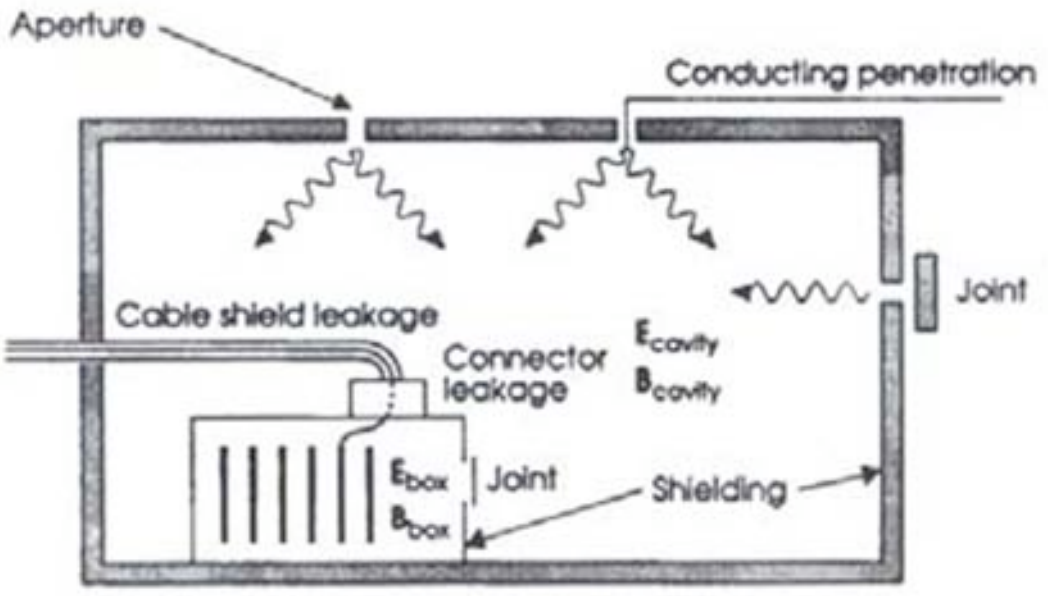

Figure 16. Back Door Coupling (From: Pace, 2007)

The backdoor coupling method is more feasible for the e-bomb scenario since the EMP is direct or via some apertures exposing the wires at the potential target system (See Figure 16). Because, the wiring and electronic equipments are vulnerable to electromagnetic interference and electromagnetic pulse effects, especially when they are not shielded against them, this method is the best fit and will be used in this study.

B. MODEL COUPLING RESULTS AND EVALUATIONS

The CEMPAT transmission-line coupling calculation program is used in this study for determining the best data,determining the roles that specific parameters have on the coupling event, and for calculating the induced voltages and currents on the cables of the system using those best values. Detailed information about the principles used in the CEMPAT analysis program can be found in Appendix.

The data that are user-entered into the CEMPAT program to calculate the induced voltages and currents on the cables are:

- Cable diameter,
- Cable length,
- Cable height above the ground,
- Incident angle,
- Driving field function : Double exponential pulse,
- Loading : Impedance values,
- Driving field : High altitude, overhead
- Soil conditions on the target field : Dielectric constant and finite ground conductivity,
- Observation point : Measurement point, which is always at the target nodes.

Each of those data affecting the electromagnetic coupling to the system cables are candidates for producing coupling data. For this wide domain of possible parameter values, some suitable values were needed and variation analysis of each data parameters was evaluated using the CEMPAT program to find the best value for each data. Best, in this case, means determining the one parameter value that helps optimizing coupling results to their highest possible values.

In order to perform this variation of parameters investigation, some reasonable data parameters were first picked based on either best practice or general familiarity with expected coupling levels and a 'Base Cable Configuration' created for reference. Those data parameters can be seen in Table 5.

PARAMETER	Length	Height	Diameter	E-Field	Incident Angle (Θ)	Ground Cond (σg)	Dielectric Const (εr)	ZL	ZR
VALUE	30 m	0.1 m	0.1 cm	5 kV/m	90°	1.0E-02	10	318 Ω	318 Ω

Table 5. Base Cable Configuration Data Parameters

After establishing the base configuration, the CEMPAT program was run for moderate variations of other excluding parameter values to test each variation response for the best resulting coupled current. (Basic configuration data parameters were tested by exchanging them one-by-one with other parameters and judging the effect on the resulting current). Independent parameter variation effects were assumed throughout this evaluation to simplify the analysis (i.e., the data were varied one at a time, but not more).

The transmission line medium and the base cable configuration can be seen in Figure 17. The transmission line is exposed to the E threat, created by the e-bomb, with a 90 degrees incident angle (Θ). In addition, it has a height above earth ground composed of conductivity (σ) and dielectric constant (ε). Matched impedance values are used at grounded both ends based upon the

cable height and diameter. The coupling measurement is observed by the CEMPAT program at the right end of the transmission line, indicated with an arrow.

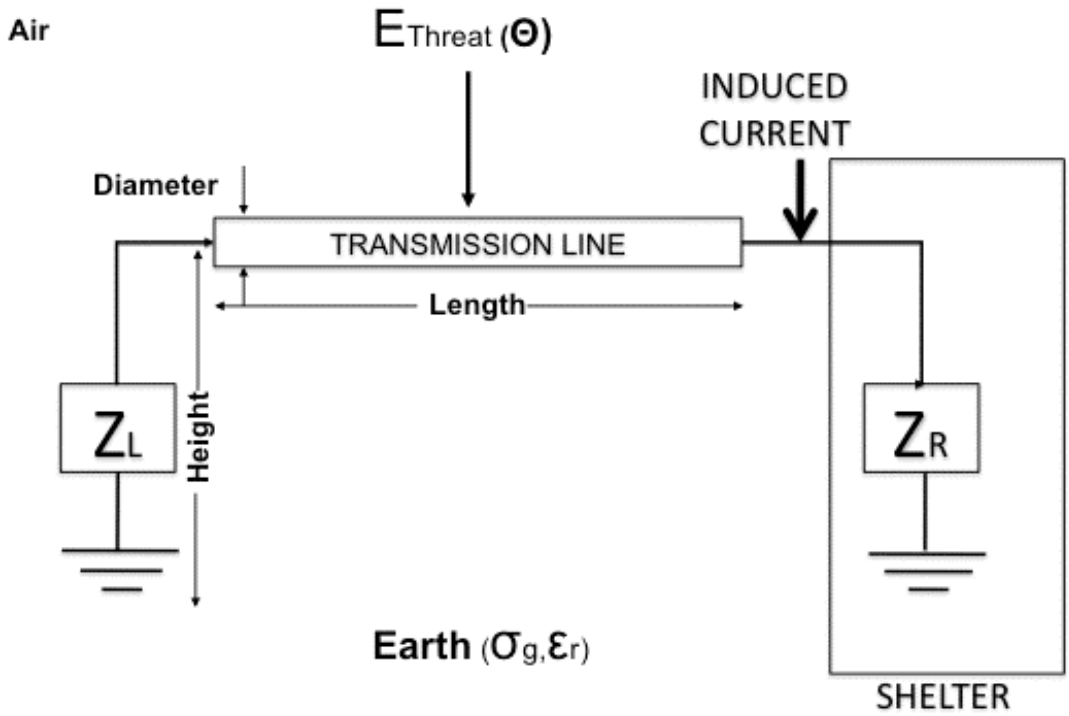

Figure 17. Transmission Line Configuration

Outputs of the baseline parameter values out of CEMPAT program run can be seen in Table 6 and the parameters used are scalars representing response features of the coupled current. The scalars used in Table 6 are called waveform norm attributes and are briefly described in material that follows and further described in the Appendix.

PAA (Amps)	PAD (Amps/Sec)	PAI (AmpsxSec)	RI (AmpsxSec)	RAI (Ampsx√Sec)
2.51E+01	6.10E+08	4.06E-06	7.32E-06	8.64E-03

Table 6. Outputs of the baseline parameter values

Following the baseline parameters run, the CEMPAT program was run for each slightly modified baseline configuration, and results tables, for each run, were created consisting of those model outputs results. All unvaried outputs on the table were matched to the baseline configuration, and the best (highest) resulting coupled current value was picked to be used on the real run with the IADS topological model. The CEMPAT program outputs, i.e., threat electric field, coupled voltages & currents, are available as ASCII text files in time, frequency and in impulse-function formatted outputs. A time domain representation example for the ground-interacted electric field LAN cable current response is shown in Figure 18.

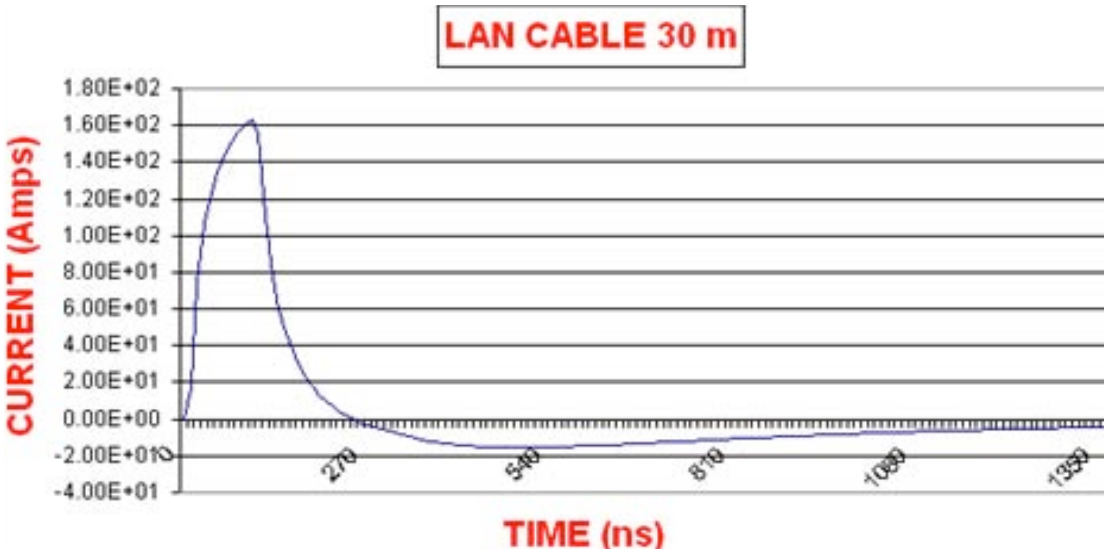

Figure 18. Time Response Plot of Far E-Field Coupling to a Cable

Detailed information about the CEMPAT program outputs related to coupling can be found in Appendix. They are briefly described here:

PAA : Peak Absolute Amplitude, indicates the size of the response

PAD : Peak Absolute Derivative, indicates the variation in the response

PAI : Peak Absolute Impulse, indicates the absolute value of the content (area under the curve) of the response

RI : Rectified Impulse, indicates the value of the rectified area under the curve of the response

RAI : Root Action Integral, indicates the square root of the normalized energy of the response.

As can be analyzed on the time response plot shown in Figure 18, peaks and absolute values of under-curve integration are the most beneficial waveform metrics for comparing the responses and determining best coupling purposes. These two scalars provide information related to the size of the coupled signal and its energy content. They are both directly related to the potential for upset or damage that might be caused. The higher those values, the more coupling effect can be expected to be achieved for a specific cable and node termination configuration. Since they best describe the important effects, all output plots for current responses in this report will only use the Peak Absolute Amplitude (PAA) and Root Action Integral (RAI) scalars to capture the major coupling assessment results of interest in this study.

Each data parameter determination table that follows will identify the difference in response norm attributes between the run outputs with respect to the range of parameter values considered reasonable. By this, the ratio of variation difference vs. output results can be examined, as can be depicted through these response scalars. The largest responder is identified and shown as a Highlighted row entry in each table.

1. Cable Diameter Determination

CABLE DIAMETER (centimeters)	PAA (Amps)	PAD (Amps/Sec)	PAI (AmpsxSec)	RI (AmpsxSec)	RAI (Ampsx√Sec)
4	2.96E+01	7.18E+08	4.38E-06	7.95E-06	1.03E-02
2	2.91E+01	7.08E+08	4.22E-06	7.64E-06	9.90E-03
0.6	2.78E+01	6.72E+08	4.15E-06	7.50E-06	9.33E-03
0.1	**2.51E+01**	**6.10E+08**	**4.06E-06**	**7.32E-06**	**8.64E-03**

Table 7. Cable Diameter Determination Test Results.

From the data shown in Table 7, it is clear that as the cable diameter increases, the response scalars indicate that higher PAA and RAI values are to be expected. This finding led to a decision to use the largest possible diameter cable that could be found from a literature search of a fielded system cables for each type (power, signal, LAN) of cable to ensure that is supporting the largest response a possible upper bound conditions.

2. Cable Length Determination

CABLE LENGTH (meters)	PAA (Amps)	PAD (Amps/Sec)	PAI (AmpsxSec)	RI (AmpsxSec)	RAI (Ampsx√Sec)
70	2.71E+01	4.81E+08	8.38E-06	1.55E-05	1.43E-02
45	2.71E+01	4.51E+08	5.84E-06	1.07E-05	1.12E-02
30	**2.51E+01**	**6.10E+08**	**4.06E-06**	**7.32E-06**	**8.64E-03**
15	2.01E+01	6.67E+08	2.11E-06	3.62E-06	5.25E-03

Table 8. Cable Length Determination Test Results

From the data shown in Table 8, as the cable length increases, the current response metrics indicate a higher PAA and RAI value. Nevertheless, there is an exception to that direct proportionality relation. After a specific length is achieved, the PAA value does not increase further. This is a known physical relationship for true cable coupling that is called the integration length of the cable. The peak value of the cable is expected to increase with increasing length up to the integration length. As Table 8 indicates, the integration length for this cable is just about 45 meters. For lengths exceeding 45 meters, the PAA value does not increase any further. From an analysis and modeling perspective, these data indicate that the target system cabling needs to be no longer than 45 meters.

3. Cable Height above the Ground Determination

HEIGHT (meters)	PAA (Amps)	PAD (Amps/Sec)	PAI (AmpsxSec)	RI (AmpsxSec)	RAI (Ampsx√Sec)
1	3.19E+01	1.04E+09	4.58E-06	8.36E-06	1.04E-02
0.5	2.82E+01	7.48E+08	4.28E-06	7.76E-06	9.36E-03
0.1	**2.51E+01**	**6.10E+08**	**4.06E-06**	**7.32E-06**	**8.64E-03**

Table 9. Height Above the Ground Determination Test Results

From the data shown in Table 9, as the height above the ground increases, the response of the CEMPAT program indicates that higher PAA and RAI values will result. As described before, a representative height decision for each cable of the system depends on the target nodes characteristics like their height above the ground along with the shape and configuration of a specific node.

One possible reason for low peak values at very low cabling heights is that coupling relates to the total field near an imperfect ground. As is well known, the electric field at the plane of the ground must be zero, so reduced coupling at lower heights is expected. A cable positioned too close to the ground would be unlikely to couple large surface currents for large distances. This is why cables are buried in survivable communications configurations.

4. Incident Angle Determination

INCIDENT ANGLE	PAA (Amps)	PAD (Amps/Sec)	PAI (AmpsxSec)	RI (AmpsxSec)	RAI (Ampsx√Sec)
90°	**2.51E+01**	**6.10E+08**	**4.06E-06**	**7.32E-06**	**8.64E-03**
70°	2.55E+01	6.42E+08	3.83E-06	6.89E-06	8.33E-03
60°	2.59E+01	6.84E+08	3.54E-06	6.38E-06	7.92E-03
50°	2.54E+01	7.42E+08	3.14E-06	5.67E-06	7.31E-03
30°	2.28E+01	8.79E+08	2.07E-06	3.74E-06	5.33E-03
20°	1.86E+01	8.60E+08	1.43E-06	2.58E-06	3.86E-03

Table 10. Incident Angle Determination Test Results

The data in Table 10 identifies the response characteristics of the baseline cable as the angle of incidence for the horizontally polarized threat field changes. The indicated angle is relative to the cable run, or the elevation angle. The largest PAA response of the CEMPAT program to the incident angle determination is centered around 60 degrees (60 +/- 10). There is a significant drop below 30 degrees. Even though the PAA value is reducing somewhat above 60 degrees, it is a slight reduction and so is not expected to make a major difference between 60 and 90 degrees.

On the other hand, examining the RAI value, it has the same response with PAA at less than 30 degrees while it keeps increasing above 60 degrees.

However, 90 degrees, which is a broadside incident, is picked out of the incident angle determination test since decided threat model and the bomb drop altitude requires it to be so from a practical perspective. Nevertheless, it is obvious that there is no big loss by using a 90-degree incident angle vice 60 degrees.

5. Load Determination

LOAD (Ω) (Z_{Left} & Z_{Right})	PAA (Amps)	PAD (Amps/Sec)	PAI (AmpsxSec)	RI (AmpsxSec)	RAI (Ampsx√Sec)
318&SHORT	4.27E+01	1.06E+09	7.43E-06	1.32E-05	1.48E-02
OPEN&SHORT	4.70E+01	1.32E+09	4.30E-06	6.01E-05	3.68E-02
0.2&SHORT	4.09E+01	1.06E+09	5.05E-05	5.05E-05	3.32E-02
318&318	**2.51E+01**	**6.10E+08**	**4.06E-06**	**7.32E-06**	**8.64E-03**

Table 11. Loading Determination Test Results

Table 11 indicates the results obtained when loading the basis cable with a variety of different termination configurations. The largest current result for the transmission line and loading came out of the one end short-circuited configuration. It is likely that the other end of the cable is loaded with the cable characteristic impedance for normal cases as it is used to connect to terminal equipment. According to those results, signal cable and LAN cables are modeled to issue the characteristic impedance (matched) on the left side and the right hand is a very low impedance (0.2 ohms). For power cabling, it is more likely expected to be not a characteristic impedance but a low impedance value to ensure good grounding and current returns. Therefore, 2 ohms arbitrarily picked for its left-hand side load. Finally, for the telephone line it was decided to be a two-wire line (parallel wire) cable and to establish matched impedance for both ends, just as it would be expected to be configured in the real conditions.

The general formulas to calculate the characteristic impedances of the LAN and signal line cabling can be found from the common-mode cable impedance shown in equation 9

$$Z_0 = 60ln\left(\frac{2h}{a}\right) \quad (9)$$

where

h : Height above the ground

a : Radius of the cable thickness

And for the two wire balanced telephone cable in equation 10 (Inan and Inan, 2000).

$$Z_0 = 120 \times ln\left(\frac{d}{2\times a} + \sqrt{\left(\frac{d}{2\times a}\right)^2 - 1}\right) \quad (10)$$

where

d : Distance between cables

a : Radius of the cable thickness

The LAN cable, signal cable, and telephone cable characteristic impedances as calculated with the corresponding formulas identified above are: 456 ohms, 331 ohms, and 193 ohms, respectively. Each of these impedance values was analytically confirmed (at least approximately) by establishing a model of each cable type and forming Thevenin impedance from a ratio of the open-circuited voltage to the short-circuited current (the average of the ratio was the Thevenin impedance).

The reason that the cable impedances are composed of only resistance is because reactance configured on these loads, although attempted, had no effect on the PAA and RAI values. The results out of the CEMPAT program regarding the capacitance trials, can be seen in Table 12.

CAPACITANCE	PAA (Amps)	PAD (Amps/Sec)	PAI (AmpsxSec)	RI (AmpsxSec)	RAI (Ampsx√Sec)
100 µF	4.04E+02	1.06E+10	5.11E-04	5.12E-04	3.30E-01
100 nF	4.04E+02	1.06E+10	5.11E-04	5.12E-04	3.30E-01
100 pF	4.04E+02	1.06E+10	5.11E-04	5.12E-04	3.30E-01

Table 12. Capacitance Determinations

6. Soil Conditions on the Target Field: Dielectric Constant and Finite Ground Conductivity Determination

Since the system of interest model was designed for deployment on a medium hill to represent the expected IADS field configuration, the dielectric constant and the finite ground conductivity effects on coupled currents were evaluated using the values depicted in Table 1. For study purposes and examining their effects on coupling, the CEMPAT program was run over a reasonable range of possible values to determine the impact on resulting stress.

DIELECTRIC CONSTANT	PAA (Amps)	PAD (Amps/Sec)	PAI (AmpsxSec)	RI (AmpsxSec)	RAI (Ampsx√Sec)
15	2.49E+01	5.63E+08	4.06E-06	7.31E-06	8.61E-03
10	**2.51E+01**	**6.10E+08**	**4.06E-06**	**7.32E-06**	**8.64E-03**
5	2.53E+01	6.60E+08	4.06E-06	7.32E-06	8.68E-03

Table 13. Dielectric Constant Determination Test Results

As can be seen in Table 13, there is not a major difference between the values for both PAA and RAI. They are almost identical to each other. However, the analysis results show that the PAA and RAI values are inversely proportional to tested dielectric constant values (i.e., the largest current amplitude results from the smallest dielectric constant).

FINITE GROUND CONDUCTIVITY	PAA (Amps)	PAD (Amps/Sec)	PAI (AmpsxSec)	RI (AmpsxSec)	RAI (Ampsx√Sec)
1	4.00E+00	1.91E+08	4.94E-07	9.06E-07	1.25E-03
1.E-02	**2.51E+01**	**6.10E+08**	**4.06E-06**	**7.32E-06**	**8.64E-03**
1.E-05	5.36E+01	5.32E+08	2.29E-05	2.83E-05	2.83E-02

Table 14. Finite Ground Conductivity Determination Test Results

Table 14 shows that the PAA and RAI values are inversely proportional with analyzed finite ground conductivity values as well. The CEMPAT program was run for three dielectric constant values, each one is a thousand times bigger than the previous one, and the output results show that the more conductive the ground, the more shorting out of the threat magnetic field is to be expected.

7. Driving Field Function and Driving Field

The double-exponential pulse used in the CEMPAT program is shown in equation 11, which follows. The user-selectable α and β values are chosen to replicate the temporal and spectral content of an unclassified representation of HEMP (See Appendix) and as was discussed earlier in this report, the amplitude for the e-bomb was determined by analysis. A HEMP waveform was selected as a representative "reasonable worst-case" condition that would represent an e-bomb. The amplitude, however, was scaled to best represent the expected e-bomb outputs under the conditions of the attack scenario previously shown in Figure 11. To derive the e-bomb field amplitude a previously developed NPS student MATLAB program (Ertekin, 2008) was used which calculates far-field electric field as a function of range for three hypothetical classes of e-bombs (off-the-shelf, moderate output, an a high-output device). Detailed information how the specific amplitude value was determined is discussed in 'The Scenarios and Bounding Cases" section of this study.

$$E(w) = E_0 \times \left[\frac{1}{j \times w + \alpha} - \frac{1}{j \times w + \beta} \right] \tag{11}$$

Where

E_0 : $9x10^3$ (V/m)

α : $4x10^6$ 1/s

β : $4.79x10^8$ 1/s

ω : $2\times\pi\times f$.

8. Overall Determination Results

The best determined parameters from the previous analyses sets establishes the configuration details which optimize coupling results to their highest possible values, out of the above boldfaced determining results tables are gathered and can be observed in Table 15. This table constitutes the "reasonable worst case" conditions needed to determine delivered currents, voltages and power at the modeled IADS nodes.

	VALUE	PAA (Amps)	PAD (Amps/Sec)	PAI (AmpsxSec)	RI (AmpsxSec)	RAI (Ampsx√Sec)
CABLE DIAMETER	4 (cm)	2.96E+01	7.18E+08	4.38E-06	7.95E-06	1.03E-02
CABLE LENGTH	45 (m)	2.71E+01	4.51E+08	5.84E-06	1.07E-05	1.12E-02
HEIGHT	1 (m)	3.19E+01	1.04E+09	4.58E-06	8.36E-06	1.04E-02
INCIDENT ANGLE	90°	2.51E+01	6.10E+08	4.06E-06	7.32E-06	8.64E-03
LOAD (ZLeft & ZRight)	OPEN&SHORT	4.70E+01	1.32E+09	4.30E-06	6.01E-05	3.68E-02
CAPACITANCE	100 (F)	4.04E+02	1.06E+10	5.11E-04	5.12E-04	3.30E-01
DIELECTRIC CONST	5	2.53E+01	6.60E+08	4.06E-06	7.32E-06	8.68E-03
GROUND CONDUCTIVITY	1.E-05	5.36E+01	5.32E+08	2.29E-05	2.83E-05	2.83E-02

Table 15. Overall Determination Results

IV. THE SCENARIOS AND BOUNDING CASES

The e-bomb scenario and conventional weapon scenario will be introduced in this chapter along with their performance and results based upon the CEMPAT program, MATLAB program and a special Unclassified weaponeering calculations program, Joint Munitions Effectiveness Manual (JMEM).

A. THE E-BOMB SCENARIO

In this section, relations between the geometry, frequency, and E-Field will be described. These relations will be shown based upon some formulas and the far E-Field value will be determined according to the calculated results. Following this determination, the CEMPAT program output results, which are created by a run including the best determination values along with that E-Field value, will be shown in a table, summarizing the effects of the e-bomb on the selected system of interest.

1. Geometry and Frequency Considerations

The geometry, frequency, and E-Field relations will be outlined here in details along with some formulas.

a. The Far E-Field

The far E-Field amplitude value of the double exponential pulse is required that would be expected to be produced by the hypothetical e-bomb. That value is determined by using a previously developed MATLAB program that calculates the E-field with a set of descriptive formulas that extend the fields in the waveguide to those that would drive the dish antenna, and finally be projected from the aperture plane to the far field. The E (far field) formula can be derived in that order as follows (Ertekin, 2008):

$$Z_{1,0} = Z_0 \times \left[1 - \left(\frac{\lambda}{2 \times a} \right)^2 \right]^{-\frac{1}{2}} \quad (12)$$

where

$Z_{1,0}$: The waveguide impedance in TE_{10} mode (Ω)

Z_0 : Wave impedance of free space ($\mu / \varepsilon = 120\pi$)

λ : Operating wavelength ($\lambda = \frac{c}{f}$, where the c is the speed of light in free space, 3×10^8 m/s) (m)

a : Larger dimension of the waveguide (m).

Once the model waveguide impedance is determined, the peak electric field (E-field) in the guide can be approximated by equation 13:

$$E_{\max}(waveguide) = \sqrt{\frac{4}{a \times b} \times Z_{1,0} \times P_{avg}} \quad (13)$$

where

$Z_{1,0}$: Model impedance of waveguide (Ω)

P_{avg} : Average power of HPM source (Watts)

a : Larger dimension of the waveguide (m)

b : Smaller dimension of the waveguide (m).

A reasonable value of average power was arbitrarily determined as 20 Mega Watts, which is a suitable value for selected power generator of the e-bomb.

Using a parabolic dish antenna, like the one in Figure 19, the peak electric field at the aperture can be estimated by the focal length of the antenna without using its dimensions.

$$E_{peak}(aperture) = E_{\max}(waveguide) \times \frac{a \times b}{F \times \lambda} \qquad (14)$$

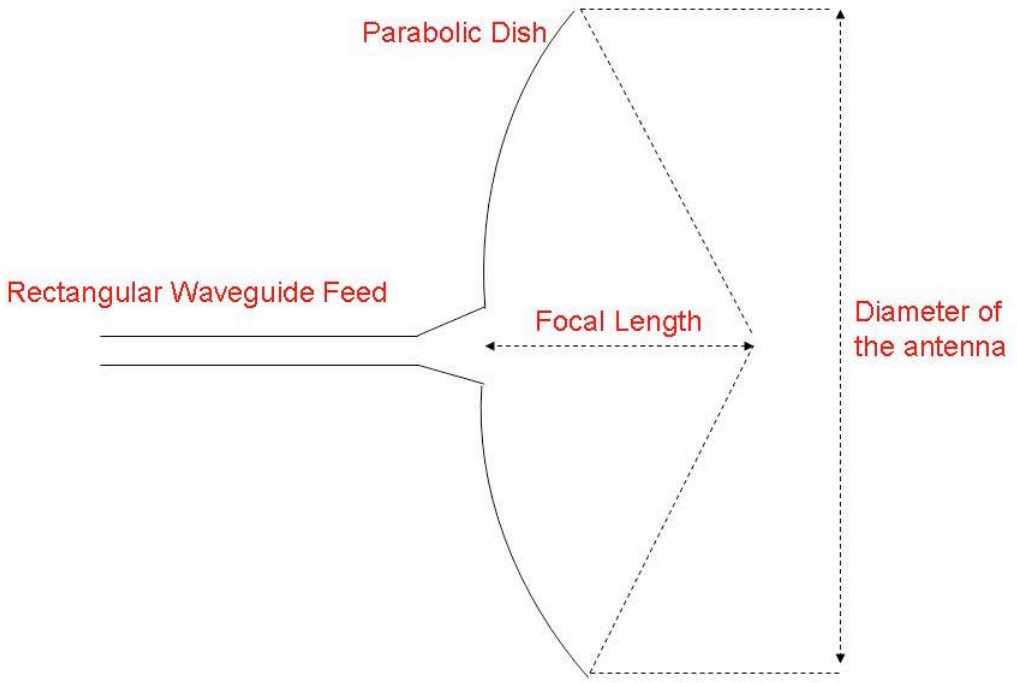

Figure 19. Details of the Proposed Parabolic Dish Antenna (From: Ertekin, 2008)

Once the electric field at the aperture of the antenna is found, the far field parameters for the peak electric field on the antenna boresight may then be estimated by equation 15.

$$E_{peak}(F) = E_{peak}(Apt) \times \left(\frac{A}{r \times \lambda} \right) \qquad (15)$$

where

r	:	Target distance from the e-bomb (m)
E_{peak} (F)	:	E-field strength from the e-bomb at the distance r (V/m)
A	:	$\pi \frac{D^2}{4}$ for the parabolic antenna (m^2).

Out of this field-defining MATLAB program, an E-field vs. distance plot was created. Among the inputs of the program, only the frequency value is variable and others are either selected or decided before, based upon the best coupling considerations. The output of the program is a plot mapping distance vs. range (altitude in the case of the vertically delivered e-bomb). Observation of Figure 20 shows that the electric field is inversely proportional to the range away from the antenna (as expected). The described program output can be used at a specific range to designate the value of the expected E-field at that range (the detonation altitude) that might be produced by an e-bomb.

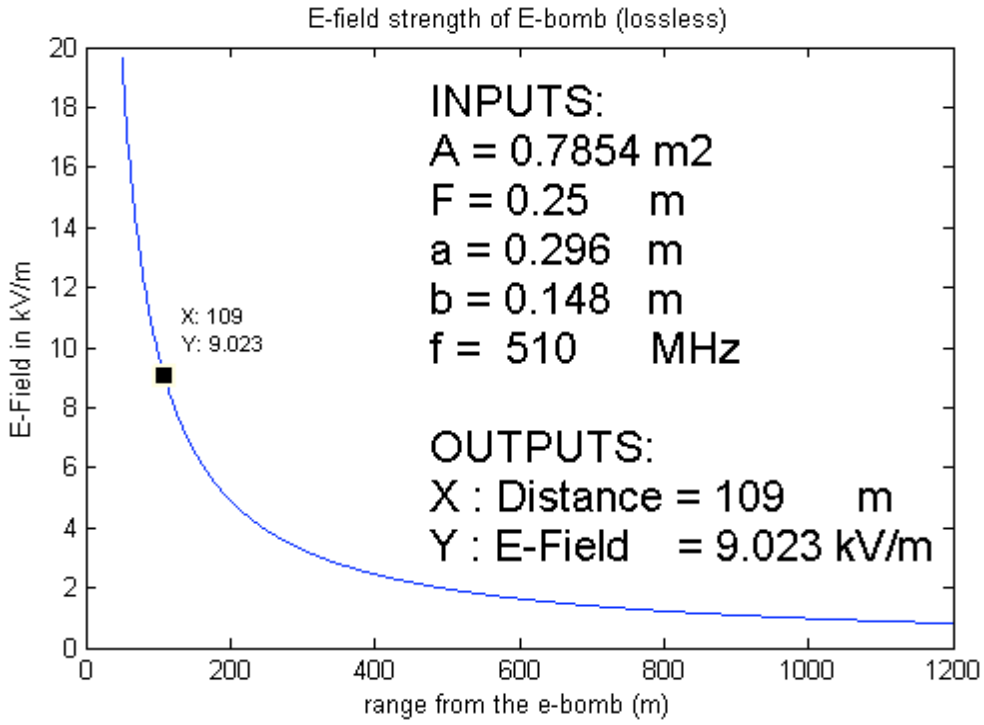

Figure 20. E-field vs. Range (Altitude) Plot Example

A : The Dish Antenna Area (m^2)

F : Focal Length of the Dish Antenna (m)

a : Length of WR1150 waveguide (m)

b : Height of WR1150 waveguide (m)

f : Frequency (Hz)

As an example run to be illustrated in here, the program was run for 510 MHz, which is the cut-off frequency of the e-bomb that WR1150 waveguide provides, and Figure 20 was created as a result of the MATLAB program run. At this frequency, the e-bomb creates a 9 kV/m far E-Field value at 109 meters altitude, which is in the middle of the curve on the plot. This E-Field curve when evaluated at a different point on this range curve produces for example a 10.58 kV/m field strength at 93 meters altitude.

b. Frequency and Altitude

Replacing the components in the E (Far Field) formula with their equivalents it can be revised as:

$$E_{peak}(FarField) = E_{\max}(waveguide) \times \frac{a \times b \times A \times f^2}{F \times r \times c^2} \quad (16)$$

Where:

A : The Dish Antenna Area (m^2)

F : Focal Length of the Dish Antenna (m)

a : Length of waveguide (m)

b : Height of waveguide (m)

f : Frequency (Hz)

c : Speed of light (m/s)

r : Range (Altitude) (m).

This form of the formula lets one to see the effects of each component to the far E-field. A, b, a, F components are determined and c component is constant in the formula while f and r components are variable. The major effect to the E-field comes from the operating frequency since it has a squared effect, and it is directly proportional to the waveguide E-field. On the other hand, the distance (detonation altitude) from the weapon to the target is inversely proportional to the E-field, as would be expected.

Another consideration is the relation between frequency and distance, as we can recall from the 'Geometry of the Attack' section. The operating frequency is directly proportional to the distance.

c. The Far E-Field Determination

Based on the information given above, the MATLAB program was run to predict e-bomb electric fields over a hypothetical design frequency range, starting at the cut-off frequency. The corresponding distances to the random frequencies are specified in a results table. Those results are shown in Table 16.

FREQUENCY (MHz)	510	600	750	1	1.2	1.5
DISTANCE (meters)	93	110	140	190	227	285
E-FIELD (kV/m)	10.58	5.68	5.94	7.19	8.5	10.3

Table 16. The E-Field Determination Results

Table 16 provides a good picture to compare the frequency-distance-E-field relations. At first look, it seems it is beneficial to use high

frequency ranges for the e-bomb, for the purpose of getting higher E-field values. Nevertheless, since a double exponential pulse is used for coupling, high frequencies at double exponential pulse spectrum corresponds to low amplitude values of far E-field (See Figure 12). Much stronger fields are available when considering the lower frequency of the double exponential waveform. Specific information about this issue is in Appendix.

According to the entire range of calculated results shown in Table 16, an average value of far E-field coupling to the target cables was selected as 9 kV/m (with corresponding values of frequency and range of 109 meters) and formed the basis for the amplitude of the e-bomb threat field applied in the CEMPAT cable coupling program to simulate an e-bomb attack.

2. Results Evaluation

Considering each IADS cable type, and the optimum coupling results that will control response levels and considering the double exponential transient threat expected from an e-bomb weapon, the analytically determined best coupling parameters were used in the CEMPAT program to achieve optimum coupling results. In other words, the effects of the e-bomb on the model of interest are achieved and can be observed in Table 17. Actually, those results are evaluated as a summary of the assessment runs in Chapter III.

In this table, PAA and RAI values for each cable type and length can be compared and this comparison gives an idea about best or optimum coupling situations along with the height, diameter, and impedance values for the cable configurations of interest in the IADS model.

	LENGTH (meters)	PAA (Amps)	RAI (Ampsx√Sec)	RISETIME (Sec)	HEIGHT (meters)	DIAMETER (meters)	ZL (Ω)	ZR (Ω)
POWER CABLE	40	1.78E+02	1.40E-01	9.31E-08	0.5	0.06	2	0.2
	30	1.75E+02	1.34E-01	8.00E-08				
	15	1.61E+02	1.18E-01	8.50E-08				
SIGNAL CABLE	40	2.21E+02	7.76E-02	6.65E-08	2.5	0.04	331	0.2
	30	2.15E+02	6.47E-02	6.00E-08				
	15	1.86E+02	4.00E-02	3.50E-08				
LAN CABLE	40	1.68E+02	5.83E-02	6.65E-08	2.5	0.005	456	0.2
	30	1.63E+02	4.85E-02	6.00E-08				
	15	1.40E+02	2.97E-02	3.50E-08				
TELEPHONE CABLE	40	1.14E+02	4.58E-02	6.65E-08	2.5	0.0025	193	0.2
	30	1.10E+02	3.95E-02	6.00E-08				
	15	9.40E+01	2.62E-02	3.50E-08				

Table 17. The Objective Coupling Results

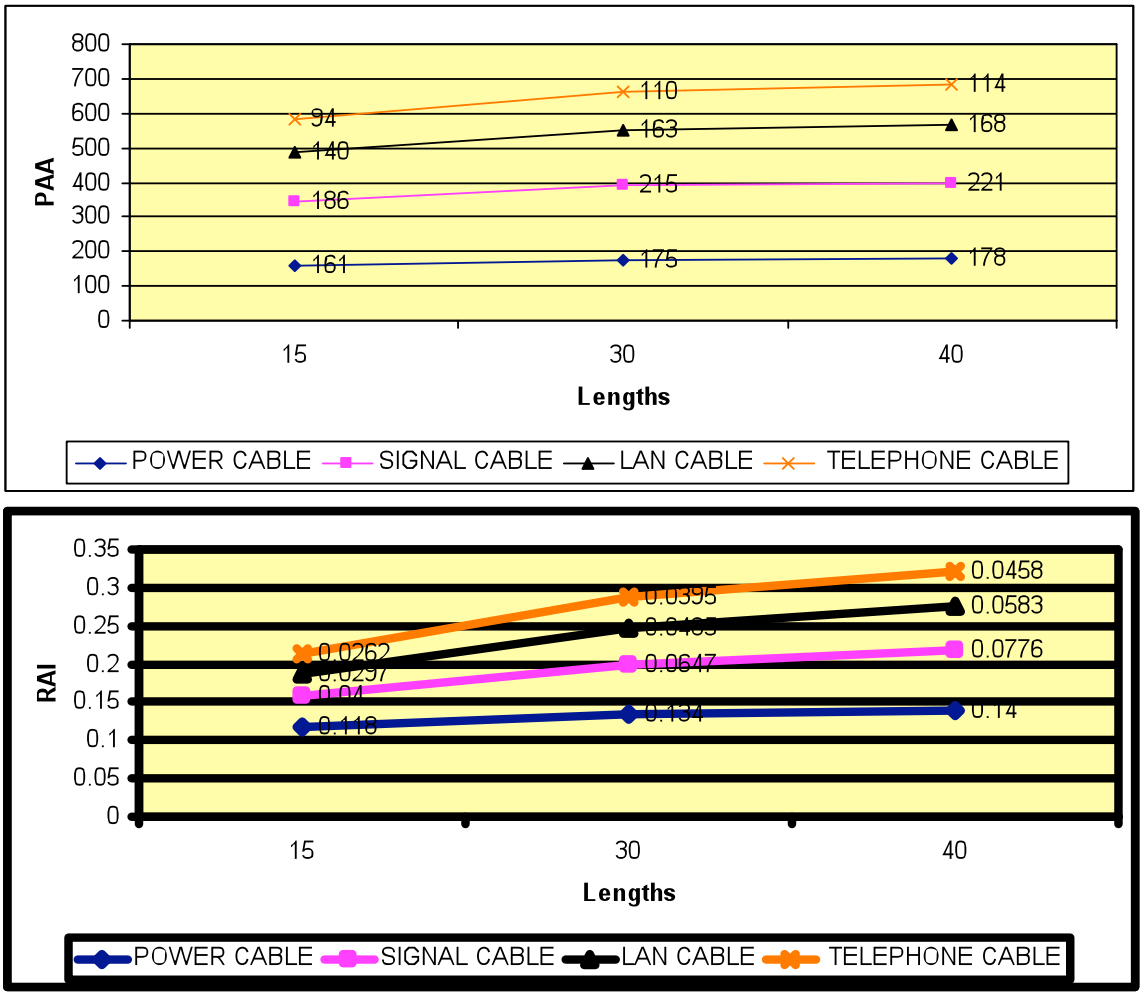

Figure 21. Length vs. PAA and RAI

A good comparison example plot for length vs. PAA and RAI, out of this table, can be observed in Figure 21. PAA and RAI reactions are directly proportional to the cable length. Nevertheless, as was mentioned in the length determination runs, after a specific cable length (integration length), PAA and RAI values do not give that proportional response to the cable length.

Figure 21 only shows the metrics from the analysis. Some response plots that were created out of the CEMPAT program for an average value of the cable lengths in the target system, which should be 30 meters configurations, can be viewed in Figure 22. These plots illustrate the reactions of each cable type (phone, power, LAN, and signal) in the target system, against the e-bomb effects.

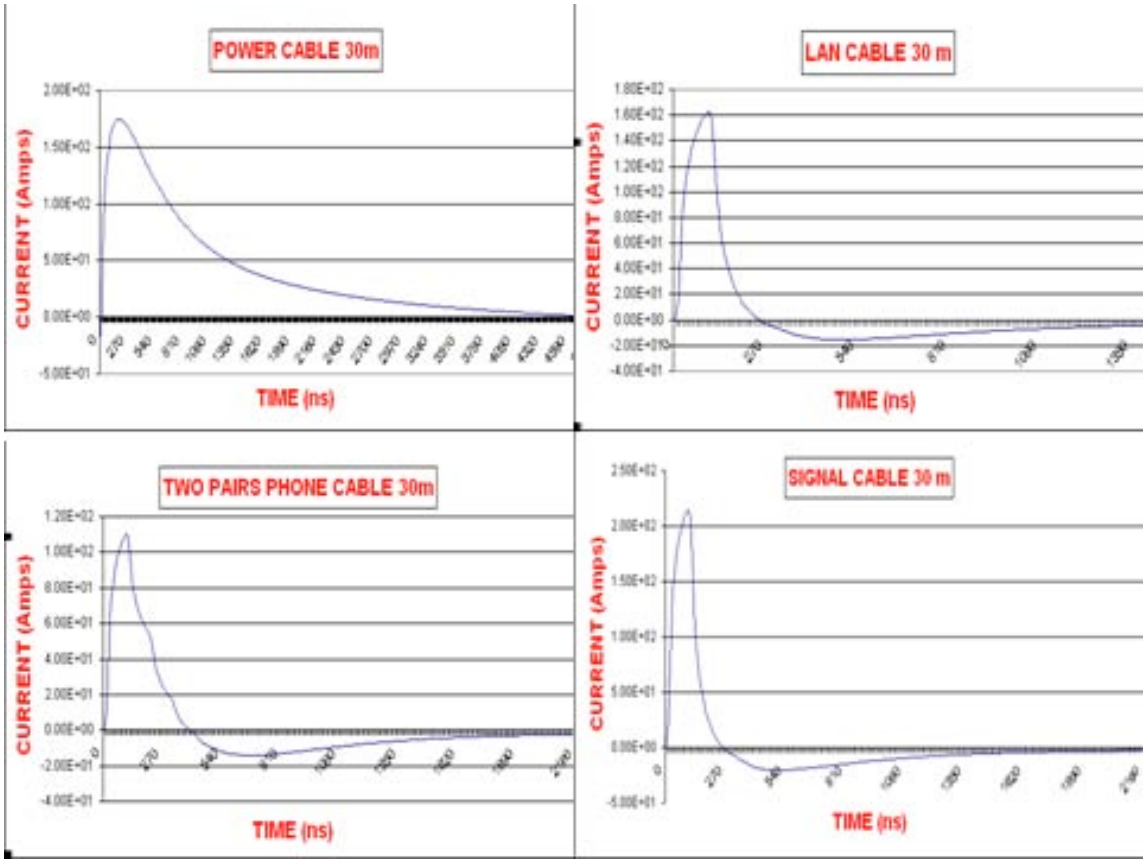

Figure 22. The CEMPAT Program Output Plots

The e-bomb effects examined in Table 17 and observed in Figure 21 and Figure 22 will be further evaluated in terms of PAA and RAI values. The next step

will be to investigate how the target system is going to respond to those effects, and how it is expected to react to the currents created by the e-bomb. The expected reactions of the target should be any upsets that can render the target system nonfunctional to the potential of the e-bomb to inflict moderate or catastrophic kill levels operationally.

B. THE CONVENTIONAL WEAPONS SCENARIO

A Guided Bomb Unit (GBU-10 Paveway II) will be tested in conventional weapon scenario to compare its effects with the e-bomb on the selected system of interest model.

The Guided Bomb Unit-10 (GBU-10) consists of an MK-84 2,000-pound general purpose or penetrating warhead with an added laser guidance. The operator illuminates a target with a laser designator, and then the munition guides to a focused laser energy reflected from the target. A picture of the GBU-10 bomb is in Figure 23.

Figure 23. GBU-10 Paveway II (From: Bombas Guidas, 2009)

According to the Air Force, the munition was used during Operation Desert Storm and hit *78 percent* of its targets. The platforms were used during Operation Desert Storm, by F-15E and F-111F aircraft mainly against bridges, Scuds, *C3I* (Command, Control, Communications, Intelligence) *nodes*, and bunkers.

There are two models of GBU-10 Laser Guided Bombs (LGB): Paveway I has fixed wings and Paveway II has folding wings. Paveway II models have these improvements: detector optics and housing made of injection-molded plastic to reduce weight and cost; increased detector sensitivity; reduced thermal battery delay after release; increased maximum canard deflection; laser coding; folding wings for carriage, and increased detector field of view. (Paveway II's instantaneous field of view is thirty percent greater than that of the Paveway I's field of view) (Military Analysis Network, n.d.).

An unclassified Joint Munitions Effectiveness Manuals (JMEM) weaponeering program is used to calculate the possible effects of the GBU-10 Paveway II on the each nodes of selected target model. In order to be able to examine the outputs of the JMEM program, some definition will be given related to program outputs and basic concepts of conventional munition operation.

1. Definitions

Some definitions that help understanding the result evaluation of the JMEM program are as follows:

a. Weaponeering

> Weaponeering is the process of determining the type of weapon, fin, sensor, fuse, etc. required to achieve a specific level of target damage. It is a key task in the force application planning cycle. The process considers target vulnerability, target damage criteria, weapon effects, munition or dispenser delivery errors and weapon and/or dispenser reliability. (Product Brochure)

Weaponeering processes are the main part and heart of an organized attack against any target.

b. Circular Error Probability

In the military science of ballistics circular error probability (CEP) is a measure of a weapon system's precision. It is defined as the radius of a circle into which a warhead, missile, bomb, or projectile will hit at least 50% of the time (The Free Dictionary).

The smaller the CEP value, the higher the probability of hit. Therefore, CEP value is very important in weaponeering calculations.

c. Types of Kills

Functional kill (F-Kill) is to render a targeted installation, facility, or target system unable to execute its primary function. (Military Dictionary-Terms Defined) An M-Kill destroys one or more of the vehicle's vital drive components (for example, breaks a track on a tank) and immobilizes the target. It does not always destroy the weapon system and the crew; they may continue to function. Catastrophic kill requires a weapon system and/or the crew is destroyed (Global Security).

Kill levels can be determined with respect to the importance level of the target and the requirement of the target to be damaged, for the perpetuation of the operation.

d. Single Sortie Probability of Damage

Single Sortie Probability of Damage (SSPD) is an index or percentage that Joint Munitions Effectiveness Manuals calculate the effectiveness of the conventional weapon blast and fragmentation (Defense Technical Information Center, n.d.).

SSPD is obtained out of weaponeering calculations and gives the probability of damage on the target. Therefore, SSPD is an important metric that helps the attacker to decide the potential of the target to be destroyed.

2. JMEM Results and Evaluations

An SA-2 integrated air defense system, which is identical to the system of interest model in this study, is selected as a target in JMEM program. SA-2 missile system has five nodes, which are identical to the nodes on this study. The JMEM program allows the user to select only one of each node at a time. So, a GBU-10 was applied to each node one–by-one, and the results related to each node attack are in Table 18.

	TARGET	SA-2 COMPUTER VAN	SA-2 GENERATOR VAN	SA-2 GUIDANCE CONTROL VAN	SA-2 GUIDELINE MISSILE ON LAUNCHER	SA-2 POWER DISTRIBUTION VAN
INPUTS	MUNITION	GBU-10 PAVEWAY II	GBU-10 PAVEWAY II	GBU-10 PAVEWAY II	GBU-10 PAVEWAY II	GBU-10 PAVEWAY II
	SPEED (TAS)	550 KNOTS	550 KNOTS	550 KNOTS	550 KNOTS	550 KNOTS
	CEP	17	17	17	17	17
	ALTITUDE	50000 FEET	50000 FEET	50000 FEET	50000 FEET	50000 FEET
	DIVE/LEVEL	LEVEL	LEVEL	LEVEL	LEVEL	LEVEL
	KILL TYPE	F-KILL	F-KILL	F-KILL	K-KILL	F-KILL
OUTPUTS	SSPD	0.79	0.78	0.79	0.79	0.79
	PASSES REQUIRED	1	1	1	1	1

Table 18. JMEM Program Run Inputs/Outputs

Most integrated air defense systems have effective altitude capability of 30,000 feet to 80,000 feet. The probability of hit decreases as the altitude gets higher. Because of that, the system of interest model effective altitude capability is assumed 50,000 feet, which is an average value in this case. According to the laser-guided bomb delivery envelope in Figure 24, a level attack is the best method, and a true speed value of 550 Knots is expectable at this altitude. Finally, the CEP value selected as 17 feet, since it is an acceptable average value and it is a default value of the JMEM program.

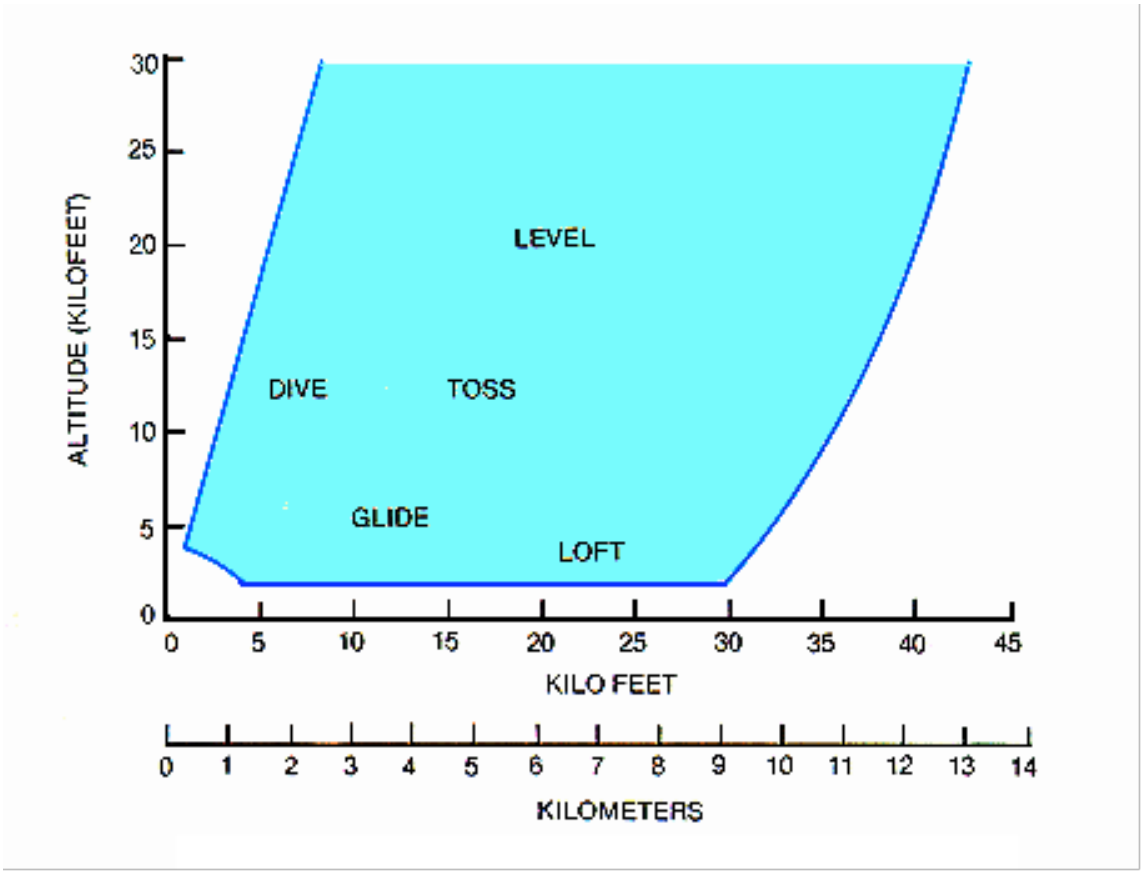

Figure 24. Representative Laser Guided Bomb Delivery Envelope (From: Military Analysis Network, 2009)

As it can be viewed in Table 18, the SSPD values are almost the same for each attack. The SA-2 missile system has five nodes while the system of interest model in this study has six nodes. Nevertheless, since all of the nodes in both systems are identical to each other, the sixth node in the system of interest model is expected to have the same results with other nodes.

The obtained results from the JMEM program for the effectiveness of the GBU-10 bomb is the same as the Air Force report from Operation Desert Storm hit percentage (78%). Out of the results, one can conclude that, in order to have a 78% SSPD on the system of interest model, six passes/attacks on the target is required.

V. DAMAGE ASSESSMENT

In this chapter, e-bomb effects on the IADS target system will be assessed by using the coupled current scalar results outlined earlier in Table 17. This assessment will be analyzed in detail based on some procedures, assumptions, and principles that will be described in the material that follows. Out of this analysis, target system node power, voltage, and energy levels, which are formed on the electronic equipment system nodes by the hypothetical e-bomb, will be calculated using the current metric values in Table 17. Once the power, voltage and energy levels are formed, these calculations will be compared to some officially reported effect threshold results derived from reputable experimental effect analysis of the current formed power, voltage, and energy on similar electronic components. Information about those experimental data table can be found in analysis assessment section of this chapter in detail.

A. THREAT ENVIRONMENT

Every node of the IADS target is interconnected to all other IADS nodes with representative, appropriate types of intra-site cabling.Those connection features vary by type and with respect to their specifications, functional purposes and mission requirements in the system. The details associated with each cable connection and cable-load characteristics will be covered separately for their individual threat environment responses and analyzed in this section for the effects levels that might be expected.

In order to be able to solve the assessment problem and follow the intended procedure analysis, Norton equivalent circuit principles will be used to describe the connection characteristics. The loads attached to the Norton equivalent circuit are assumed matched impedances. In this case, maximum power delivered to the R_L will occur at a level that is one-half of the currents induced on the cables. This is because one-half of the induced power will also be

dissipated by the Thevenin equivalent impedance in delivering load currents. A representative Norton equivalent circuit adapted to the target system nodes can be seen in Figure 25.

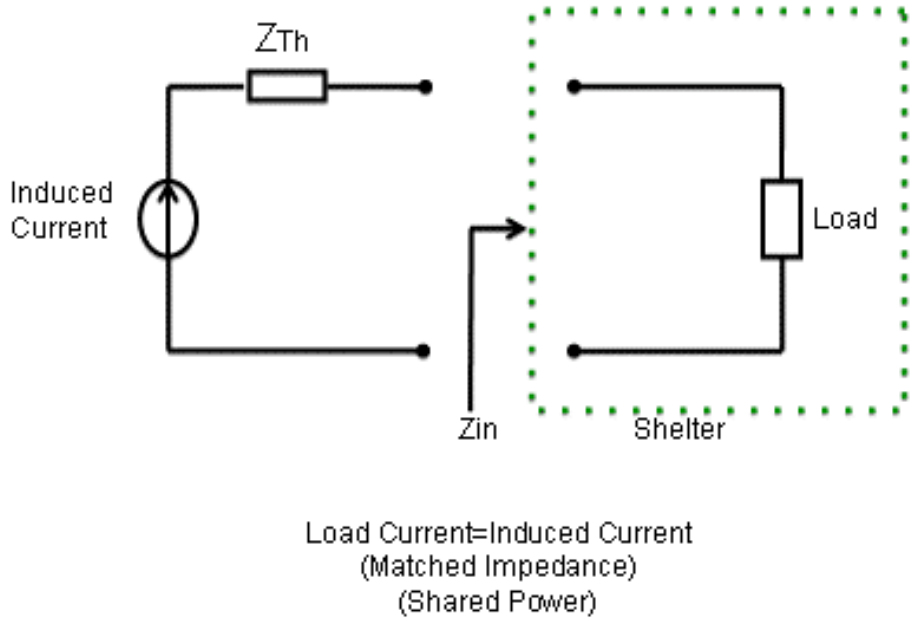

Figure 25. Adapted Norton Equivalent Circuit

1. Power Cable Threat Environment

The threat environment for the power cable can be viewed in Figure 26. The threat field is induced on the bulk power cable, which is composed of five individual wires, outside the shelter. These five wires include separate wire conductors for phase a, b, and c power connectivity along with a ground wire and a return wire. The e-bomb created current value in Table 17 represents the induced bulk current on the entire power cable. Since that bulk cable is not directly connected to the electronic components inside the shelter because each wire in the bulk cable is directly connected, those wire currents need to be calculated with respect to their relationship to the overall bulk cable current. As a reasonable approximation, dividing the induced bulk cable current by the square

root of the number of wires contained gives the wire current (See the formula in Figure 26). There is no shielding assumed for the power cabling.

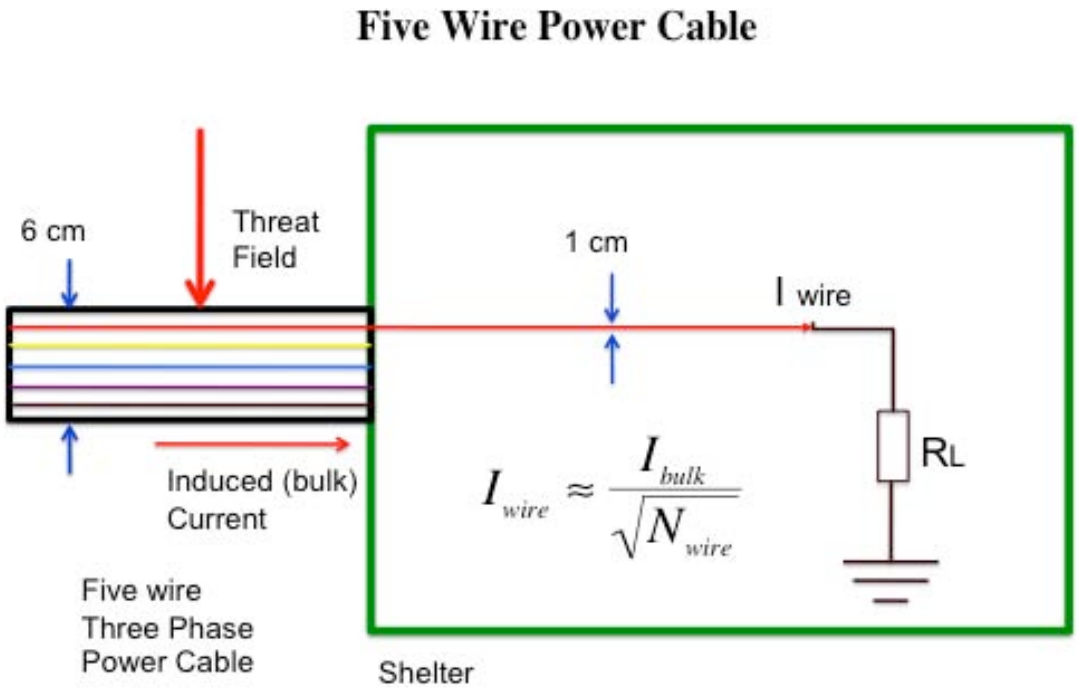

Figure 26. Power Cable Threat Environment

2. Signal Cable Threat Environment

The Signal cable threat environment can be viewed in Figure 27. As described previously, the signal and LAN cable in the IADS target system are assumed to be designed with a 30 dB shielding. This is a reasonable and expected moderate cable shielding value for such a system, because even if the shielding would be higher than 30 dB, i.e., 50 dB, possible cracks or apertures in the connection parts of the cables can occur. On the other hand, less than 30 dB shielding would not be realistic since it is a very low value for such a system. Therefore, 30 dB was selected, as it would be a moderate and reasonable shielding value for such a situation.

Being shielded, the signal cable will no longer carry all of the induced current on the bulk cable but that current will be reduced with respect to the ratio of shielding value. Since it has a 30 dB shielding, the wire current carried to the R_L or to the electronic components can be calculated by dividing the induced bulk current by 1000 (See the formula in Figure 27).

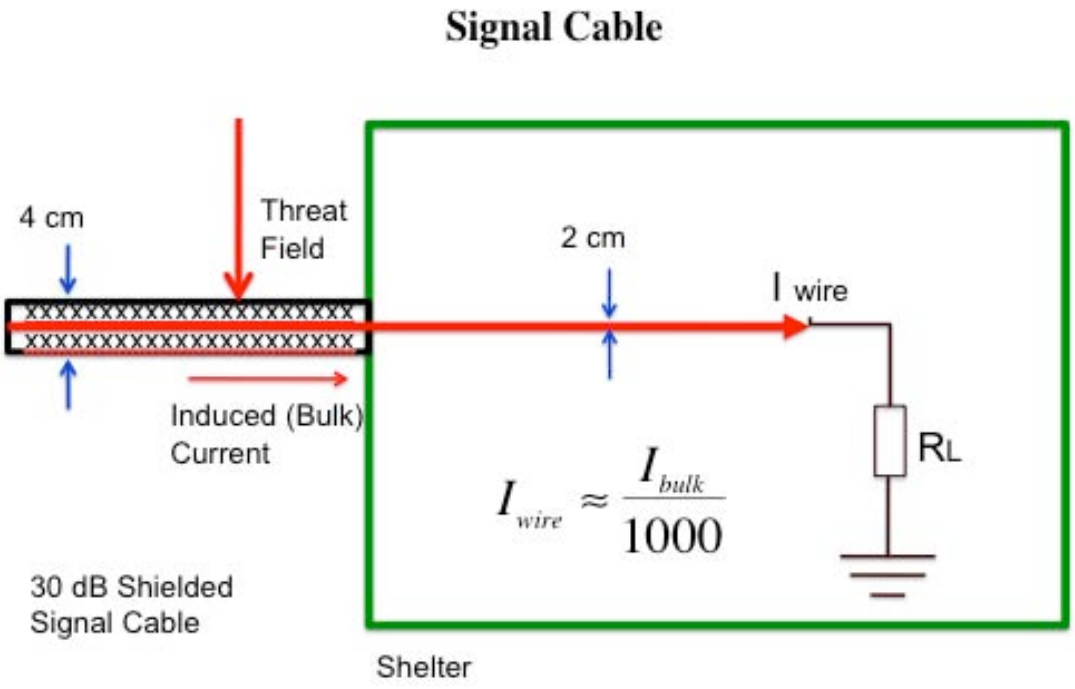

Figure 27. Signal Cable Threat Environment

3. LAN Cable Threat Environment

Figure 28 represents the threat environment for the LAN cable. LAN cabling is also assumed to be designed with a 30 dB shielding value similar to the signal cable. Therefore, the same considerations and calculations on the signal cable can be applied to the LAN cable as well.

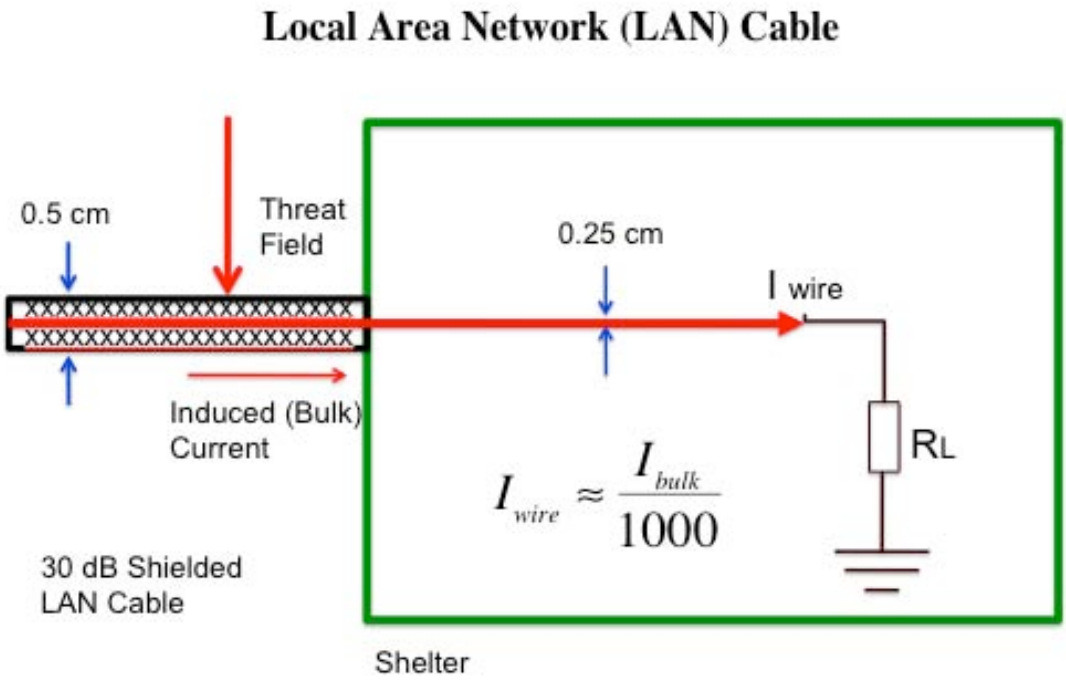

Figure 28. LAN Cable Threat Environment

4. Telephone Cable Threat Environment

The telephone line in the IADS target system was designed as a two-wire parallel cable in order to make it realistic, since it is broadly used for telephone communication lines. The threat environment for the telephone line is identical to the power cable and can be observed in Figure 29. Although the two wires in the bulk telephone cable are actually separated from each other by a plastic material, the same current sharing calculation method used earlier in the power cable threat environment can be applied to two-wire telephone cable threat environment. Hence, the wire current can be derived by dividing the induced bulk current by the square root of two (See the formula in Figure 29). No telephone line cable shielding is assumed.

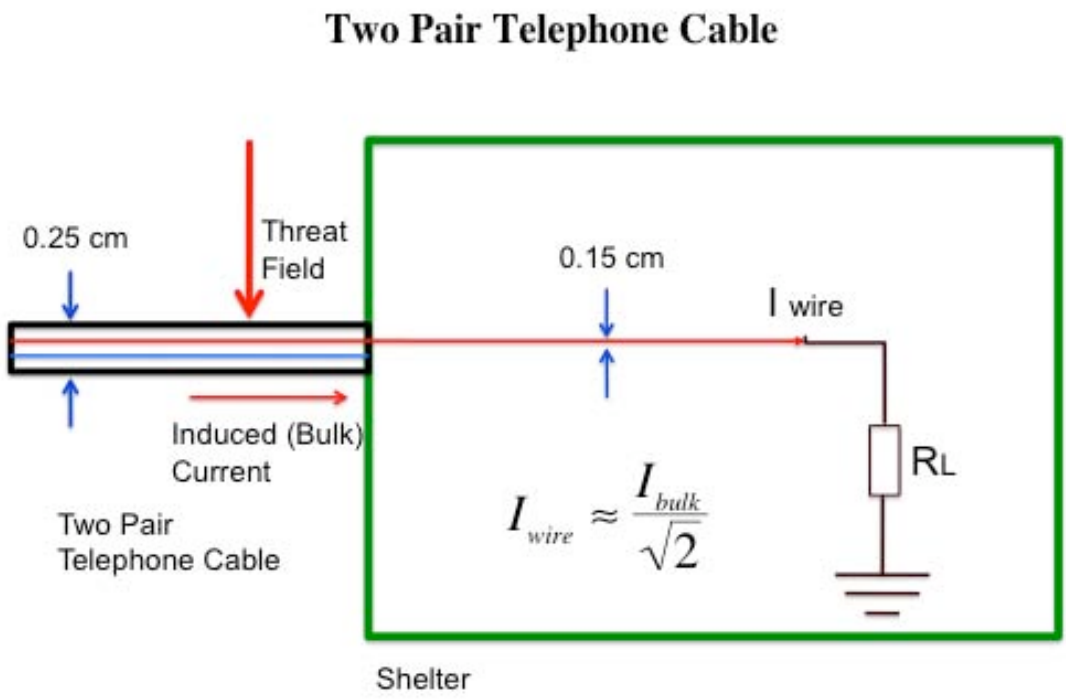

Figure 29. Telephone Cable Threat Environment

B. ANALYSIS PROCEDURE

In order to implement the analysis procedure, some first principle rules are needed. The induced wire current values at each system node will be applied to those principle rules, and then using appropriate fundamental equations, power, voltage, and energy values formed on the electronic equipment components (on R_L) will be calculated.

Since the e-bomb created current has a pulse duration, and it is resonant in nature, the fundamental formulas will be based on Root Mean Square (RMS) value of the currents as well as peak current values. RMS value, or average value, of a sinusoidal resonant current can be calculated dividing the peak current by the square root of two.

The fundamental formulas for the intended procedure to handle these currents are as follows:

Since the mentioned threshold level experimental data table, which is used in this study as a reference for comparison, involves the maximum voltage values, e-bomb created max voltage values will be calculated and used on R_L, instead of RMS voltage values. These peak value results will be compared with this threshold level experimental maximum voltage to determine the potential effects. Multiplying the peak or maximum current by the R_L impedance gives the maximum voltage on the R_L, as it is shown in equation 17.

$$V_{\max} = I_{\max} \times R_L \tag{17}$$

The RMS voltage formed on the electronic equipments can be calculated by equation 18

$$V_{RMS} = I_{RMS} \times R_L \tag{18}$$

Using this RMS voltage and RMS current values, the average power formed on the electronic equipment can be derived as in equation 19:

$$\begin{aligned} P_{avg} &= V_{RMS} \times I_{RMS} \\ V_{RMS} &= I_{RMS} \times R_L \\ P_{avg} &= I_{RMS} \times I_{RMS} \times R_L \\ P_{avg} &= (I_{RMS})^2 \times R_L \end{aligned} \tag{19}$$

The pulse durations of the induced currents are calculated by the CEMPAT program for the results of exposure to the hypothetical e-bomb. Using

these values, the average energy, to which the electronic equipment is exposed for this short period of time, can be calculated by equation 20.

$$U_{avg} = P_{avg} \times \tau \tag{20}$$

Where

τ : Pulse Duration.

C. ANALYSIS ASSESSMENT

Using the fundamental formulas for the analysis procedure, voltage, power, and energy on the electronic components, is calculated with respect to each cable type in Table 17, Appropriate analysis results tables are created, for each cable type in order to be able to examine the calculation results. Following this compilation, those analysis tables are compared to the mentioned threshold level experimental reference table created and published by the Defense Nuclear Agency (now the Defense Threat Reduction Agency).

1. Reference Data

One of the published experimental data results that will be compared to analysis procedure results in this study is the data published by Defense Nuclear Agency, which can be viewed in Figure 14. The bars on this figure represent the experimental range of values where possible damage occurrences on the device may occur when it is exposed to corresponding power levels. This chart was created based upon experimental results of standard injection susceptibility test waveforms that monitored and documented damage occurrences. As it is depicted in the chart, increasing power levels corresponding to the bars for each device can lead that device to serious damage results.

Another reference data set used to compare to the analysis procedure results can be examined in Table 19. In this table, electronic components are

categorized into four groups as high power discrete, low power discrete, CMOS, and TTL circuits. The upset and burnout threshold levels of voltage, power, and energy are available for three frequency levels: 200 MHz, 600 MHz, and 900 MHz at each corresponding electronic component. Among these three frequency levels, 600 MHz and 900 MHz are exactly in the range of the e-bomb operating frequency. Therefore, these frequency levels are very compatible for the intended comparisons.

	FREQUENCY (MHz)	UPSET VOLTAGE (mili V)	UPSET POWER (micro W)	UPSET ENERGY (pico J)	BURNOUT VOLTAGE (V)	BURNOUT POWER (W)	BURNOUT ENERGY (micro J)
Low Power Discretes	200	14.1	4	4	25	12	12
	600	24.5	12	12	42.4	36	36
	900	30	18	18	52	54	54
High Power Discretes	200	14.1	4	4	44.7	40	40
	600	24.5	12	12	77.5	120	120
	900	30	18	18	95	180	180
CMOS	200	245	1200	1200	20	8	8
	600	424	3600	3600	35	24	24
	900	520	5400	5400	42.4	36	36
TTL	200	200	800	800	14.4	4	4
	600	346	2400	2400	24.5	12	12
	900	424	3600	3600	30	18	18

Table 19. Upset/Burnout Thresholds (Pulse Width=100 nanosecond) (From: DNA, 1986)

All of the energy threshold levels in this experimental table are calculated with respect to a standard injection waveform of 100 ns in pulse duration, while the e-bomb formed energy on the electronic equipments are calculated based on the pulse durations calculated by the CEMPAT program. Actually, all of the pulse durations of the e-bomb created currents are slightly less than 100 ns, averaging about 60 ns in duration, which can possibly be viewed as a drawback for the formed energy approach of this analysis with respect to the energy threshold levels in the reference table. However, the results in Table 17 are based on transmission-line modeling of a distributed system excited by a hypothetical threat, therefore it is assumed possible that “true” current durations could be larger than the 60 ns (on the average) than the model predicts. Transmission line models are inherently high-Q, while practical systems are damped

somewhat, and responses are expected to reasonably exceed the model prediction of duration.

The electronic components indicated in this reference table are very commonly included in most electronic systems; therefore, the same components in the table are expected to be included at all of the target system nodes as well.

In the next section, the analysis procedure described above are implemented, and the results compiled into a summary table. Finally, the modeled results and the two described threshold effect reference data values will be compared and demonstrated to conclude what kind of effects the e-bomb might possibly have on the system of interest (IADS target).

2. Data Comparisons

Out of the analysis procedure and fundamental formula calculations, appropriate tables, combined with both calculation results and reference data, are created by which the calculation results can be matched with the reference data table. Those created calculation result tables are highlighted and coupled together with the experimental data tables for each cable type environment individually.

a. Power Cable Data Comparison

The e-bomb coupling results for power cable threat environment is satisfactory enough to exceed the entire experimental data threshold levels table. As it is depicted in Table 20, the power, voltage, and energy values formed on the electronic equipment by the e-bomb model are well above the upset and burnout threshold levels at the experimental data table.

In addition, the formed power values, 2.5 kW to 3 k W, correspond to the bars in Figure 14 for High Power Transistors, Silicon Controlled Rectifiers, Germanium Transistors, Rectifier Diodes, and Reference Diodes, which means that those electronic components are potential candidates for damage.

POWER CABLE

CABLE LENGTH	VOLTAGE (Peak) (V)	POWER (W)	ENERGY (Joule)
40	159.20804	3168.4	2.95E-04
30	156.5247584	3062.5	2.45E-04
15	144.0027778	2592.1	2.20E-04

	FREQUENCY (MHz)	UPSET VOLTAGE (mili V)	UPSET POWER (micro W)	UPSET ENERGY (pico J)	BURNOUT VOLTAGE (V)	BURNOUT POWER (W)	BURNOUT ENERGY (micro J)
Low Power Discretes	200	14.1	4	4	25	12	12
	600	24.5	12	12	42.4	36	36
	900	30	18	18	52	54	54
High Power Discretes	200	14.1	4	4	44.7	40	40
	600	24.5	12	12	77.5	120	120
	900	30	18	18	95	180	180
CMOS	200	245	1200	1200	20	8	8
	600	424	3600	3600	35	24	24
	900	520	5400	5400	42.4	36	36
TTL	200	200	800	800	14.4	4	4
	600	346	2400	2400	24.5	12	12
	900	424	3600	3600	30	18	18

Table 20. Data Comparison for Power Cable Environment (Model results are highlighted, threshold levels are shown below the model results)

b. Signal Cable Data Comparison

The comparison in Table 21 reflects the 30 dB shielding configuration for the signal cable. Note, that there are some threshold levels in the burnout section which could not be exceeded because of shield protection. An important observation is that all of the experimental threshold levels for upset were exceeded by the e-bomb simulation data. In addition to all power and energy threshold levels in the burnout section, the other below-threshold condition involved the voltage threshold levels for high power discretes. The experimental thresholds were not exceeded at 600 and 900 MHz as is shown.

SIGNAL CABLE

CABLE LENGTH	VOLTAGE (Peak) (V)	POWER (W)	ENERGY (Joule)
40	73.151	4.04159275	2.69E-07
30	71.165	3.82511875	2.30E-07
15	61.566	2.862819	1.00E-07

	FREQUENCY (MHz)	UPSET VOLTAGE (mili V)	UPSET POWER (micro W)	UPSET ENERGY (pico J)	BURNOUT VOLTAGE (V)	BURNOUT POWER (W)	BURNOUT ENERGY (micro J)
Low Power Discretes	200	14.1	4	4	25	12	12
	600	24.5	12	12	42.4	36	36
	900	30	18	18	52	54	54
High Power Discretes	200	14.1	4	4	44.7	40	40
	600	24.5	12	12	77.5	120	120
	900	30	18	18	95	180	180
CMOS	200	245	1200	1200	20	8	8
	600	424	3600	3600	35	24	24
	900	520	5400	5400	42.4	36	36
TTL	200	200	800	800	14.4	4	4
	600	346	2400	2400	24.5	12	12
	900	424	3600	3600	30	18	18

Table 21. Data Comparison for Signal Cable Environment (Model results are highlighted, threshold levels are shown below the model results)

c. LAN Cable Data Comparison

Since the signal and LAN cable are identical to each other with respect to their specifications, and they have the same shielding level, their response to the threat environment is identical. As it can be seen in Table 22, the comparison results correspond to the same threshold levels with the signal cable.

In addition, the formed power values for both Signal and LAN cables are 2.2 watts to 3.2 watts, which correspond to the bars for Point Contact Diodes, Microwave Diodes, and Integrated Circuits in Figure 14.

LAN CABLE

CABLE LENGTH	VOLTAGE (Peak) (V)	POWER (W)	ENERGY (Joule)
40	76.608	3.217536	2.14E-07
30	74.328	3.028866	1.82E-07
15	63.84	2.2344	7.82E-08

	FREQUENCY (MHz)	UPSET VOLTAGE (mili V)	UPSET POWER (micro W)	UPSET ENERGY (pico J)	BURNOUT VOLTAGE (V)	BURNOUT POWER (W)	BURNOUT ENERGY (micro J)
Low Power Discretes	200	14.1	4	4	25	12	12
	600	24.5	12	12	42.4	36	36
	900	30	18	18	52	54	54
High Power Discretes	200	14.1	4	4	44.7	40	40
	600	24.5	12	12	77.5	120	120
	900	30	18	18	95	180	180
CMOS	200	245	1200	1200	20	8	8
	600	424	3600	3600	35	24	24
	900	520	5400	5400	42.4	36	36
TTL	200	200	800	800	14.4	4	4
	600	346	2400	2400	24.5	12	12
	900	424	3600	3600	30	18	18

Table 22. Data Comparison for LAN Cable Environment (Model results are highlighted, threshold levels are shown below the model results)

d. Telephone Cable Data Comparison

Even though the lowest e-bomb created Peak Absolute Amplitude (PAA) and Root Action Integral (RAI) values of the induced current occurred on the telephone cable, among other cable types, the highest formed results are derived out of telephone cable threat environment. This is because it is not shielded, and it consists of only two wires. Therefore, its current is divided by square root of two but not five as power cable and not divided by any value because of the shielding effect. As a result, those circumstances let the telephone cables in the target system have the highest expected termination

equipment load currents in the target system. Consequently, just like the power cable, the telephone cable exceeds all of the threshold levels of the experimental data table as can be seen in Table 23.

TELEPHONE CABLE

CABLE LENGTH	VOLTAGE (Peak) (V)	POWER (W)	ENERGY (Joule)
40	15557.7634	313528.5	2.08E-02
30	15011.87696	291912.5	1.75E-02
15	12828.33122	213168.5	7.46E-03

	FREQUENCY (MHz)	UPSET VOLTAGE (mili V)	UPSET POWER (micro W)	UPSET ENERGY (pico J)	BURNOUT VOLTAGE (V)	BURNOUT POWER (W)	BURNOUT ENERGY (micro J)
Low Power Discretes	200	14.1	4	4	25	12	12
	600	24.5	12	12	42.4	36	36
	900	30	18	18	52	54	54
High Power Discretes	200	14.1	4	4	44.7	40	40
	600	24.5	12	12	77.5	120	120
	900	30	18	18	95	180	180
CMOS	200	245	1200	1200	20	8	8
	600	424	3600	3600	35	24	24
	900	520	5400	5400	42.4	36	36
TTL	200	200	800	800	14.4	4	4
	600	346	2400	2400	24.5	12	12
	900	424	3600	3600	30	18	18

Table 23. Data Comparison for Telephone Cable Environment (Model results are highlighted, threshold levels are shown below the model results)

VI. CONCLUSIONS AND RECOMMENDATIONS

A. CONCLUSIONS

The Chapter V data comparison tables for each type of cable investigated the possible effects of the hypothetical e-bomb on the target nodes very well. Based on the comparison results derived in those evaluation tables, at least an upset is expected on all of the electronic equipment at each considered node. Moreover, all of the equipment connected to the power and telephone cables are possible candidates for being completely damaged (burned out). Nevertheless, voltage threshold levels for both upset and damage of some electronic components, i.e., low power discretes, CMOS and TTL circuits, connected to the power and telephone cable were shown to exceed those that are predicted by the voltage values formed from the outputs expected from a hypothetical e-bomb.

Shielding on the signal and LAN cables played a very important role on protecting the sensitive electronic devices connected to those nodes from transient current surges created by the e-bomb. Therefore, it is concluded that shielding is a very important factor for such an IADS to be adequately protected against EMI or EMP effects. In this analysis, a 30 dB shield was assumed for signal and LAN cabling, and it appears easily achievable. This study determined that the degree of shielding (30 dB) was very effective on the electronic schemes considered. On the other hand, shielding can sometimes be penetrated because of any cracks or gaps at any connection points. A very effective shielding method, including an assurance margin, should be selected since it plays such an important role, and precautions should be taken against those cracks and gaps on the cables in order to eliminate the penetrations. A starting point for that shielding requirement would appear to be the 30 dB shield used in this study for those cables.

A previously published, and open-source in format, theoretical design of an e-bomb (Kopp, 1996) showed that some components such as power

generator, vircator, and antenna shape/diameter, along with delivery system configurations are very challenging aspects that must be tackled to implement the concept of an e-bomb. A limiting set of factors for the e-bomb design investigated in this study were the cut-off frequency and the length of the waveguide feeding the dish antenna, because they determine the cut-off frequency and the overall e-bomb spectral performance range. If another method could solve this problem, and support extending the frequency coverage over what was explored here could be developed, then the simulated e-bomb effects could be even more of a deterrent.

In the Modeling and Electromagnetic Coupling chapter, the data determination tables provide a very good opportunity for examining the best coupling values associated with this study. Those coupling data values were carefully computed from first principles and expected to accurately depict the modeled configuration since they were calculated from accepted and proven CEMPAT transmission-line coupling program runs, and the range of all model values were all within reasonable limits. Eventually, those tables are expected to be very beneficial for understanding the variations and behaviors of those true coupling data should it ever be collected.

From an operational view, this study shows the possible benefits of using an e-bomb in an attack against an IADS system. In delivery, the attack can most likely involve only one aircraft that is positioned well above the IADS' effective altitude range but still be expected to have an effect on the entire distributed system as analyzed in this study.

It is claimed in this study that six separate DMPIs could be taken out of the theater by the e-bomb attack with only one pass over the target. Even if the maximum expected effects could not be achieved, it could cause temporary malfunction on the target system, and that provides an advantage for the rivals. On the contrary, this study claims that an attack against the same target, which has six nodes, using conventional munitions will need six passes or six separate

attacks to the target. This situation leads an operation plan to consider much more criteria, i.e., more support, more protection, more cost, than it does for an e-bomb attack.

In addition, assuming that the system of interest was not mobile and its nodes were covered with very robust fixed facilities that conventional munitions could not penetrate, an e-bomb attack could be desired since it does not deal with the features associated with the physical infrastructures but, instead, interacts with and effects the node electronic equipment.

In addition, the enemy may not even realize an e-bomb attack on electronically equipped targets has occurred since the platform is dropped off high above the ground and the electromagnetic propagation is a transparent threat that travels at the speed of the light.

B. RECOMMENDATIONS AND FUTURE WORK

Reliability of the electronic devices involved in a modern command and control system is a broad area in the open literature; therefore, it might be possible to find another useful study with respect to the issue of the reliability of devices which would lead to an assessment of the e-bomb created current or voltage on the target system and further literature research. That research might indicate either increased, or decreased reliability would be expected other than that which was assumed in this study. One finding of this study was that the assumed shielding of 30 dB was very effective against the e-bomb coupling. With respect to reliability, a good follow-up study might look into whether that 30 dB shield would be expected to remain effective over the lifecycle of modern electronic equipped systems, which can cover several decades.

In this study, although the threshold level tables, which are created by the Defense Nuclear Agency, used to compare with the e-bomb formed voltage, power, and energy is a very feasible benchmark, some other theoretical threshold value tables that best fit the real comparison needs of e-bomb formed

values should also be created. Those extensions to this study need to include investigations into the direct feasibility of the assumed waveshape, pulse duration, and operating frequency of the e-bomb. For example, the table used in this study only covers 200 MHz, 600 MHZ, and 900 MHz frequency values, and it is still feasible with the e-bomb in this study to, perhaps, have an overall range of operating frequencies that would go as low as 200 MHz. In addition, the table is created with respect to 100 ns pulse duration while created currents pulse durations last only around 60 ns. Although having 60 ns can be considered a benefit for a more precise energy comparison result, it is still not the best match with the table. If it were more than 100 ns and the energy threshold level was exceeded, then it would cause conflictions that it might have thought as it was because of the longer pulse duration.

Therefore, it would be more beneficial to create a threshold level table, which is particularly relevant to the e-bomb waveshape, frequency range, and created current pulse duration. Another opportunity for creating such a theoretical table would provide that the e-bomb design considerations and decisions would be based on the e-bomb specification, configuration, and operational feature requirements with respect to its wave shape, frequency range, instead of on available data of threshold upset/damage effects. Therefore, the e-bomb platform shape, operational features and specifications of the e-bomb, and the created table would best match each other. If realizable, the weapon design could be extended into new performance regions, previously thought impractical or impossible.

APPENDIX: RESPONSE ANALYSIS VIA TRANSMISSION LINE MODELING

This following was written by Lt. Col. Terry Smith, military faculty, Information Sciences Department, Graduate School of Operations and Information Sciences, at the Naval Postgraduate School, to complement the author's work.

Using transmission line theory and an appropriate set of first principle equations, bulk cable currents induced by threat electromagnetic environments on single and/or multiple conductors near the earth's surface can be analyzed. Formulas for the first principles are provided in this Appendix describing the electromagnetically coupled currents, voltages and impedance relationships used in a transmission-line model meant to represent "real" system topologies and configurations for an Integrated Air Defense System (IADS).

a) CEMPAT Introduction:

The transmission-line modeling program used in support of this report is the Harry Diamond Laboratories (now Army Research Laboratory) developed CEMPAT code. CEMPAT (which was created and refined by one of HDL's support contractors, Mission Research Corporation) provides capabilities to simulate the electromagnetic effects on a distributed transmission line system, which includes the interaction of single and multiple conductors, along with provisions for handling ground interaction effects and using a user-defined electromagnetic field operating environment. This section briefly describes the CEMPAT simulation program which was designed and developed to calculate voltages and currents on the intrasite conducting power and signal cables that may appear in deployed mobile ground based C^4I facilities.

- Background:

In the early 1990's, the U.S. Army's Harry Diamond Laboratories (HDL) conducted a series of experimental and analytic efforts in support of their Defense Standards and Specifications Program (DSSP). HDL's goal was to develop and demonstrate high altitude electromagnetic pulse (HEMP) hardening technologies for transportable ground-based command, control, communications, and intelligence systems (C^4I) with inherent time-urgent functions. HDL's focus was the development of standards and specifications appropriate for transportable systems. In addition, the HDL MIL-STD-188-125 Technical Working Group was involved in resolving several technical issues essential for the preparation and support of a draft military standard appropriate for transportable systems with time-urgent functions.

- Scope:

Modeling & Simulation (M&S) of critical-function transportable systems must be appropriate for all types of expected deployed mobile system interface connections and must also address the range of possible electromagnetic threat environments that the deployed system may reasonably be expected to encounter. To that end, an existing modeling tool that is readily available, and has demonstrated performance in

handling all perceived system configurations (cable lengths, diameters, loading, and soil conditions in the vicinity of cabling) was desired. In addition, an important consideration in choosing the modeling tool to be used for assessment of the Integrated Air Defense System (IADS) susceptibility to an E-bomb is that the electromagnetic environment threat coverage capability must be scalable and deemed appropriate for the evaluation from the perspective of considering all possible angles of incidence and threat incident field polarization from a hypothetical E-bomb source. All of these considerations were account for in the choice to use CEMPAT (a tool that the advisor of this thesis helped develop, and that was extensively used in HDLs specifications and standards program).

- Approach

The general approach was to analytically determine the expected voltages and currents through the use of validated transmission line coupling codes (CEMPAT). Parameter variations were initially used to investigate the consequences to these coupled currents and voltages as a function of field orientation, cable loading configurations, cable lengths, and soil parameter conditions. Results were noted and used to tweak (or optimize) the target system configuration used throughout this study. A ``reasonable worst case" current and voltage situation was identified in the cable analysis to bound from above the expected system response conditions and to enhance confidence in the overall study findings.

In summary, the problem at hand involved the proper definition of the equivalent threat sources, the geometry and configuration of the operational IADS system targeted by the electromagnetic threat, and a summary of the expected currents and voltages that would result from a "representative" coupling model. That defined representative model was then used in a carefully defined electromagnetic environment to represent expected outputs from an E-bomb electromagnetic field environment. Details are provided in the body of this report as to the assumptions made to create this electromagnetic environment and the modeled IADS configuration.

- General Problem Considerations

The HDL-developed CEMPAT code was used to calculate these cable current and voltage responses. As discussed previously, CEMPAT was developed by the Army as a general-purpose analytical assessment tool for typical HEMP problems. CEMPAT was written in FORTRAN 77 and compiled for use by personal computers. CEMPAT includes an integrated set of subroutines that allow users to define the electromagnetic environment (wave shape features, angle of arrival and ground electromagnetic conditions) and setup the configuration of a simulated IADS system cable with user adjustable parameters such as diameter, length, and complex load values on each end of the modeled cable. CEMPAT output formats are available in either the time-domain or frequency-domain and are formatted as plot files that describe the coupled current and voltage anywhere along the cable length. CEMPAT evaluations are

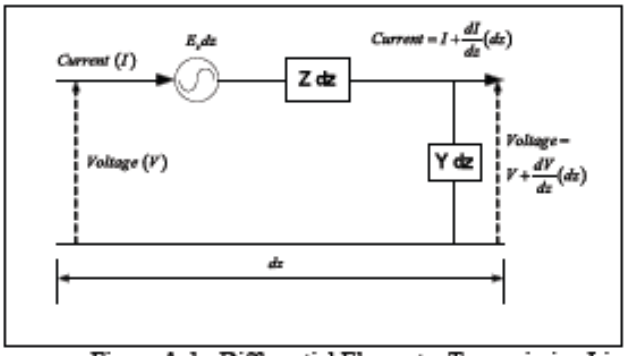

Figure A-1: Differential Element – Transmission Line

limited to the conditions leading to a horizontally polarized incident electric field. This is not expected to be a significant limitation, however, because previous studies have indicated that the condition leading to large coupled currents from a vertically polarized incident wave are appropriate for angles of attack that are very near grazing. Since the electromagnetic environment threat for this study will arrive from near-overhead, peak currents from vertical polarization drive are not expected.

b) Transmission line equations[1]:

In the analysis of electromagnetic wave coupling to transmission lines, the source driving the line is distributed along it's length. An elemental length, *dz*, of a longer transmission line being driven by an elemental voltage source is shown in Figure A-1. For time-harmonic signals, voltage and current along the transmission line element are described using the following expressions:

$$\frac{\partial V}{\partial z} = E_z - Iz; \quad \frac{\partial I}{\partial z} = -VY;$$

where:

V = *Voltage*, I = *Current*, E_z = z – *directed Electric f ielc*

z = distance *along the transmission line*

After differentiating the *Voltage* equation, and substituting the result back into the *Current* equation, we arrive at a pair of second-order, linear, differential equations that describe the voltage & current at any position along the elemental segment of transmission line:

$$\frac{\partial^2 V}{\partial z^2} - \gamma^2 V = \frac{\partial E_z}{\partial z}; \quad \frac{\partial^2 I}{\partial z^2} - \gamma^2 I = E_z Y$$

where:

γ = *complex propagation* constant= $\alpha + j\beta$

$$\alpha = \textit{attenuation}\ \text{constant} = \omega\left\{\frac{\mu\varepsilon_c}{2}\left[\sqrt{1+\left(\frac{\sigma}{\omega\varepsilon_c}\right)^2}-1\right]\right\}^{0.5}$$

$$\beta = \textit{phase}\ \text{constant} = \omega\left\{\frac{\mu\varepsilon_c}{2}\left[\sqrt{1+\left(\frac{\sigma}{\omega\varepsilon_c}\right)^2}+1\right]\right\}^{0.5}$$

σ = *conductor conductivity*; ω = *radian f requency*

$$\varepsilon_c = \textit{complex}\ \text{dielectric constant} = \varepsilon_o\left(\varepsilon_r - \frac{j\sigma}{\omega\varepsilon_o}\right); \quad \varepsilon_r = \textit{relative}\ \text{dielectric constant};$$

$$\varepsilon_o = \textit{f ree- space}\ \text{dielectric constant} = 8.854\times10^{-12}\left(\frac{F}{m}\right)$$

[1] Edward F. Vance, "*Coupling to Cables*", DNA Handbook, Chapter II, December 1974.

Each of these second-order, linear, differential equations has associated with it two linearly independent solutions (a homogeneous and particular solution). Solving the developed relationship for the current *I (z)*:

$$I(z) = I(\text{homogeneous}) + I(particular) = I_h(z) + I_p(z)$$

where:

$$I_h(z) = K_1 \exp^{-\gamma z} + K_2 \exp^{+\gamma z}; \quad I_p(z) = P(z)\exp^{-\gamma z} + Q(z)\exp^{+\gamma z}$$

$$\therefore \quad I(z) = \left[K_1 + P(z)\right]\exp^{-\gamma z} + \left[K_2 + Q(z)\right]\exp^{+\gamma z}$$

where:

$$P(z) = \frac{1}{2Z_o}\int_{z_1}^{z} E_s(z')\exp^{+\gamma z} dz'; \quad Q(z) = \frac{1}{2Z_o}\int_{z}^{z_2} E_s(z')\exp^{-\gamma z} dz'$$

$$Z_o = \sqrt{\frac{Z}{Y}} = \text{ line characteristic impedance} = 60\cosh^{-1}\left(\frac{2h}{a}\right)$$

The characteristic impedance for the modeled transmission-line is appropriately represented as a common-mode (or bulk cable transmission line) characteristic impedance for a cylindrical conductor over an infinite conducting ground plane[2] as is shown in Figure A-2.

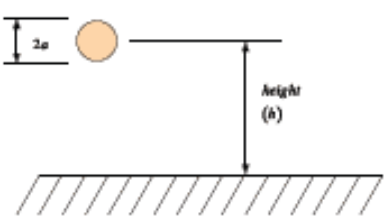

Figure A-2: Impedance Geometry

The two constants K_1 and K_2 are determined from the impedances of the cable (Z_1 and Z_2) located at distances $z = z_1$ and $z = z_2$, where $z_2 > z_1$ (see Figure A-3) as in conventional transmission-line theory.

$$K_1 = \rho_1 \exp^{\gamma z_1}\left[\frac{\rho_2 P(z_2)\exp^{-\gamma z_2} - Q(z_1)\exp^{+\gamma z_2}}{\exp^{+\gamma(z_2 - z_1)} - \rho_1\rho_2\exp^{-\gamma(z_2 - z_1)}}\right]$$

$$K_2 = \rho_2 \exp^{-\gamma z_2}\left[\frac{\rho_1 Q(z_1)\exp^{+\gamma z_1} - P(z_2)\exp^{-\gamma z_1}}{\exp^{+\gamma(z_2 - z_1)} - \rho_1\rho_2\exp^{-\gamma(z_2 - z_1)}}\right]$$

$$\rho_1 = \frac{Z_1 - Z_o}{Z_1 + Z_o}; \quad \rho_2 = \frac{Z_2 - Z_o}{Z_2 + Z_o}; \; ref\,lection\,coef\,f\,icen(s\;\; l\&t\;\; ri\}$$

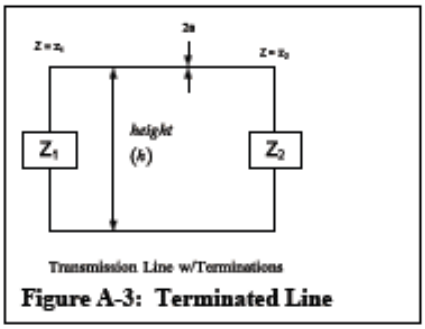

Figure A-3: Terminated Line

A similar development using the second-order differential equation for voltage yields:

$$V(z) = Z_o\left\{\left[K_1 + P(z)\right]\exp^{-\gamma z} - \left[K_2 + Q(z)\right]\exp^{+\gamma z}\right\}$$

Where all constants are derived in the same fashion as those previously identified in the current derivation.

[2] S.A. Schelkunoff and H.T.Friis, "*Antennas Theory and Practice*", John Wiley & Sons: NY, 1952.

Specific Evaluation Case: Derivation of the current expression for a loss-less ($\alpha = 0$, $\gamma = j\beta$) transmission line of overall length equal to L starting at $z_1 = 0$ and extending to $z_2 = L$ (and evaluating the current at the two ends of the line).

$$P(0)=0;\quad P(L)=\frac{E_z}{2\gamma Z_o}\left[\exp^{+\gamma L}-1\right];\quad Q(0)=\frac{-E_z}{2\gamma Z_o}\left[\exp^{-\gamma L}-1\right];\quad Q(L)=0;$$

$$I(0)=\left[K_1+0\right]+\left[K_2+Q(0)\right]=K_1+K_2+Q(0)$$

$$I(L)=\left[K_1+P(l)\right]\exp^{-\gamma L}+K_2\exp^{+\gamma L}$$

Solving the above expression for the current at the left end of this transmission line (i.e. *I(0)*) and using the previously defined reflection coefficients, constants *P(z)* and *Q(z)* for each end of the cable and considering the expression for the applied electric field:

$$I(0)=\frac{\rho_1\rho_2P(L)\exp^{-\gamma L}-Q(0)\rho_1\exp^{+\gamma L}}{\exp^{+\gamma(L)}-\rho_1\rho_2\exp^{-\gamma(L)}}+\frac{\rho_1\rho_2Q(0)\exp^{-\gamma L}-\rho_2P(L)\exp^{-\gamma_1}}{\exp^{+\gamma L}-\rho_1\rho_2\exp^{-\gamma L}}+Q(0)$$

$$I(0)=\frac{\rho_1\rho_2P(L)\exp^{-2\gamma L}-Q(0)\rho_1+\cancel{\rho_1\rho_2P(L)\exp^{-2\gamma L}Q(0)}-\rho_2P(L)\exp^{-2\gamma L}+Q(0)\left[1-\cancel{\rho_1\rho_2P(L)\exp^{-2\gamma L}}\right]}{1-\rho_1\rho_2\exp^{-2\gamma L}}$$

$$I(0)=\frac{(\rho_1-1)\rho_2P(L)\exp^{-2\gamma L}+Q(0)(1-\rho_1)}{1-\rho_1\rho_2\exp^{-2\gamma L}}=\frac{(1-\rho_1)\left[Q(0)-\rho_2P(L)\exp^{-2\gamma L}\right]}{1-\rho_1\rho_2\exp^{-2\gamma L}}$$

$$I(0)=\frac{(1-\rho_1)\left[\frac{-E_z}{2\gamma Z_o}\left[\exp^{-\gamma L}-1\right]-\rho_2\frac{E_z}{2\gamma Z_o}\left[\exp^{+\gamma L}-1\right]\exp^{-2\gamma L}\right]}{1-\rho_1\rho_2\exp^{-2\gamma L}}$$

$$I(0)=\frac{E_z(1-\rho_1)}{2\gamma Z_o}\frac{\left[1-\exp^{-\gamma L}-\rho_2\left[\exp^{-\gamma L}-\exp^{-2\gamma L}\right]\right]}{1-\rho_1\rho_2\exp^{-2\gamma L}}$$

Working with the leading term that describes the applied field:

$$\frac{E_z(1-\rho_1)}{2\gamma Z_o}=\frac{E_z\left(\frac{\cancel{Z_1}+Z_o-\cancel{Z_1}+Z_o}{Z_1+Z_o}\right)}{2\gamma Z_o}=\frac{2E_zZ_o}{2\gamma Z_o(Z_1+Z_o)}=\frac{E_z}{\gamma(Z_1+Z_o)}$$

$$\therefore\quad I(0)=\frac{E_z}{\gamma(Z_1+Z_o)}\frac{\left[1-\exp^{-\gamma L}-\rho_2\left[\exp^{-\gamma L}-\exp^{-2\gamma L}\right]\right]}{1-\rho_1\rho_2\exp^{-2\gamma L}}$$

A similar development for the current expression at the end of the transmission line ($z = L$) follows:

$$I(L)=\left[K_1+P(L)\right]\exp^{-\gamma L}+K_2\exp^{+\gamma L}$$

$$I(L)=\frac{\rho_1\rho_2P(L)\exp^{-2\gamma L}-Q(0)\rho_1\exp^{+\gamma L}}{\exp^{+\gamma(L)}-\rho_1\rho_2\exp^{-\gamma L}}+\frac{\rho_1\rho_2Q(0)-\rho_2P(L)}{\exp^{+\gamma L}-\rho_1\rho_2\exp^{-\gamma L}}+P(L)\exp^{-\gamma L}$$

$$I(L)=\frac{\cancel{\rho_1\rho_2P(L)\exp^{-2\gamma L}}-Q(0)\rho_1\exp^{-\gamma L}-\cancel{\rho_1\rho_2P(L)\exp^{-2\gamma L}}+P(L)\exp^{-\gamma L}+Q(0)\rho_1\rho_2\exp^{-\gamma L}-\rho_2P(L)\exp^{-\gamma L}}{1-\rho_1\rho_2\exp^{-2\gamma L}}$$

$$I(L)=\frac{-Q(0)\rho_1\exp^{-\gamma L}+P(L)\exp^{-\gamma L}+Q(0)\rho_1\rho_2\exp^{-\gamma L}-\rho_2P(L)\exp^{-\gamma L}}{1-\rho_1\rho_2\exp^{-2\gamma L}}$$

$$I(L)=\frac{Q(0)\rho_1\exp^{-\gamma L}\left[\rho_2-1\right]+P(L)\exp^{-\gamma L}\left[1-\rho_2\right]}{1-\rho_1\rho_2\exp^{-2\gamma L}}=\frac{\left[1-\rho_2\right]\left[P(L)\exp^{-\gamma L}-Q(0)\rho_1\exp^{-\gamma L}\right]}{1-\rho_1\rho_2\exp^{-2\gamma L}}$$

$$I(L)=\frac{\left[1-\rho_2\right]\left[\frac{E_s}{2\gamma Z_o}\left[\exp^{+\gamma L}-1\right]\exp^{-\gamma L}+\frac{E_s}{2\gamma Z_o}\left[\exp^{+\gamma L}\right]\rho_1\left[\exp^{+\gamma L}-1\right]\right]}{1-\rho_1\rho_2\exp^{-2\gamma L}}$$

$$I(L)=\frac{E_s\left[1-\rho_2\right]}{2\gamma Z_o}\left[\frac{1-\exp^{-\gamma L}+\rho_1\exp^{-2\gamma L}-\rho_1\exp^{-\gamma L}}{1-\rho_1\rho_2\exp^{-2\gamma L}}\right]$$

$$I(L)=\frac{E_s}{\gamma(Z_2+Z_o)}\left[\frac{1-\exp^{-\gamma L}+\rho_1\left(\exp^{-2\gamma L}-\exp^{-\gamma L}\right)}{1-\rho_1\rho_2\exp^{-2\gamma L}}\right]$$

These two expressions above (*I(0) & I(L)*) are the desired results leading to the CEMPAT code that is used to describe the currents at the beginning and at the end of a transmission line of length equal to L. These currents are directly proportional to the z-component of the incident electric field, which will be described next.

c) Description of the Incident Field (derived from Vance, pages 11-19 thru 11-25):

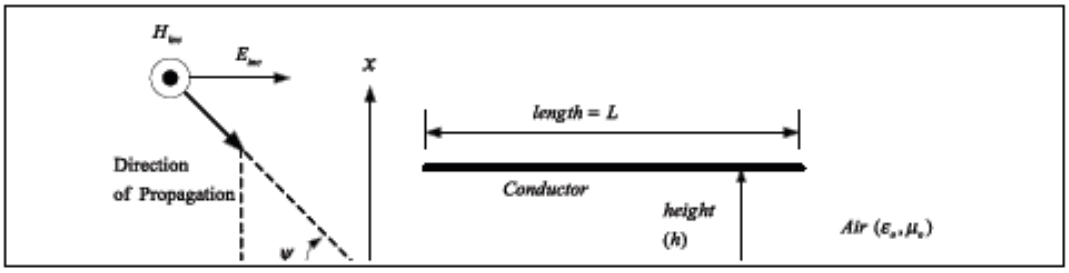

For horizontally polarized fields, the electric field component in the direction of the wire (E_s) is used to excite the transmission line elevated above the earth at height (*h*) (See Figure A-4). Assuming a loss-less case, the total applied electric field (incident + reflected) using a double exponential waveshape for the incident "threat" waveform can be identified as:

$$E_s(h,\psi,\phi,z,\omega) = E_i(j\omega)\sin(\psi)\left[1+\Gamma_h \exp^{-2j\beta h\sin(\psi)}\right]\exp^{-j\beta z\cos(\phi)\cos(\psi)}$$

$$= E_i(j\omega)\sin(\psi)\left[1+\Gamma_h \exp^{-\left(\frac{2j\omega h\sin(\psi)}{c}\right)}\right]\exp^{-\left(\frac{2j\omega z\cos(\phi)\cos(\psi)}{c}\right)}$$

where:

$$\Gamma_h = \frac{\sin(\psi)-\sqrt{\varepsilon_r\left(1+\frac{\sigma}{j\omega\varepsilon}\right)-\cos^2(\psi)}}{\sin(\psi)+\sqrt{\varepsilon_r\left(1+\frac{\sigma}{j\omega\varepsilon}\right)-\cos^2(\psi)}}; \quad E_i(j\omega) = E_o\left[\frac{1}{C_1+j\omega}-\frac{1}{C_2+j\omega}\right]$$

Note: $\cos(\phi)\cos(\psi)$ = direction cosine for a TEM-wave approaching the transmission line along the x-axis (see Figure A-4) from directly above (broadside incidence):

and:

$\omega = 2\pi f = radian\ frequency\left(\frac{radians}{\sec}\right)$

$\phi = azimuth\ angle\ of\ incidence\ from\ the\ x\text{-}\ axis$

$\Psi = elevation\ angle\ of\ incidence\ from\ the\ soil\ surface$

Horizontal Polarization refers to an incident electric field parallel to the plane of the earth's surface

$\beta = k = \text{phase constant} = \frac{2\pi}{\lambda} = 2\pi f\sqrt{\mu\varepsilon} = \frac{\omega}{c}$

$\varepsilon_c = complex\ permittivity\ of\ the\ medium\left(for\ free\ space\ \varepsilon_c = \varepsilon_o = 8.85x10^{-12}\left(\frac{F}{m}\right)\right)$

$\mu_c = complex\ permeability\ of\ the\ medium\left(for\ free\ space\ \mu_c = \mu_o = 4\pi x10^{-7}\left(\frac{H}{m}\right)\right)$

$\sigma = conductivity\ of\ the\ soil\left(\frac{S}{m}\right)$

E_o, C_1 *and* C_2 are constants used to describe the generalized "threat" waveform

A.1: HEMP THREAT ENVIRONMENT

As indicated in the coupling expressions above, a threat field must be defined for the coupling analysis effort. For this study, the waveshape for the hypothetical E-Bomb (which doesn't exist) was derived based on an unclassified representation for the high-altitude electromagnetic pulse (HEMP) threat.

HEMP was used because it is known to produce hostile operating environments and also is well-established in terms of its usage and utility. The Department of Defense High-Altitude Electromagnetic Pulse (HEMP) environment standard, DoD-STD-2169[3], identifies the time dependent electric-field environment for the early-time (E_1 - less than 1 millisecond), intermediate-time (E_2 - 1 microsecond to 1 second), and late-time (E_3 - greater than 1 sec) phases of HEMP. In general, high altitude refers to burst elevations exceeding 30 km above ground level. Unclassified versions of the DoD-STD-2169 environment are readily available and commonly used. DoD-STD-2169's early-time phase, or E_1, is of principal interest for relatively small objects such as the IADS configuration.

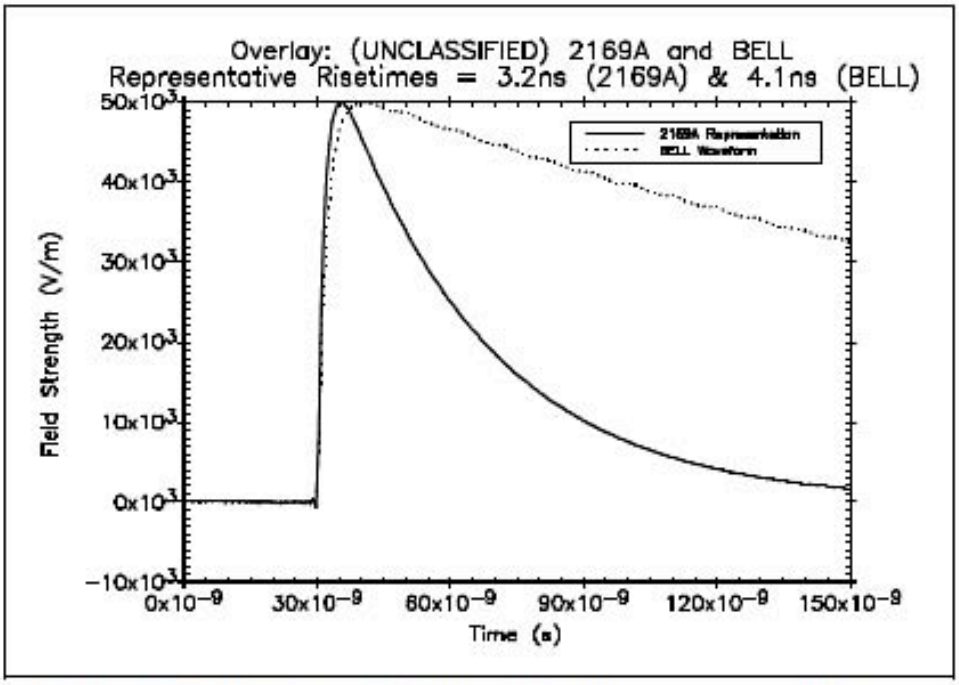

Figure A-5. HEMP early-time criterion environment representations.

To illustrate the early-time HEMP E_1 fields, a qualitative representation of two time dependent criterion electric field waveshapes related to the criterion environments of interest to this report are shown in Figure A-5. The HEMP threat preceding DoD-STD-2169 is included (dotted line) along with a representative fast pulse waveshape that will be used throughout this work. The earlier HEMP environment[4] was the so-called "Bell" waveform which is analytically represented by the difference of

[3] DoD-STD-2169A, "*Military Standard, High-Altitude Electromagnetic Pulse Environment*," December 1987 (SECRET).

[4] Sherman, et.al., EMP Engineering and Design Principles, Bell Laboratories, Loop Transmission Division, 1975.

two exponentials with peak electric field of about 50 kV/m, an approximate risetime of 4 nanoseconds, an exponential decay time of 250 nanoseconds and fluence (energy flow across a unit area) of about 90 micro Joules per square centimeter. Contrast this waveshape with the fast-rise pulse for DoD 2169A. Note that there is significant change in both variation and content between these two waveshapes. A generalization of the kinds of changes introduced by DoD-STD-2169 include: 1) a faster risetime, 2) narrowing of the pulse width and therefore less total waveform energy, and 3) associated increased high frequency spectrum content. Both waveshapes shown in Figure A-5 are UNCLASSIFIED, qualitative in nature, representations of classified criterion environments.

The two HEMP threats shown in Figure A-5 that are applicable to our assessment of IADS hardening are described analytically below:

1) the Bell handbook HEMP threat (which is probably a good representation for most of the IADS system components), and

2) an UNCLASSIFIED representation of the E_1 component of the 2169A HEMP threat (titled *EMP-1*).

Both HEMP threats are analytically represented as double exponential waveforms with parameter coefficients as follows:

$$E(t) = E_1 * \left(\exp^{-\alpha t} - \exp^{-\beta t}\right) \quad \left(\frac{V}{m}\right)$$

$$E(\omega) = E_1 * \left[\frac{1}{\alpha + j\omega} - \frac{1}{\beta + j\omega}\right] \left(\frac{V*s}{m}\right)$$

Where:

$$E_1 = \frac{E_0}{\exp^{-\alpha t_m} - \exp^{-\beta t_m}} \; ; \; t_m = \frac{\ln\left(\frac{\alpha}{\beta}\right)}{\alpha - \beta}$$

EMP-1:		*BELL:*	
E_0	$= 50.0E3\ V/m$	E_0	$= 50.0E3\ V/m$
α	$= 3.0E7\ s^{-1}$	α	$= 4.0E6\ s^{-1}$
β	$= 4.76E8\ s^{-1}$	β	$= 4.76E8\ s^{-1}$
$\left(\frac{E_1}{E_0}\right)$	$= 1.285$	$\left(\frac{E_1}{E_0}\right)$	$= 1.050$

A.2: WAVEFORM NORM ATTRIBUTES

The system response (voltage, current, charge, etc.) stemming from HEMP excitation is called stress. The time-dependent stress waveform F(t) can be expressed as:

$$F(t) = \left| A_{stress} \right| \; x \; f(t$$

where: f(t) is a normalized waveshape descriptor and A_{stress} is a positive valued stress amplification factor with the engineering units of (volts, current, charge, etc.).

There is considerable difficulty in manipulating and storing large numbers of stress data files. Each response waveform may consist of tens of thousands of data points and is unique from all other response files. The unique features of each waveform is also different (i.e., amplitude, energy, frequency spectrum, etc.). To overcome difficulties in working with such a large ensemble of data, waveform norm attributes (norms) are often used to describe certain important waveform features[5,6]. These norms have proven to be much more convenient when comparing or archiving responses from modeling and analysis or testing efforts. Norms are scalar "*figures of merit*" that measure a property or an attribute of a waveform. These norms (or properties) are selected to be representative of the characteristics of a waveform that are relatable to damage mechanisms in equipment (generally electronic equipment).

The norms described here and shown in Table A-1 provide several measures of the size of a waveform. For each of the five norms a mathematical description, a title and acronym, a frequency bound (where one exists), and a short description of the related failure modes where this particular norm might indicate is given in Table A-1. Norms are calculated from experimental or analytic waveforms by translating these mathematical descriptions into numerical algorithms. Inspection of the mathematical operations show that they highlight not only the waveform amplitude but the waveform variation produced primarily by the high frequency components and the signal content produced primarily by the low frequency waveform components.

The Peak Absolute Amplitude (PAA) characterizes the peak current of the waveform. Peak Absolute Derivative (PAD) characterizes maximum high frequency content and time rate of change. Peak Absolute Impulse (PAI) is representative of maximum charge transfer. Rectified Impulse (RI) is related to total charge transfer without regard to direction. Root Action Integral (RAI) is related to energy absorbed (resistive heating) by the component.

The general assumption is made that all reasonable damage mechanisms are covered when describing a waveform by this five norm set. Damage assessment is made by considering the signal energy content. The total energy content of a stress waveform at a junction is represented by the root action integral and rectified impulse norm attributes, respectively. Thus, two of these five norm quantities identified measure the capability of an HEMP waveshape to damage a device directly exposed to it. The other norms (peak absolute amplitude, peak absolute derivative, and peak absolute impulse) are required because there are other failure mechanisms (upset for example) and because devices not directly exposed to the stress can

---

[5] "*B-1B EMP Test Program Concept Plan*", Air Force Weapons Laboratory, Kirtland AFB, NM, 31 March 1986.

[6] R.E. Thomas, et.al., "*Waveform Norm Attributes White Paper*", Air Force Weapons Laboratory, Kirtland AFB, NM, 11 April 1989.

also be damaged. In these latter situations energy is not the relevant measure of the capability of the stress to induce malfunctions. Hence other norm attributes are required to cover these faults.

Upset assessment related to a signal are dependent upon the parameters of a waveform that affect the state of a logic circuit. State changes are functions of logic timing, logic threshold levels, and software control features. Clearly, the peak absolute value of a stress waveform will directly affect the potential to cross a logic threshold level and possible toggling the logic state. Previous norm assessment programs[7] have shown that there is also an inverse proportionality to frequency relationship when calculating the potential for system upset. Therefore, failure is more strongly influenced by the variation of the stress waveform at higher frequencies than the stress signal alone. In other words, high frequency upsets are controlled by the derivative of the stress. The derivative of the stress is bounded from above by the peak derivative. The results from the mentioned norm assessment program also showed that "unreasonable" values are highly dependent upon time integrations of stress. The probability of observed failures then increases with increases in the peak absolute impulse norm and the root action integral norm.

To sum, experimental data employ that no single norm is an adequate descriptor of the controlling factors leading to failure and that the "size" of the stress must be described by an ensemble of attributes that can potentially lead to failures.

The set of five mathematical norm attributes used in this report are described below and identified in Table A-1 (where the units associated with stress current is shown). Strict conformance with mathematical norm properties is important to ensure the integrity of the scalar and the information that it reprepresents as it is processed using normal signal processing methods. These required properties include:

A norm attribute (N) of a waveform *f(t)* is written as:

$$N = \|f(t)\|$$

Norm attributes must have the following properties:

$$\|f(t)\| \geq 0 \text{ with } \|f(t)\| = 0 \text{ if } f(t) = 0$$

- This property requires that the norm attribute have a positive value with no bias

$$\|A f(t)\| = A\|f(t)\|$$

- The norm must be linearly scalable.

$$\|f_1(t) + f_2(t)\| \leq \|f_1(t)\| + \|f_2(t)\|$$

- and finally, the norm of the superposition of two waveforms must be less than or equal to the sum of the norms of each waveform.

---

[7] R.J. Hansen, *"Subsystem EMP Strength Verification Methods: Upset Detection and Evaluation for Military Systems,"* DC-FR-4088.330-1, Kaman Sciences Corporation, Dikewood Division, Albuquerque NM (9 October 1988).

Table A-1. Waveform Norm Attributes

NORM	NAME	TIME	FREQUENCY	Related Failure Modes
PAA (A)	Peak Absolute Amplitude	$\lvert f(t)\rvert_{max}$	$\leq \frac{1}{\pi}\int_{-\infty}^{\infty}\lvert F(\omega)\rvert d\omega$	- In band coupling - Toggling of some digital circuitry - Dielectric breakdown
PAD $\left(\frac{A}{s}\right)$	Peak Absolute Derivative	$\left\lvert \frac{df(t)}{dt}\right\rvert_{max}$	$\leq \frac{1}{\pi}\int_{-\infty}^{\infty}\lvert \omega F(\omega)\rvert d\omega$	- Wire to wire coupling - Below band coupling - ESA voltage breakdown
PAI $(A \cdot s)$	Peak Absolute Impulse	$\left\lvert \int_{-\infty}^{t} f(\tau)d\tau\right\rvert_{max}$	$\leq \frac{1}{\pi}\int_{-\infty}^{\infty}\left\lvert \frac{F(\omega)}{\omega}\right\rvert d\omega$	- Above band coupling - Toggling of some digital circuitry - Peak charge transfer
RI $(A \cdot s)$	Rectified Impulse	$\int_{-\infty}^{\infty}\lvert f(t)\rvert dt$	No frequency bound	- Adiabatic junction heating - Stacked above band coupling - Some voltage breakdown effect
RAI $\left(A \cdot s^{0.5}\right)$	Root Action Integral	$\sqrt{\int_{-\infty}^{\infty} f(t)^2 dt}$	$\sqrt{\frac{1}{\pi}\int_{-\infty}^{\infty}\lvert F(\omega)\rvert^2 d\omega}$	- Adiabatic joulean heating - Metalization burnout

LIST OF REFERENCES

Abrams, M. (2003). Dawn of The E-bomb. *IEEE spectrum*: 26–30.

Albuquerque, N.M. (2009). Boeing laser avenger shoots down unmanned aerial vehicle in tests. Retrieved May 27, 2009, from http://boeing.mediaroom.com/index.php?s=43&item=504

Benford, James, Swegle, John A., & Schamiloglu, Edl. (2007). *High Power Microwaves*. 2nd ed. New York, London: Taylor and Francis.

BLU-82 Commando Vault. Daisy clutter. Retrieved June 16, 2009, from http://www.globalsecurity.org/military/systems/munitions/blu-82.htm

Bombas Guidas. Retrieved June 23 2009, from http://www.revistanaval.com/armada/flotaero/gbu.htm

CBS News March 25, 2003. Retrieved May 27, 2009, from http://www.cbsnews.com/stories/2003/03/25/iraq/main546081.shtml.

Defense Talk. Retrieved June 16, 2009, from http://www.defencetalk.com/pictures/data/4854/medium/Nellis_07_BLU-82_15000_Bomb-271.jpg

Defense Technical Information Center. (n.d.) Retrieved June 25, 2009, from http://www.dtic.mil/cgibin/GetTRDoc?AD=ADA497498&Location=U2&doc=GetTRDoc.pdf

Deveci, Mert Bayram. (2007). *Directed Energy Weapons: Invisible and Invincible.* Master's thesis, Naval Postgraduate School, Monterey, CA.

DNA EMP Engineering Handbook Tor Ground Based Facilities. (1986). *Volume II-Design and Engineering*, DNA-H-86-60-V2, Defense Nuclear Agency, Washington, DC 20305=1000.

Determining The Focal Length of a Parabolic Dish. Retrieved June 20, 2009, from http://www.satsig.net/focal-length-parabolic-dish.htm.

Ertekin, Necati. (2008). *E-Bomb : The Key Element Of The Contemporary Military-Technical Revolution*. Master's thesis, Naval Postgraduate School, Monterey, CA.

Global Security. Retrieved June 24, 2009, from http://www.globalsecurity.org/military/library/policy/army/fm/20-32/chap1.html.

Headquarters Department of Army. (2002). *Patriot Battalion and Battalion Operations.* FM 3-01.85. Retrieved July 11, 2009, from http://www.militarynewbie.com/pubs/FM%203-01.85%20Patriot%20Battalion%20and%20Battery%20Operations.pdf.

Ianoz, Michel. (2008). *A Comparison Between HEMP and HPM Parameters. Effects and Mitigation Methods*. 2008 Asia-Pacific Symposium on Electromagnetic Compatibility & 19th International Zurich Symposium on Electromagnetic Compatibility, Singapore.

Inan, Umran S., & Inan, Aziz S. (2000). *Electromagnetic waves*. Prentice Hall, Inc.

Introduction to the Patriot Air Defense Missile System. Retrieved July 11, 2009, from http://www.scribd.com/doc/2900138/ad0415a-introduction-to-the-patriot-air-defense-missle-system

JP1-02 DoD Dictionary of Miltary and Associated terms. (2001).

Kopp, C. (1993). *A doctrine for the use of electromagnetic pulse bombs.* Air Power Studies Centre. Paper No.15.

Kopp, C. (1996). *An introduction to the technical and operational aspects of the electromagnetic bomb.* Air Power Studies Centre. Paper No.50.

Kopp, C. (2006). Directed Energy Weapons-Part 1. *Defense Today.*

Microwave Encyclopedia, Microwaves101.com. Retrieved August 12, 2008, from http://www.microwaves101.com/content/downloads.cfm

Microwaves101. Retrieved August 12, 2008, from http://www.microwaves101.com/content/downloads.cfm

Military Analysis Network. (n.d.) *Guided Bomb Unit (GBU-10) Paveway II.* Retrieved June 23, 2009, from http://www.fas.org/man/dod-101/sys/smart/gbu-10.htm

Military Dicrionary-Terms Defined. Retrieved June 24, 2009, from http://www.militaryfactory.com/dictionary/military-terms-defined.asp?term_id=2258

Pace, Phillip E. (2007). Joint Network-Enabled Electronic Warfare-1 (EC3700) Course Notes. Fall 2007. Naval Postgraduate School, Monterey, CA.

Patriot Battalion Equipment and Organization. Appendix B. Retrieved July 11, 2009, from http://www.globalsecurity.org/space/library/policy/army/fm/44-85/Appb.htm.

Patriot TMD. Retrieved July 10, 2009, from http://www. security.org/space/systems/patriot.htm.

Product Brochure. Retrieved June 24, 2009, from http://jmem.northropgrumman.com/Brochure.htm.

Schamiloglu, E. (2004). *High Power Microwave Sources and Applications*. 2004 IEEE MTTS, Forth Worth, Texas.

Schleher, D. Curtis. (1999). *Electronic warfare in the information age*. Boston: Artech House.

Shoot to not kill: a peak at our nonlithal arsenal. (2003). Available online at http://www.popsci.com/scitech/article/2003-04/shoot-not-kill

Smith, Terry. Appendix: Response Analysis via Transmission Line Modeling. In *Simulated e-bomb effects on electronically equipped targets*. In press, master's thesis, Naval Postgraduate School, Monterey, CA.

The Free Dictionary. Circular error probability. Retrieved June 24, 2009, from http://encyclopedia.thefreedictionary.com/Circular+Error+Probability

Valouch, Jan. Electromagnetic directed energy weapon for eliminating electronic systems. Retrieved July 09, 2009, from http://www.army.cz/mo/obrana_a_strategie/1-2003eng/valouch.pdf

Vance, Edward F. (1987). *Coupling to shielded cables*. Florida: Robert E. Krieger Publishing Co.

Wilson, Clay. 2006. *High altitude electromagnetic pulse (HEMP) and high power microwave (HPM) devices: threat assessments*. CRS Report for Congress, Order Code RL32544. Retrieved June 2, 2009, from http://www.fas.org/man/crs/RL32544.pdf.

Zacharias, Richard, Pennock, Steve, Poggio, Andrew, & Ray, Scott. (1992). Tools and techniques for estimating high intensity RF effects*. IEEE AES Systems Magazine.*

THIS PAGE INTENTIONALLY LEFT BLANK

INITIAL DISTRIBUTION LIST

1. Defense Technical Information Center
   Ft. Belvoir, Virginia

2. Dudley Knox Library
   Naval Postgraduate School
   Monterey, California

3. Lt. Col. Terry Smith
   IW/EW Program Officer
   Monterey, California

4. Dr. Dan Boger
   Department of Information Science
   Monterey, California

5. Enes Yurtoğlu
   7th Main Jet Base Erhac
   Malatya, Turkey

6. Kara Harp Okulu
   Kara Harp Okulu Kütüphanesi
   Ankara, Turkey

7. Deniz Harp Okulu
   Deniz Harp Okulu Kütüphanesi
   İstanbul, Turkey

8. Hava Harp Okulu
   Hava Harp Okulu Kütüphanesi
   İstanbul, Turkey

9. Elektronik Harp Destek Merkezi
   Ankara, Turkey